The Role of Cytokinin Homeostasis in the Regulation of PIN7

BY KHULUD SALEM ALBALAWI, MSc

Thesis submitted to the University of Nottingham for the degree of Doctor of Philosophy

July 2022

Abstract:

Phytohormones regulate virtually every aspect of plant growth and development. The interaction between auxin and cytokinin determines the vascular pattern in the root. One key node of crosstalk between these hormones, involves cytokinin promoting the transcription of the auxin efflux transporter PIN-FORMED 7 (*PIN7*). However, the mechanism by which this occurs is not known. A forward genetic screen to identify novel loci regulating *PIN7::PIN7:GFP* in the root identified a number of mutants. One of them, in a mutant called 56B2, is in the promoter of the *CYTOKININ OXIDASE/DEHYDROGENASE 5* (*CKX5)* gene. In this project the phenotype of this mutant was characterised in detail. It has been shown that in addition to mis-expression of *PIN7* in the root tip, this mutant also shows reduced sensitivity to cytokinin and defects in organ formation in both lateral roots and leaves. It was demonstrated that CKX5 is expressed in the root vascular cylinder, lateral root primordia, and the shoot apical meristem. These are all regions consistent with the phenotypes that was observed in 56B2. To test whether the mutation in the *CKX5* promoter causes mis-expression of *CKX5* in root tips, reporter lines were developed for *CKX5* with either wild-type or 56B2-like promoters. Surprisingly, these showed no difference in *CKX5* levels in the root meristem. Then variation in natural accessions has been looking and two closely related lines (Kardz 1 and 2) that differ from each other with exactly the same substitution present in 56B2 were identified. It has been shown that several of the phenotypes present in 56B2 are shared with Kardz-2, but that *CKX5* levels are not altered in the root tip. As cytokinin is known to be transported from shoots to root via the phloem, the results are consistent with a hypothesis in which cell non-autonomous regulation of *CKX5* causes the root

phenotype shown in 56B2. A series of experiments were presented that could explore this further.

Acknowledgement

I am deeply grateful to my supervisor Dr. Anthony Bishopp for his invaluable advice and continuous support. Words of thanks are not enough to express my thanks and gratitude for his patience during my PhD study. I would like to thank every member in "Root group" for their support and help either in academic or personal level especially in pandemic period we felt as international student surrounded by our families. Also, I would like to extend my sincere thanks to A20 lab member George, Alex, Britta, John, Jingyi, Elina and Kartika for their assistance and cherished memories I got by spending time with them in the lab. I would like to thank Kamal and Nicky for their hard job they have made it to make our work in the lab easy. I would like to thank Tabuk University for funding opportunity to study at University of Nottingham.

I would like to express my sincere gratitude to my lovely family parent, sisters, brothers for their support and believes on me. A heartfelt thanks to my husband for his patient, understanding and continuous support. I have surrounded by your love and believe over the years even we live in different countries.

I would like to offer special thanks to my friends Dalia, Doha, Shiah, Abrar and Amrah for their support that made my study in the UK a wonderful time as I have another family not just friend.

Thanks, from my bottom heart to my lovely kids Deem and Ahmad. They are the main supporter to me during my PhD journey. Thank you for their patience and understanding throughout my study. Finally, thanks God for giving me the strength and ability to finish this project.

ABBREVIATIONS

AHK: Arabidopsis HISTIDINE KINASE.

AHPs: Arabidopsis histidine-phosphotransfer proteins.

ARF: auxin response factor.

ARRs: Arabidopsis response regulators.

AuxREs: auxin response elements.

BA: 6-Benzyladenine.

cDNA. Complementary DNA

CKX5: OXIDASE/DEHYDROGENASE 5.

4-cl-IAA: 4-chloroindole-3-acetic acid

Col-0: Columbia-0

CRISPR/Cas9: clustered regularly interspaced short palindromic repeat

CZ: central zone

cZ: cis-zeatin.

DNA: Deoxyribonucleic Acid

dNTPs:Deoxyribonucleotide triphosphate

DZ: Differentiation Zone

E. coli: Escherichia coli

EMS: Ethyl methanesulfonate.

EZ: Elongation Zone

GFP: green fluorescent protein.

GUS: β- glucuronidase.

IAA: Indole-3-acetic acid.

IBA: indole-3-butyrie acid.

iP: isopentenyladenine.

ipt: ISOPENTENYLTRANSFERASE.

Kan: Kanamycin

LRP: Lateral Root Primordium

mRNA: Messenger Ribonucleic Acid

MZ: Meristem Zone

NASC: Nottingham Arabidopsis Stock Centre

OC: Organizing Centre

PCR: Polymerase Chain Reaction

PI: Propidium Iodide.

PIN7: PIN-FORMED 7.

PZ: Peripheral Zone

qRT-PCR: quantitative real time polymerase chain reaction

RAM: Root Apical Meristem

RZ: Rib Zone

SAM: Shoot Apical Meristem

tZ: trans-zeatin.

TZ: Transition Zone in root

T-DNA: Transfer DNA

UV: Ultraviolet

wol: Wooden leg

Ws: Wassilewskija

WT: Wild type

^{o}C.:Degree Celsius

µl: Microlitre

Table of Contents

List of Figures:

Chapter 1. Introduction

1.1 Arabidopsis thaliana as a model plant

Arabidopsis thaliana is a small annual weed that belongs to the mustard family (Brassicaceae). *Arabidopsis* was first described in 1577 by Johannes Thal based on collections from the Harz Mountains of Northern Germany. Although both the genus and species name date to 1842, when it was re-named as *A. thaliana* by Gustav Heynhold (Krämer, 2015). *A. thaliana* grew natively in Europe and Central Asia, but nowadays has spread across many places in the world (Al-Shehbaz and O'Kane, 2002).

The length of the *Arabidopsis* life cycle is determined by two key traits, flowering time and seed dormancy (Pigliucci, 2002). Broad variation exists between *Arabidopsis* accessions regarding both of these traits and plants can be described as either annual and biennial (Pigliucci, 2002). Summer annuals germinate in the spring and flowering in summer of the same year, while winter annuals germinate in the autumn and overwinter as rosettes and flower the next year. When natural accessions are grown in greenhouse conditions without a long period of cold treatment (known as vernalization) flowering is delayed dramatically (Napp-Zinn, 1987).

The life cycle fast cycling in *A. thaliana* line (such as the commonly used Col-0) is approximately 8 weeks (from germination to mature seed). The different stages of its life cycle from seed to mature plant are completed within nearly 59 days (Figure 1.1). *A. thaliana* has small white flowers and produces about 20-30 seeds in each silique (Meinke et al., 1998, Komaki et al., 1988).

Arabidopsis was the first flowering plant to have its genome sequenced, and this was published in 2000 (The Arabidopsis Genome, 2000). It has a relatively small genome with genome size approximately 157 Mbp with 5 chromosomes and about 25,500 genes (The Arabidopsis Genome, 2000). Over the years a suite of advanced molecular biology techniques and tools have been developed to enable to researchers to examine function of individual genes. These include a genome browser on TAIR (Swarbreck et al., 2007), an extensive collection of mutant lines held at stock centres in Europe and USA (arabidopsis.info, abrc.osu.edu), and an extensive literature base, with the search string "*Arabidopsis*" listing over 80 000 papers on the NIH PubMed server.

This wealth of research in *Arabidopsis* is possible due to its extreme experimental tractability. It has been adopted as a model plant due to its small size, rapid lifecycle and the ease at which it can be grown in the lab. Moreover, *A. thaliana* is self-fertilizing and produce thousands of seeds from a single individual. Transgenics can be made easily and efficiently with *Agrobacterium tumefaciens* by using the floral dipping technique (Bent, 2000).

Figure 1.1: The life cycle of *Arabidopsis thaliana* (Col-0). The figure shows the different stages of development from seed until mature plants (approximately 8 weeks after germination). Image taken from (Krämer, 2015).

1.2 Global Food Security

Humanity is facing a great challenge in providing food security for an ever-growing world population. According to the Food and Agriculture Organization (FAO) of the United Nations, 795 million people were suffering from chronic malnutrition around the world in 2014-2016 (FAO et al., 2015). The human population is expected to exceed 8 billion people by 2050 (Sadik, 1997). Therefore, according to the FAO's estimation, food production will have to increase by 70% between 2005 and 2050 to feed this population (FAO,2009). To find a balance between food production and population growth, crop yields must improve. Unfortunately, environmental stresses such as drought, high salinity, nutrient-deficiency and adverse temperature affect the growth

and the productivity of plants. Moreover, each year, large areas of land are lost due to irrigation issues and soil erosion.

It is possible to increase food security by decreasing food waste and loss by capturing more of the food produced for people consumption (Cole et al., 2018). Employing technology for food preservation and stabilisation to increase product shelf life (such as heat treatment or high pressure processing to reduce microbes) will also play a role (Martindale, 2017). Likewise, reducing over-consumption (Cole et al., 2018) by providing education to allow an understanding the danger of obesity contribute to alter the consumer behaviour would in turn feed into improved global food security.

Moreover, shifting the diets towards reducing meat consumption will increase food security. According to published data, the global food system would have about 70% more calories available to humans, if the crops grown to feed animal were instead consumed by people (Pimentel and Pimentel, 2003). As a result, the number of people that could be fed based on our existing agricultural land would rise (Cassidy et al., 2013).

Furthermore, improving existing crop plants will increase food security. Whilst, work is needed in the crops we use today, it makes sense to inform this based on what we have learnt from model plants. To that end, *Arabidopsis* is providing a wealth of information on the molecular mechanisms many traits that would be of agricultural interest. This information can be used to identify components within signalling pathways that controlling specific aspects of growth and development that would be desirable for breeders. In some cases, it may be possible to modify existing crop genomes using CRISPR/Cas technologies to target genes identified in *Arabidopsis*.

This approach may allow the introduction into crop plants of desired traits, such resilience to biotic and abiotic stresses.

Currently, examples exist where knowledge of fundamental signalling pathways have accelerated the development of novel crop species. One example of synergy between crop improvements and knowledge in model organisms relates to how alterations in cytokinin homeostasis can affect grain yield in rice (Ashikari et al., 2005). Natural variation in the expression of the *OsCKX2* gene regulates the number of reproductive organs and increases grain yield in rice (Ashikari et al., 2005). *CKX2* is a member of a family of genes that degrade cytokinin (detail in section1.5). Prior to this work, it was known that overexpression of *CKX genes* reduced the endogenous level of cytokinin and activity of the shoot apical meristem and seed production in *Arabidopsis* (Werner et al., 2001b).

1.2 *Arabidopsis* development

Plants differ from animals in that they have the ability to produce new organs continuously throughout their life cycle. This continuous organogenesis relies on the activity of stem cells. These stem cells are located at root and shoot tips and are called apical meristems. Undifferentiated cells within these meristems self-renew and generate daughter cells which then differentiate to specific cell identities. The shoot and root apical meristems grow and produce the aboveground and underground parts of the plant body, respectively.

1.3.1 Root development

Roots are the hidden organs of the plants that lie under the soil, providing the nutrients and water required for plant growth, as well as structural support for the aerial part. *A.*

thaliana has been used as a model for studying root development due to its simple cellular organization.

During *Arabidopsis* embryogenesis, the zygote divides to form a 1-cell embryo. Through a series of divisions this then gives rise to a, 2-cell, octant, dermatogen, globular, transition structure, before finally becoming a heart stage embryo (Figure 1.2) (ten Hove et al., 2015). An asymmetric division of zygote produces a small apical cell and larger basal cell, which divides to form the suspensor (Yoshida et al., 2014). The primary root of *Arabidopsis* is initiated at the globular stage from the upper cell of the suspensor (hypophysis) (Tian et al., 2014). An asymmetric division of the hypophysis produces an upper cell which gives rise to the quiescent centre and the larger basal cell which gives rise to the columella (Laux et al., 2004). The quiescent centre is a small group of cells that rarely divide and are surrounded by the stem cells. Together these form the stem cell niche and produce the primary root meristem (Dolan et al., 1993). The stem cells divide asymmetrically to produce the different cell types and tissues seen in the primary root, namely, epidermis, cortex, endodermis, stele, columella and lateral root cap (De Smet and Beeckman, 2011). The primary root meristem is located at the root tip, and forms all cells and tissues that comprise the growing root.

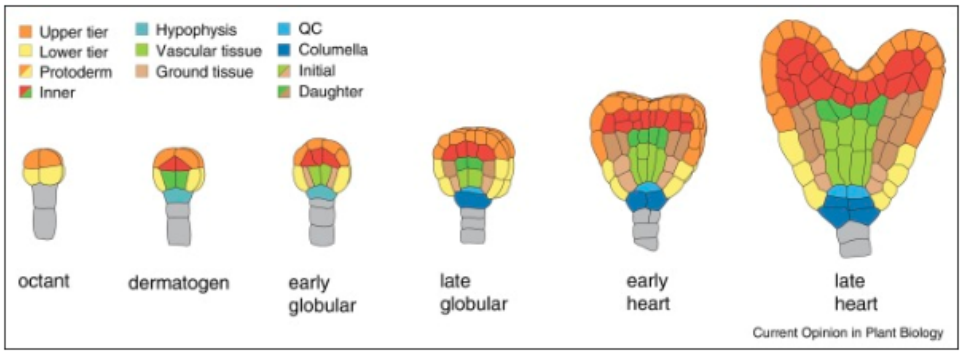

Figure 1-2: Stages of the development of *Arabidopsis* embryo.

This figure reproduced from (Smit and Weijers, 2015).

Roots have a radial structure in which the vascular cylinder (stele) is surrounded by endodermis, cortex and epidermis. The root comprises of four different zones: The meristem zone (MZ), the transition zone (TZ), the elongation zone (EZ), and the differentiation Zone (DZ) (Figure 1.3) (Verbelen et al., 2006, Ubeda-Tomás et al., 2012). The meristematic zone contains the stem cell niche and is the source of all divining cells. The boundary between division and elongation zone is the transition zone (TZ) where cells cease dividing and start to grow in length. Cells continue to grow throughout the elongation zone. As they reach the differentiation zone they stop elongating and differentiate to their final cell fate.

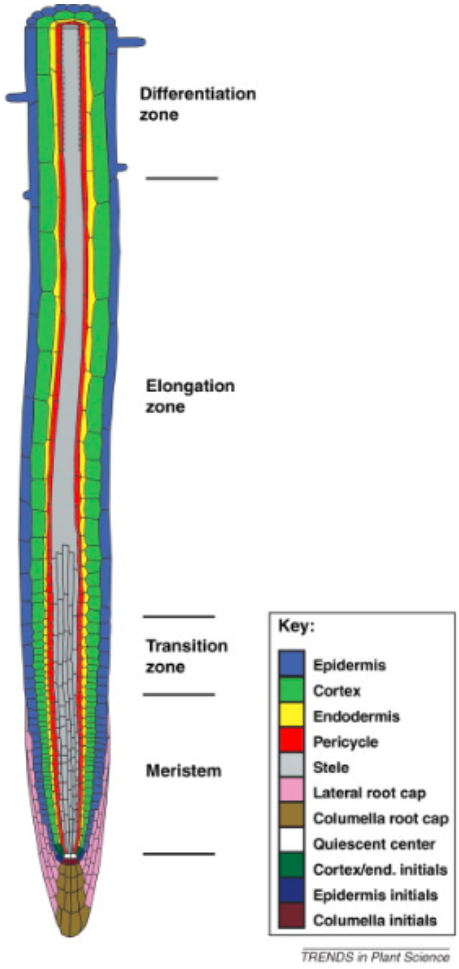

Figure 1.3: Development zones within the primary root of Arabidopsis. In the Meristem Zone cells divide. In the transition zone cells stop dividing. In the elongation zone cells elongate, and in the differentiation zone cells reach their final cell fate. The figure is reproduced from (Ubeda-Tomás et al., 2012).

The initiation of lateral roots is a postembryonic process. Vascular tissue within the primary root is surrounded by a single layer of tissue called the pericycle. In *Arabidopsis,* Lateral roots initiate from the pericycle founder cells opposite the xylem pole (Dolan et al., 1993). Lateral roots initiation starts by anticlinal division of the pericycle founder cells. These divisions occur several times to create single layer of primordia (called stage I). Next, the inner and outer layer are formed by a series of periclinal cell divisions (stage II). Next, cells divide both anticlinally and periclinally through stages (III – VII) to form a dome-shaped primordium that emerges through the

endodermis, cortex and epidermis of the parental root (Figure 1.4) (Dubrovsky et al., 2001, Casimiro et al., 2001).

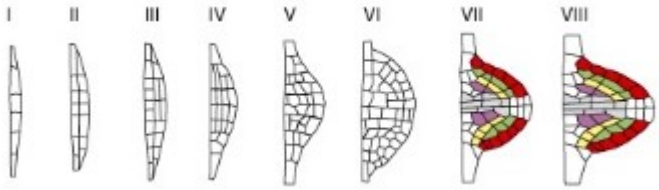

Figure 1.4: The initiation and formation of lateral root primordium in *Arabidopsis*. The image shows the eight stages of primordium development. Figure taken from (Péret et al., 2009).

1.3.2 Shoot development

In *Arabidopsis*, the precursor cells for shoot apical meristem are formed by the upper four cells of the eight cell embryo, while the hypocotyl is produced by the lower cells (Boscá et al., 2011). A round of periclinal divisions then occurs in the eight-cell embryo to separate the inner cells to produce a 16-cell globular stage embryo (Xue et al., 2020, Boscá et al., 2011). The shoot apical meristem (SAM) is established during the globular stage through subsequent periclinal cell divisions.

In the mature plant, the SAM is composed of three zones: the Central Zone (CZ), the Peripheral Zone (PZ), and the Rib Zone (RZ) (Figure 1.5) (Xue et al., 2020). The stem cell niche is located beneath the central zone and comprised of the organizing centre (OC) and cells directly in contact with it. The central zone is comprised of stem cells dividing slowly and is surrounded by the peripheral zone, composed of cells dividing rapidly (Steeves and Sussex, 1989). Some resultant stem cells are moved from the

CZ to the PZ then grow to the lateral organs (Steeves and Sussex, 1989). The cells that form the stem are produced in the rib zone.

During the postembryonic development in *Arabidopsis,* the SAM and axillary meristems form the rosette leaves. On the onset of reproductive growth, the SAM transitions into the inflorescence. Next, the floral meristems are produced by the inflorescence meristem and these produces floral organs (Kaufmann et al., 2010).

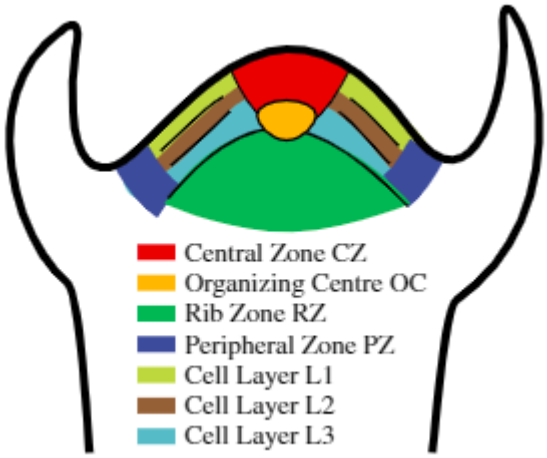

Figure 1.5: Schematic shows the zones of SAM. The Central Zone, Organizing Centre, Rib Zone and Peripheral Zone and three layers L1, L2, and L3. Figure is reproduced from (Matte Risopatron et al., 2010).

1.3 The plant hormone auxin

The name auxin comes from the Greek word auxein which means to grow. The phytohormone auxin is vital for plant growth and development. Auxin has been shown to be the major regulator of meristem activity. In the nineteenth century, the German botanist Julius Von Sach discovered that plants have chemical signals which regulate their metabolism, growth and morphologies (Taiz & Zeiger, 2010). These chemical messengers are released from one part of the plant and transported to another, and

are responsible for the coordination of growth and the formation of plant organs. Moreover, he suggested that the distribution of these messengers may be affected by the external factors such as light and gravity.

The first growth hormone studied in plants was auxin. Many physiological processes were investigated and found to be controlled by auxin action, such as vascular development, apical dominance, responses to light and gravity root and shoot architecture and organ patterning (Woodward and Bartel, 2005). Studying auxin regulation, action and interaction is essential to understand many aspects of plant growth and development. It can be said that auxin is a crucial molecular factor in plant biology; it is arguably principal in developmental processes from embryogenesis to senescence as well as in environmental responses (Salehin et al., 2015).

Four native auxins have been identified in the plants: Indole-3-acetic acid (IAA), 4-chloroindole-3-acetic acid (4-cl-IAA), indole-3-butyrieacid (IBA) and 2-phenylacetic acid a (PAA) (Lavy & Estelle, 2016). IAA is the most abundant auxin occur in the plants (Haagen-Smit et al., 1946).

Auxin is mainly synthesized in the shoot tip and tender leaves of plants and transported to the basal part of stem by polar auxin transport carriers along the main stem (Firml et al., 2003). IAA is also synthesised in roots (Zhao, 2012). Polar auxin transport is determined via auxin-effluxes and auxin-influx carriers. The localization of these carriers at the plasma membrane determines the direction of auxin flow. Moreover, auxin can also move via passive diffusion through the plasmodesmata between adjacent cells thus transport the auxin from cells with high concentration into low concentration cells (Mellor et al., 2020).

Auxin is perceived in the nucleus via an SCF complex, comprising members of the Aux/IAA transcriptional repressors family, auxin response factor (ARF) transcription factors, and the TIR1/AFB1-AFB5 F-box proteins (Salehin et al., 2015, Peer, 2013). These are represented by large gene families: *Arabidopsis* contains 29 *AUX/IAA* genes, 23 *ARFs* genes and 5 members of *TIR/AFB* family. The ARFs bind DNA and act as transcription factors, with the Class A ARFs being associated with transcriptional activation. At low concentrations of auxin, the Aux/IAA proteins bind to the ARFs to block their function (Szemenyei et al., 2008, Schaller et al., 2015). In the presence of elevated auxin, the Aux/IAAs form a co-receptor with TIR1/AFB1-AFB5 (Calderon-Villalobos et al., 2010, Schaller et al., 2015), leading to ubiquitination of Aux/IAAs. These are then degraded by the 26S proteasome, which de-represses the activating ARFs (Figure 1.6) (Ulmasov et al., 1999). The expression of auxin-regulated genes is modulated by the activator ARFs through their binding to auxin response elements (AuxREs) in their promoters (Schaller et al, 2015).

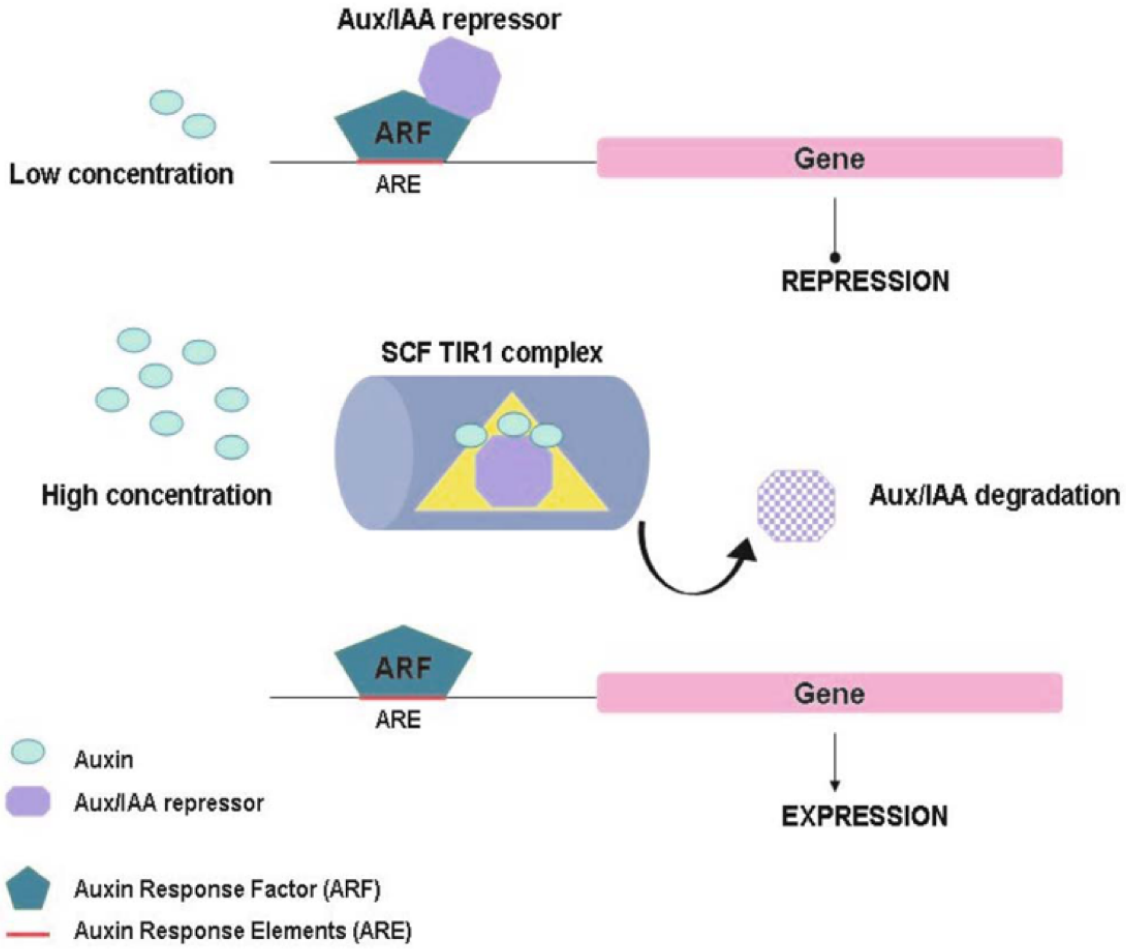

Figure 1.6: Schematic showing how transcription of auxin dependent genes is regulated

At low concentration of auxin, Aux/IAA binds to ARF and repress its activation. At high concentration of auxin, release ARF by degraded Aux/IAA via SCF TIR1 complex. Image from (Teotia et al., 2008).

1.4 Polar auxin transport; the PIN proteins

Auxin is unique amongst phytohormones due to the role of polar transport in determining asymmetries within the plant (Petrášek and Friml, 2009). Indole-3-Acetic Acid (IAA) is a weak organic acid. Therefore, in the low pH environment of the apoplast (~5.5), IAA is present in an undissociated form (IAAH) and can diffuse through the plasma membrane. In the higher pH of the cytoplasm (~7.0) they dissociate, and form IAA^{-}. These polar ions cannot diffuse across the cell membrane and must be moved

by efflux transporters (Figure 1.7). Collectively, these transporters direct auxin down from the shoot towards the root, a process known as polar auxin transport.

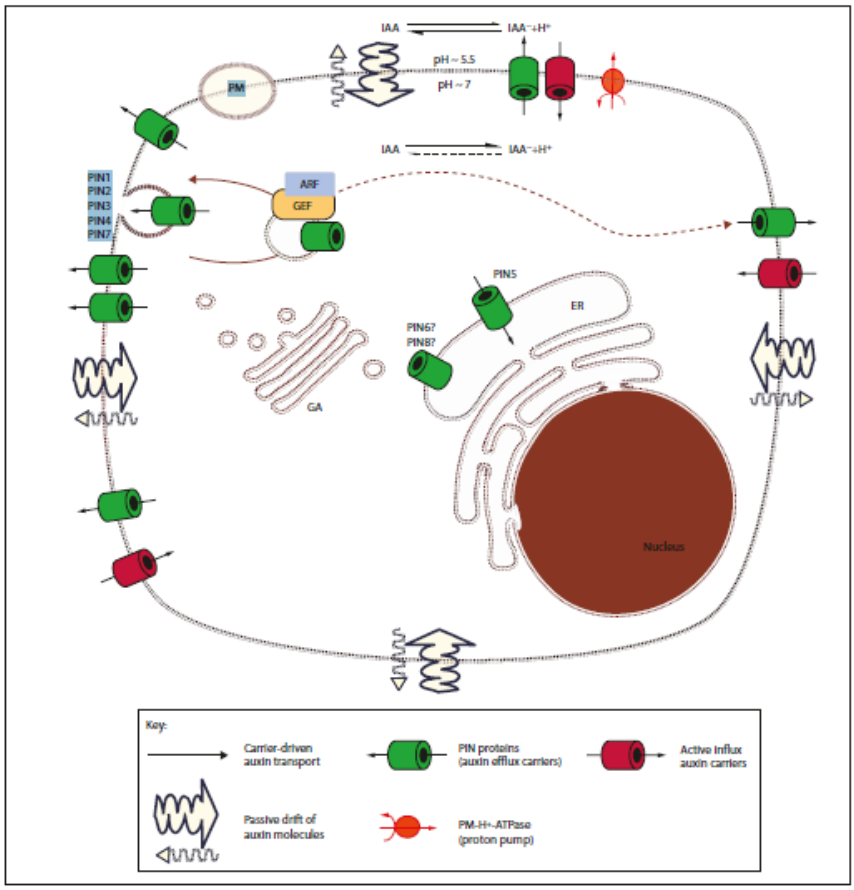

Figure 1.7: The influx and efflux transporters of Auxin.

Schematic shows the movement of auxin which is facilitated by auxin influx and efflux carriers. In the pH in the apoplast, some auxin molecules can access to the cell directly by passive diffusion that molecules stay protonated (un-ionized;(IAA)). While auxin require carriers to transport in its ionized (dissociated) form (IAA- + H+). The auxin influx carriers transport and enter the ionized auxin molecules into cells. auxin molecules in the higher pH in the cytoplasm undergo complete dissociation. The 'long' PIN subfamily of the auxin-efflux carriers localize asymmetrically at the plasma membrane and determine the direction of auxin efflux. PM, plasm membrane; ER, endoplasmic reticulum; GA, Golgi apparatus. (Křeček et al., 2009).

The PIN formed protein family contain 8 members. The structure of the eight *Arabidopsis PIN* genes can be used to divide them into two subfamilies. *PIN1, PIN2, PIN3, PIN4, PIN6* and PIN7 have a long central loop and are called 'long-looped' PINs. These have been shown to catalyse auxin efflux at the cellular level as they are

localized to the plasma membrane (Ganguly et al, 2010). *PIN5* and *PIN8* have a very short central loop and are these called 'short-looped' PINs and are localized on the ER and are involved in intracellular movement of auxin (Mravec et al., 2009). In *Arabidopsis*, the eight *PIN* genes have various spatiotemporal gene expression profile. *PIN1::GFP*, *PIN3:: GFP*, *PIN4::GFP*, and *PIN7::GFP* were observed in the vascular tissue and *PIN2: GFP* in the epidermis and cortex cells (Blilou et al., 2005, Bishopp et al., 2011a).

Friml et al. (2004) proved that the long-looped members of the PIN-FORMED (PIN) family of proteins-controlled auxin efflux. This work showed that these are asymmetrically localized at the plasma membrane and direct the auxin flow (Figure 1.8) in the root of *Arabidopsis.* In the vascular tissues of the RAM, PINs 1,3 and 7 direct auxins acropetally (rootward) due to their basal localization (Figure 1.8) (Blilou et al., 2005). PIN4 is expressed in the QC and columella and redistributes auxin (Friml et al., 2002a). PIN2 is localize on the basal membranes of the cortex cells and on the apical membranes of epidermis cells to direct auxin shootward (Figure 1.8). This flux pattern known is collectively known as the "reverse fountain" (Mironova et al., 2012, Blilou et al., 2005).

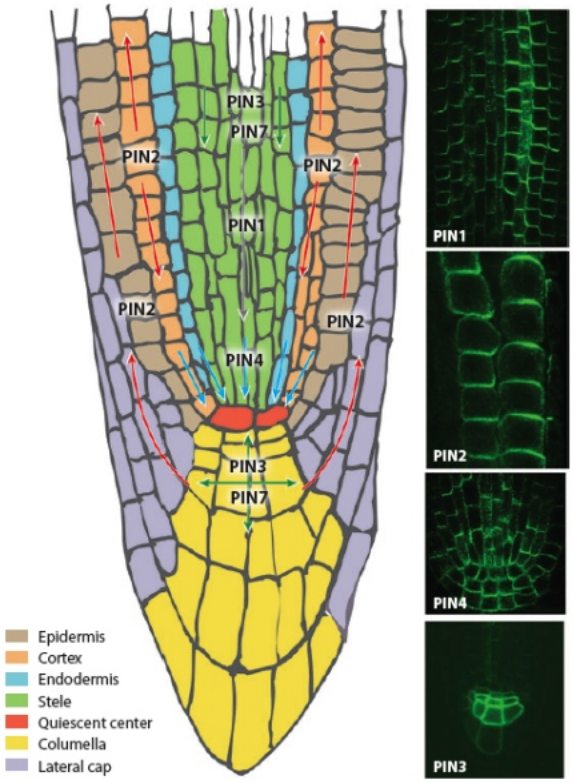

Figure 1.8: Localization of PIN proteins in the root tip of *Arabidopsis*.

Schematic shows the polar flow of auxin mediated by PINs in the root tip. PIN1 is located to the basal membrane of stele cells, PIN2 is localized at the apical of epidermis cells and at the basal of cortex cells, PIN3 in the columella, PIN4 in the QC and surrounding cells. Taken from (Kleine-Vehn and Friml, 2008).

Due to their tissue specificity, different *pin* mutants have been associated with different phenotypes. *PIN1* is involved in auxin basal movement (Blilou et al., 2005), initiation of organ (Galweiler et al., 1998) and formation of flower bud (Okada et al., 1991). *PIN2* is involved in the gravitropism (Chen et al., 1998), where it modulates recycling of auxin through the cortex cells(Blilou et al., 2005), and *pin2* mutants have a defective gravity response (Abas et al., 2006, Müller et al., 1998). Active auxin transport has been connected to the PIN3(Friml et al., 2002b), PIN4(Friml et al., 2002a), and PIN7 protein (Friml et al., 2003). *PIN3* contributes towards the early steps in the formation of lateral root as well as the tropic responses (Chen et al., 2015, Friml et al., 2002b).

Around the auxin maximum in the root meristem, the PIN4 protein located in a polar manner and stabilizes the formation of a local auxin maximum (Friml et al., 2002a). *PIN7* is involved in the formation and maintenance of the apical basal auxin gradient during embryogenesis as well as in root acropetal auxin transport (Blilou et al., 2005). *PIN7* is also involved in the gravitropism response and it negatively regulates the radial growth of root system (Ruiz Rosquete et al., 2018). Moreover, in the earliest stages of embryogenesis four PINs (PIN1,3,4, and 7) are expressed. Single mutants of *pin1*, *pin4* and *pin7* all show weak defects in embryo development, whilst multiple mutants have more serious effects (Friml et al., 2003, Blilou et al., 2005).

.

1.5 Cytokinin homeostasis

The plant hormone cytokinin promotes cell division and differentiation (Mok and Mok, 2001a). Kinetin was the first isoform of cytokinin discovered. It was identified in the 1950s by Skoog and Miller due to its ability to induce plant cell division (Miller et al., 1955). Different cytokinins have subsequently been identified, but all have the structure of N6-substituted adenine derivatives (Mok and Mok, 2001a). Cytokinins are involved in many aspects of plant development, such as root growth and branching, control of apical dominance in the shoot, and leaf senescence (Mok and Mok, 1994).

Natural cytokinins can be divided into two groups depending on their side chain. Aromatic cytokinins contain an aromatic derived side chain while Isoprenoid cytokinins, contain an aliphatic side chain of isoprenoid origin (Strnad, 1997, Mok and Mok, 2001b). Isoprenoid cytokinins can be further divided based on the variations in the cytokinin side chain and stereoisomeric configuration into isopentenyladenine (iP),

trans-zeatin (tZ), dihydrozeatin, and cis-zeatin (cZ) groups (Sakakibara, 2006, Antoniadi et al., 2015).

The concentrations of cytokinins have to be adjusted in different cell types to optimize the development and growth. A balance between synthesis and catabolism regulates cytokinin homeostasis. The level of cytokinin in plant tissue is partly controlled by the catabolic enzymes, cytokinin oxidases (CKX) (Werner et al., 2001b). Cytokinin oxidases (CKXs) catalyse the irreversible degradation of cytokinin by transforming active cytokinin such as zeatin to adenine by selectively degrading unsaturated N6-iso-prenoid side chains (Mok and Mok, 2001b). Cytokinin oxidases have been isolated from maize (Houba-Hérin et al., 1999, Morris et al., 1999), *Arabidopsis* (Werner et al., 2001b), and orchids (Yang et al., 2003).

Arabidopsis has seven members of the *CKX* gene family (*CKX1* to *CKX7*) (Schmülling et al., 2003). The different *CKX* genes are expressed in different tissues and have different subcellular localizations. CKX7 is the only *Arabidopsis* isoform localized to the cytosol (Köllmer et al., 2014, Niemann et al., 2018). The other CKXs contain a hydrophobic N-terminal domain that imports them either into the ER or vacuole and may results in their transport via the secretory pathway (Schmulling et al., 2003). Over-expression of CKX7 has modest effects on plant development (Köllmer et al., 2014) whilst over-expression of other CKXs (especially CKX1 and 3) leads to strong phenotypes (Werner et al., 2003). This suggests that depletion of different pools of cytokinin in different sub cellular compartments may have significant effects on development (Romanov et al., 2018). Additionally, CKX family members also show tissue-specific expression patterns (Werner et al., 2003). CKX1 is present at the shoot apex, lateral shoots, young flowers and vascular tissues in the root tip. CKX2 is present in the SAM and in stipules. CKX3 is only likely to be expressed at weak levels but

seems to be mostly in the shoot. CKX4 is strongest in trichomes, stipules and in the root cap. CKX5 is predominantly expressed in leaves, the SAM, flowers and at the RAM. CKX6 is mostly in the vascular system of cotyledons, leaves and roots as well as in guard cells. CKX7 is expressed in vascular tissues and in the female gametophyte (Köllmer et al., 2014)

Decreasing the level of cytokinin by over-expression of CKX1 and 3 causes strong phenotypes with inhibiting the development of shoots but promoting growth of the primary root (Werner et al., 2001b, Werner et al., 2003). Due to genetic redundancy, loss-of-function *ckx* mutants do not show clear phenotypes, although phenotypes can be observed in multiple mutants. For example, the *ckx3 ckx5* double mutant shows larger inflorescences and floral meristems (Bartrina et al., 2011), although it should be noted that recently *ckx2* mutants have been shown to have a subtle phenotype in which the angle of lateral roots is altered (Waidmann et al., 2019).

1.6 Cytokinin signalling

The pathway of cytokinin signal transduction is similar to bacterial two-component signalling systems and involves a multi-step phosphorelay (Figure 1.9) (Ferreira and Kieber, 2005). The crucial components in the cytokinin signalling are sensor kinase receptors to perceive the signal, histidine phosphotransfer proteins to transfer the signal and response regulators that regulate transcription of cytokinin.

During the previous two decades, there has been considerable progress in revealing the molecular mechanism of cytokinin action. In 2001 several papers identified the first cytokinin receptor in *A. thaliana, CRE1* Cytokinin Response 1 (CRE1) (Inoue et al., 2001)/ *Arabidopsis* Histidine Kinase 4 (AHK4) (Suzuki et al., 2001, Ueguchi et al., 2001). In addition, two other receptors, AHK2 and AHK3 were identified based on

homology (Ueguchi et al., 2001). All three receptors contain a conserved extra-cellular cytokinin-binding domain called the CHASE domain, a histidine kinase domain and a receiver domain (Ferreira & Kieber,2005). Cytokinin binds to the CHASE domain and causes phosphorylation of a conserved histidine residue in the histidine kinase domain. This phosphate is relayed through a conserved aspartate residue of the receiver domain, onto a conserved histidine residue of the *Arabidopsis* Histidine Phosphotransfer proteins (AHPs) (Lomin et al., 2012, Werner and Schmülling, 2009). The subcellular localization of the receptors has been controversial, although the largest body of evidence supports the concept that they are predominantly localized to the ER (Caesar et al., 2011, Wulfetange et al., 2011).

The downstream phosphorylation targets of the AHK cytokinin receptors are the AHPs. In *Arabidopsis* there are five AHPs (AHP1-5) that contain the conserved histidine necessary for phosphorelay (Suzuki et al., 1998, Miyata et al., 1998). AHP proteins continually translocate between the nucleus and the cytoplasm where they target and phosphorylate the ARRs (Punwani et al., 2010). Another protein called AHP6 is structurally similar to the authentic AHPs. However, it is lack of the conserved histidine residue that is required for the phosphorelay, and it is considered to be a pseudo-AHP (Mähönen et al., 2006, Lomin et al., 2012). AHP6 most likely acts as a negative regulator of cytokinin signal transduction because it is in competition with AHP1-5 for interaction with activated receptors (Hwang et al., 2012).

The *ARR* genes can be divided into two groups based on their sequence similarities, domain structure and transcriptional response to cytokinin; these are type A and type B *ARRs* (D'Agostino et al., 2000, Mason et al., 2004).

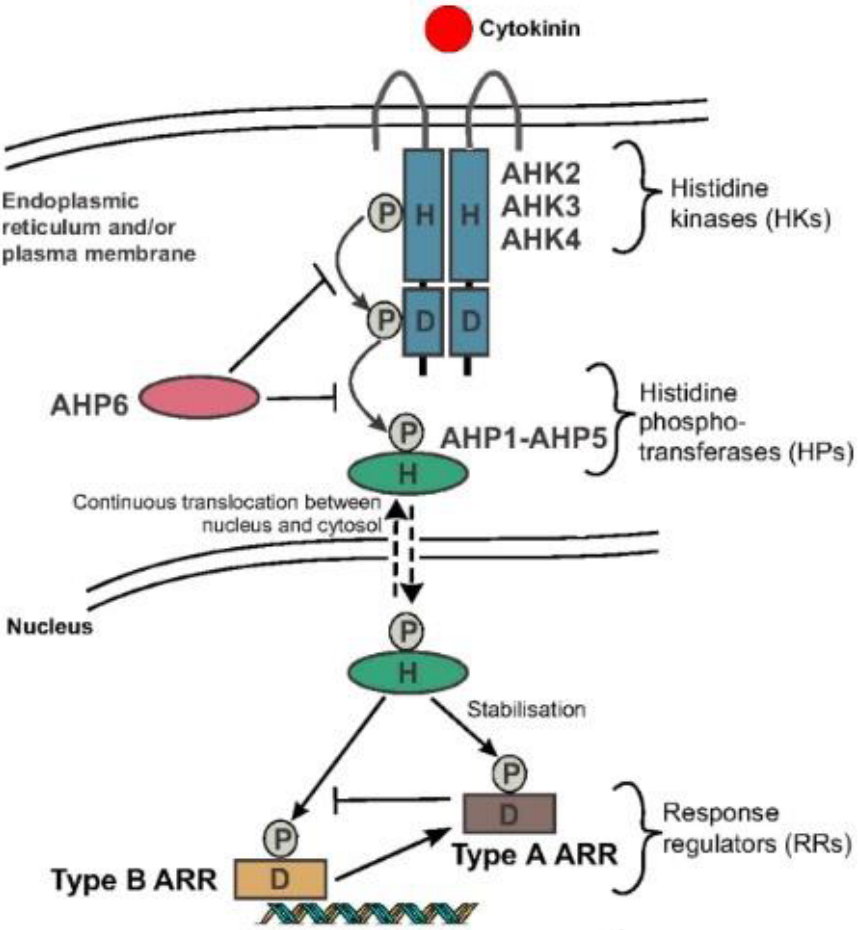

Figure 1.9: Cytokinin signalling occurs through a two-component system.

The cytokinin *Arabidopsis* histidine kinases (AHKs) which are cytokinin receptors are found in the plasma membrane and the endoplasmic reticulum. A phosphorelay is induced when cytokinin binds to the AHK proteins. The receptor transfers a phosphoryl group within the receptor from a conserved His (H) to an Asp (D) residue and then transferred it to the five *Arabidopsis* histidine phosphotransferase proteins (AHP1-AHP5). The Arabidopsis response regulators (ARRs) are phosphorylated by the AHPs as they transport between the cytosol and the nucleus. Taken from (El-Showk et al., 2013)

The type-B ARRs are transcription factors contain a DNA binding domain and activate the transcription of primary cytokinin response genes (Brenner et al., 2012). There are 11 type-B ARRs transcriptional activators in *Arabidopsis* that act as positive regulators (Mason et al. 2004), and their expression is not induced by cytokinin (Lomin et al., 2012). In contrast, type A response regulator genes, considered as primary response genes for cytokinin, are rapidly activated by these hormones (Brandstatter and Kieber,

1998, Brenner et al., 2005). Type-A ARRs consist of a family of 10 proteins that lack the DNA binding domain (To et al., 2004). The induction of Type A ARRs by cytokinin generates a negative feedback loop to restrict the signalling pathway (Hwang and Sheen, 2001). There is considerable redundancy between components, but the triple mutant in *ARR1*, *ARR10*, and *ARR12* leads to roots that are nearly completely insensitive to cytokinin that have strong reduction in cytokinin induction of multiple type-A ARR transcripts compared to wild-type (Mason et al., 2005).

1.8 Cytokinin and auxin crosstalk

Auxin and cytokinin phytohormones regulate many aspects of plant growth and development in combination. Hormonal interaction can occur at the different steps of signalling pathways, transport or biosynthesis. Interaction between auxin and cytokinin affects various developmental aspects such as regulation of apical meristems, organogenesis and root architecture. The regulatory interactions between these two hormones are sometimes characterized as antagonistic and sometimes as agonistic (Schaller et al., 2015).

The balance between auxin and cytokinin is crucial to regulate organogenesis (Skoog and Miller, 1957). When callus culture is exposed to a high auxin: cytokinin ratio this promotes root organogenesis, whereas if the ratio of auxin: cytokinin is low this promotes shoot development (Nordstro¨m, 2004). There are two step to produce shoots *de novo* through tissue culture. Firstly, to induce cell division and callus formation, by exposing plant tissue to an auxin inducing medium. Secondly, the callus is transferred to medium inducing shoot or root to stimulate tissue differentiation; that

medium contains different ratios of auxin to cytokinin, with an elevated ratio of cytokinin to auxin favouring shoot formation (Sugimoto et al., 2010).

During *Arabidopsis* embryogenesis, an antagonistic interaction between auxin and cytokinin is vital to specify the embryonic root stem cell niche (Müller and Sheen, 2008). Auxin signalling promotes the transcription of the type-A *ARRs*, *ARR7* and *ARR15,* in the hypophysis (Müller and Sheen, 2008). These then suppress cytokinin signalling to establish the embryonic stem cell niche at the root pole (Müller and Sheen, 2008).

The balance between cell division and differentiation rate is crucial for root growth and maintenance of meristem size. The phytohormones auxin and cytokinin control this balance (Ioio et al., 2007). Root meristem size is decreased in plants treated with cytokinin as a result of a progressive decrease in the number of meristematic cells. In contrast, the root meristem increases in loss-of-function mutants in cytokinin biosynthesis and signalling mutants due to the accumulation of meristematic cells (Ioio et al., 2007). For example, the triple mutant of *Isopentenyltransferase ipt3,ipt5,ipt7* has severely reduced cytokinin biosynthesis and shows an increase in the number of meristemic cells. In a similar manner, overexpression of *CKX1* in the TZ tissue reduces the level of cytokinin and plants show larger meristems than wild type (Ioio et al., 2007). On the other hand, the application of exogenous auxin causes an increase in the meristem size, as auxin enhances cell division in the meristem (Blilou et al., 2005). *PIN* auxin efflux facilitator mutant plants produce shorter meristem compared with wild-type (Ioio et al., 2007, Blilou et al., 2005). An antagonistic interaction between auxin and cytokinin occurs through the *SHY2* (short hypocotyl 2) gene, which belongs to the auxin repressor *Aux/IAA* gene family (Ioio et al., 2008b). *SHY2* is induced in the TZ by

cytokinin via a direct activation of transcription by the type-B ARRs (Ioio et al., 2008a, Moubayidin et al., 2010). SHY2 is an Aux/IAA and in the absence of auxin it binds to ClassA ARFs such as *ARF5* prevent transcription. This results in fewer cell divisions and induces premature cell differentiation (Ioio et al., 2008a).

Auxin and cytokinin have antagonistic effects on the initiation of lateral root organogenesis. Cytokinin acts as an inhibitor on lateral root organogenesis, and plants with reduced the levels of cytokinin exhibit more lateral roots (Werner et al., 2003) while plants that have cytokinin-hypersensitive mutants show fewer lateral roots (To et al., 2004). In addition, *ahk2 ahk3* mutants are less sensitive to cytokinin and exhibit increased responsiveness to auxin in lateral root formation (Chang et al., 2013). This crosstalk is mediated partially through the modulation of polar auxin transport by cytokinin, where cytokinin polarized PIN1 on either anticlinal or periclinal membranes (Marhavý et al., 2014). This causes redirection the auxin flux toward the apex of the primordia to promote lateral root development (Marhavý et al., 2014).

The root vascular cylinder of the model plant *Arabidopsis* has been exploited as a model for pattern formation. The primary root of the model plant *Arabidopsis* exhibits a bisymmetry pattern with four poles opposite each other similar to the compass directions (Scheres et al., 1994). In the north and the south, there are two xylem poles occupied by a single protoxylem cell and in the central axis connecting by metaxylem. In the east and west there are two phloem poles (Figure 1.10) (Vaughan-Hirsch et al., 2018).

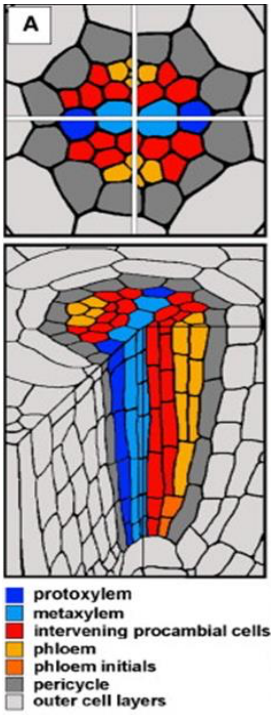

Figure 1.10: Bisymmetric pattern of *Arabidopsis* vascular root.

Schematic shows the central xylem axis flanked by two phloem poles at 90° to each other.

The specification of protoxylem identity is the earliest patterning event within the vascular cylinder. The largest auxin response is present within xylem axis cells and in the protoxylem (Bishopp *et al*., 2011), whilst the highest cytokinin response is found within the cells in the phloem/procambial domains (Mähönen et al., 2006).

Bishopp *et al* (2011) illustrate that these exclusive domains of auxin and cytokinin signalling output are maintained because a pair of mutually inhibitory interactions. Firstly, the inhibitor of cytokinin, AHP6, is a direct auxin target (Bishopp et al., 2011a), Secondly, the subcellular localization and expression of the PIN class of auxin transporters is regulated by cytokinin. Cytokinin promotes *PIN7* transcription indirectly in its expressed in the procambial cells flanking the xylem axis (Figure 1.11b) (Bishopp *et al*., 2011). In addition, cytokinin effects the subcellular location of PIN1, affecting

distribution of auxin. It was found that PIN1 localized to the lateral membrane in cells that have high cytokinin signalling such as procambium (Bishopp *et al*., 2011). Bishopp et al. (2011) showed that the expression of *PIN7* is induced in the high cytokinin signalling in procambial cells and PIN1 and PIN7 localized on lateral membranes of these cells (Figure 1.11). Whilst the core of this interaction module is clear, little is known about how cytokinin regulates *PIN7* in this context.

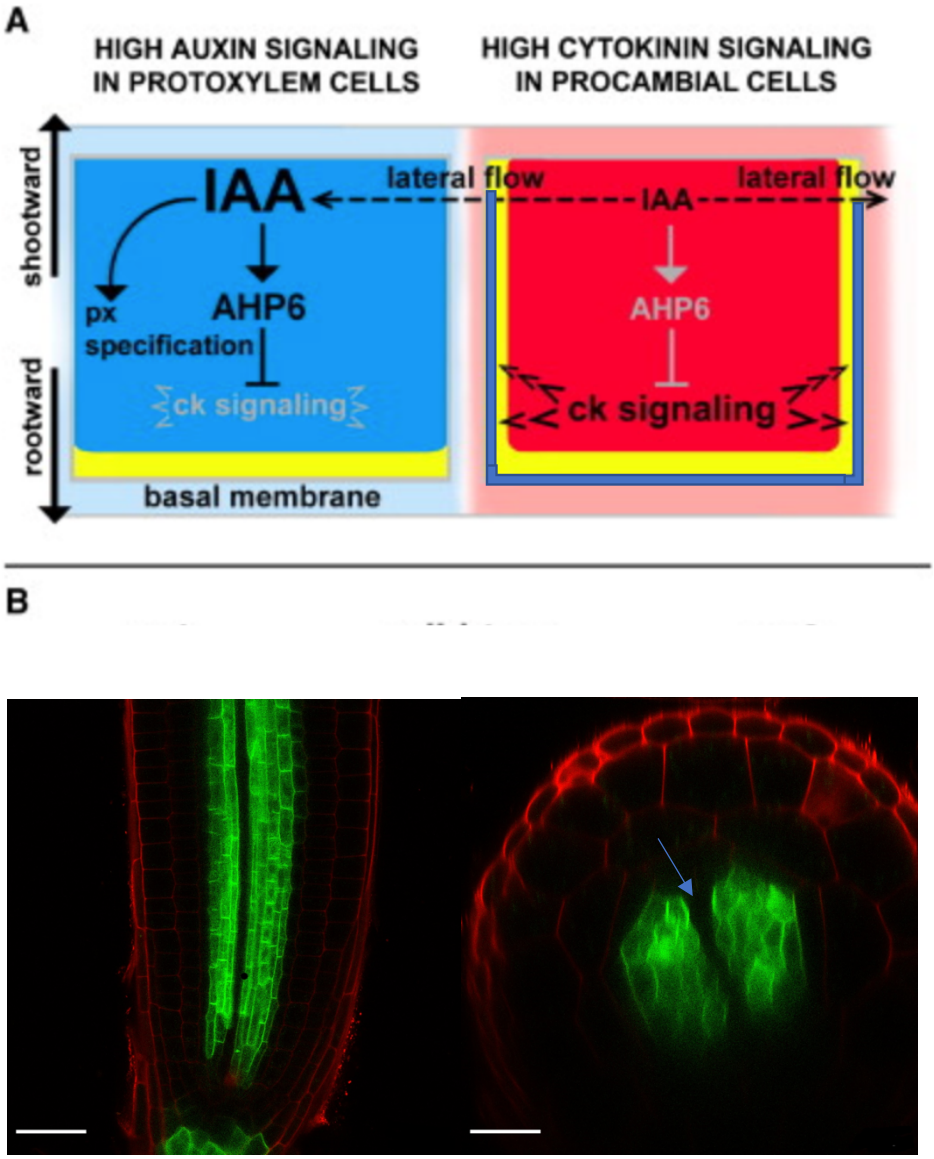

Figure 1.11: The mutually inhibitory interaction between auxin and cytokinin.

A) In the vascular cylinder of the *Arabidopsis* root meristem, protoxylem (px) cells (shown in blue) show high auxin and low cytokinin signalling, while high cytokinin and low auxin signalling observe in procambial cells (shown in red). The mutually inhibitory interaction between theses hormones response can be propagated into two domains. High cytokinin signalling in the procambial cells promote the expression of *PIN7* and localized PIN1 and PIN7 on the lateral membrane of cells instead of basal membrane only (the subcellular localization of PIN1 and PIN7 are displayed in yellow and bule respectively), black arrowheads show the effect of cytokinin signalling on PINs subcellular localization. This subcellular localization of PINs leads to the exit of auxin from procambial cells and accumulation in the protoxylem (the movement of auxin is shown by the dashed line). High auxin signalling in protoxylem localized PIN1 in the basal membrane (represented in yellow), as well as enhancing the transcription of cytokinin signalling *AHP6* and the specification of protoxylem fate. Taken from Bishopp et al., (2011). B) pPIN7:PIN7:GFP is expressed in the intervening procambial cells flanking the xylem axis. The xylem axis is indicated by blue arrows. Scale bars=50μm.

1.10 Identification of novel factors regulating *PIN7* expression.

To identify factors regulating PIN7 expression in the root tip, an ethyl methanesulfonate (EMS) mutagenisis of Col-0 *PIN7::PIN7:GFP* was performed by Dr. Anthony Bishopp, University of Nottingham. A forward genetic screen of this material was performed by Ben Goodall to detect mis- expression of PIN7::PIN7:GFP in the root tip. The rationale here was to identify upstream candidate regulators that regulate *PIN7* transcription in a cytokinin-dependent manner.

90 seed pools were generated, and a PhD student (Ben Goodall) screened approximately ~ 120 M2 seedlings via fluorescent screening microscope. Plants showing a phenotype in the initial screen were then observed via confocal microscopy. Among the 90 seed pools, nearly ~160 mutants were selected from the M2 screen. These were propagated to produce M3 seed. Nearly ~36 mutant M3 lines that showed reduction in the expression of PIN7 in the root tip by confocal microscopy were selected for further analysis. The endogenous expression of *PIN7* was measured by qRT-PCR for the selected M3 mutant lines. The endogenous *PIN7* was reduced in the majority of mutants compared to the control Col-0 and *PIN7::PIN7:GFP* which means that the transcription of *PIN7* is effected by the mutation.

The selected homozygous M3 mutant lines that reduced *PIN7* were back-crossed to the parental non-mutagenized *PIN7::PIN7:GFP*. The crosses were propagated to produce segregating mutant stocks F2. The mutation causing reduction of *PIN7* is recessive as 25% of individuals F2 generations which produced segregating mutant stocks reduced PIN7 expression. The EMS mutagenesis causes multiple mutations in the genome of selected mutant line but only one of these responsible for *PIN7* reduction. So, the causative mutation will have 100% varied read frequency compared

to the reference genome in back-crossed segregating population. Then eleven confirmed M3 mutants with reduced PIN7:: PIN7:GFP phenotypes were selected for genomic re- sequencing and candidate genes were selected based on having a variant frequency of polymorphism relative to Col.0 above 0.85. The 11 mutants that were sequenced identified candidates potentially affecting *PIN7* transcription. From the polymorphisms observed there were no mutations in genes associated with transcriptional activity. However, one of the strongest candidates was in the 56B2 line and was found in the promoter of the *CKX5* gene, which was investigated in this work.

56B2 mutant had 12 possible candidates that might reduce PIN7 expression in the root tip (Table 1). One of the strongest candidates of 56B2 is mutation in the promoter of AT1G75450 (*CKX5)* located in poly (dA- dT) tract, whereby a thymine is substituted to a guanine. It is important to note that in 2006 *CKX* gene renamed At5G21482 used to be called *CKX5* but is currently called *CKX7*. Throughout this thesis the post 2006 nomenclature is used. Naturally occurring stretches of poly (dA- dT) sequences have previously been shown to act as upstream promoter elements to control expression; for example, the yeast his3 gene contains a 17 bp region containing 15 thymidine residues and deletion of this indicates it is required for constitutive expression (Struhl, 1985). In the 56B2 mutant, in which we see a mutation in a similar sequence (poly (dA- dT) tract), there is an increase in the expression of *CKX5* and a reduction in the transcription of *PIN7.* Therefore, it was predicted that as in yeast these poly (dA-dT) tracts may affect the basal level of gene transcription – in this case for *CKX5*.

Table 1: The associated candidate genes for regulation of *PIN7* that carried SNPs due to EMS mutagenesis identified from sequencing of the 56B2 mutant.

Table includes core information, the position of mutation in the gene, the nucleotide changes induced, variant read frequency. The highlighted one is mutation in the *CKX5* promoter.

Sequenced Mutant	Chromosome	Mutation Position	Reference Nucleotide	Variant Allele	Variant Frequency	Associated Gene	Description	Common Name	Additional information
56B2	3	6675034	C	T	0.74	AT3G19270	intron_variant	CYP707A4	
56B2	3	16494443	C	T	0.71	AT3G45090	missense_variant		Glu to Lys
56B2	3	16322443	C	T	0.70	AT3G44780	missense_variant		Asp to Asn
56B2	5	7498566	G	A	1.00	AT5G22570	upstream_gene_variant, 1859bp	WRKY38	acacataagagatatatatat
56B2	4	9182904	T	A	1.00	AT4G16220	intron_variant		
56B2	4	9182916	T	A	1.00	AT4G16220	intron_variant		
56B2	5	13449789	T	C	1.00	AT5G35195	upstream_gene_variant, 40bp		ggtttttatattatattatat
56B2	1	28319216	A	C	0.87	AT1G75450	upstream_gene_variant, 1152bp	CKX5	accattcaaaaaaaaaaaaaa
56B2	1	499387	C	T	0.82	AT1G02450	upstream_gene_variant, 907bp	NIMIN1	gattttaacccgcggtatatc
56B2	4	1520058	C	T	0.79	AT4G03430	missense_variant	STA1, EMB2770	Arg to His
56B2	3	15644148	C	T	0.79	AT3G43740	missense_variant		Arg to Trp
56B2	3	2506201	C	T	0.74	AT3G07850	missense_variant		Glu to Lys

1.11 Aims and experimental objectives

This project will explore whether the alterations in *PIN7* observed in the 56B2 mutant are due to changes in the expression of *CKX5* (AT1G75450). The predicted expression of *CKX5* based on the Gene Investigator Atlas is in the root through procambium flanking xylem axis (Brady et al., 2007), therefore it is proposed that *CKX5* may influence *PIN7* transcription by modulating cytokinin levels and hence response. In addition, the expression of CKX5 in the vascular tissue suggests a function in controlling cytokinin catabolism (Werner et al. 2006).

This investigation will test the following hypothesis: the mutation in the *CKX5* promoter causes the alteration in the expression of CKX5 in the root procambial tissue, and that it an associated decrease in cytokinin levels that would reduce transcription of *PIN7* indirectly.

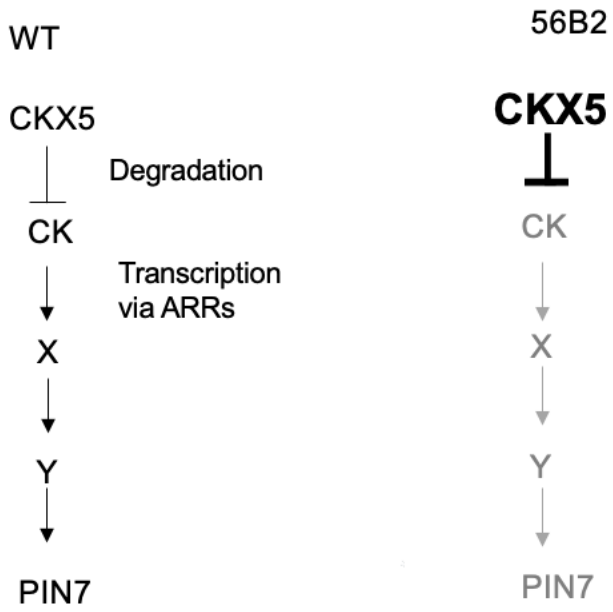

Figure 1.12: Hypothesised placement of *CKX5* in the regulation of PIN7 transcription.

It is known that *CKX5* is one of the cytokinin oxidase genes that degrade cytokinin (CK). It is known that cytokinin enhances the expression of *PIN7* indirectly, that means through the transcription factor ARRs cytokinin promotes multiple factors to regulate PIN7. The hypothesis is that the mutation in the poly(dA-dT) tract in 56B2 increases the transcription of *CKX5* and cause elevated mRNA level (shown in bold font in diagram) compared to WT. This increasing the level of CKX5 would result greater the catabolism of cytokinin and therefore would reduce the level of PIN7 indirectly (shown in grey font).

To do this, firstly I tested whether a polymorphism in the *CKX5* promoter caused the altered of PIN7 levels seen in the 56B2 mutant. To test this, *CKX5* levels in the 56B2 mutant were measured (chapter 3). It was known that CKX5 degrades cytokinin so overexpression of CKX5 would reduce the cytokinin level and may cause alteration in the plant phenotype. So, the phenotype of 56B2 in the root and shoot was observed compared to wild-type in respect to cytokinin (chapter 4).

Next, the reporter markers were used (chapter 5) to provide a better understanding of the expression pattern of *CKX5* in *planta*. The GUS reporter were used to give broad

insight of the expression in the whole plants, while GFP reporter was used for specific localization in the root.

To test that altered levels of *CKX5* are responsible for the phenotype, a CRISPR/CAS9 system will be used to introduce mutations within the *CKX5* gene in the 56B2 mutant. It was hypothesised that 56B2 lines with mutations in *CKX5* would produce elevated levels of a non-functional *CKX5* gene and *PIN7* expression would be restored close to that of that of wild-type. Also, the effect that a polymorphism in the promoter would have on expression level of *CKX5* will be explored by comparing cloning two versions of the promoter, one with the endogenous sequence found in wild-type upstream of the ATG start (carried out by former student) and another incorporating the polymorphism found in the 56B2. These aims are described more clearly and in details in chapter 6.

Finally, the allelic diversity of this locus was analysed within natural accessions to test whether the polymorphism in the promoter of *CKX5* effects the expression level. By looking at the 1001 genomes resource, it can be seen that there are natural accessions that have the exact same mutation that has been observed in 56B2. Do these have similar variations in *CKX5*? What effect does this have on plant growth? To attempt to answer these questions series of experiments were presented in chapter 7 to observe the phenotype and measure the level of both *CKX5* and *PIN7*.

This study contributes to a better understanding of factor that regulate the transcription of PIN7 and provide insight into crosstalk between auxin and cytokinin. In order to study *CKX5* which could be one of upstream regulators that control the expression of *PIN7* by modulating the cytokinin level.

Chapter 2. Materials and methods

2.1 Plant material utilised

Arabidopsis thaliana (Col-0) was used as a wild-type in the experiments, except those using natural accessions. All wild type *A. thaliana* Col-0, 56B2 mutant seeds and fluorescent marker (*PIN7::PIN7:GFP* and *proCKX5:: GFP*) lines were provided by the supervisor of this project Dr. Anthony Bishopp, University of Nottingham. Natural accession from 1001 genome project seeds were ordered from NASC.

2.2 Seed sterilisation, germination and plant growth conditions

All seeds were sterilized by adding 70% (v/v) ethanol with 0.05% (v/v) triton for 10 minutes followed by incubation in 90% (v/v) ethanol for 5 minutes. Seeds were then dried on filter paper to be ready for plating. Seeds were plated out on half-strength Murashige and Skoog media (½ MS) which was prepared by adding 2.165 g/L MS then, the pH 5.8 adjusted and 1% BactoTM agar. Media was supplied with appropriate antibiotics depending on the experiment requirement (supp 3). Plates were kept in the dark at 4˚C for 2 days then transferred to the tissue culture room. Some plates were germinated under 24h days light at 21˚C, and some germinate under 16h days at 23 ˚C. After 14 days mature seedlings were transferred into plastic pots with compost consisting of Levington M3 compost. Plants were kept in the glasshouse (16h day light and 8h dark, day temperature 23 ˚C, and night temperature 18 ˚C).

2.3 Plant treatment with cytokinin

Seeds were germinated on ½ MS with appropriate amount of 6-Benzyladenine (BA) to make final concentration and without BA. Then, plates were kept as normal in dark at 4ºC for 48h then moved into growth cabinet (16h days at 23 ˚C). Images were taken

of plates after 3, 6, 9 and 12 days germination. Primary root length using RootNav software was measured. Seeds that had not germinated within 3 days were excluded from the analysis.

2.4 Genomic DNA extraction

Two techniques were used for gDNA extraction through this project; CTAB (Hexadecyltrimethylammonium bromide) which used for high quality DNA extraction for cloning applications and a crude preparation technique based on Edwards *et al.* (1991) which was generally used for preparing DNA for sequencing.

2.4.1 CTAB extraction technique

First, plant tissue (leaf) was harvested and frozen in liquid nitrogen then ground to a fine powder using a pestle, then 500µl CTAB Buffer (2% CTAB, 100mM Tris-HCl (pH 8), 20mM EDTA, 1.4M NaCl) was added. 5µl β-mercaptoethanol was added and incubated at 65˚C for 25 minutes with regular agitation. 500µl phenol: chloroform: isoamyl alcohol (25:24:1) (v/v/v) was added and tubes wwre vortexed for 10 minutes. Tubes were then centrifuged for 5 minutes at 13,000 rpm. The aqueous phase was transferred into a fresh tube and 500µl chloroform: isoamyl alcohol 24:1 (v/v) was added for second clarification. A chloroform extraction was performed to remove traces of phenol. An equal volume of isopropanol was added to the aqueous phase and incubated at -20˚C for 1 h, then was centrifuged for 10 minutes at 13,000 rpm and the supernatant was discarded. The pellet was washed in 70% ethanol, then resuspended in TE Buffer (1M Tris-cl + 0.5M EDTA).

2.4.2 Crude extraction technique

Genomic DNA was extracted using the method developed by Edwards et al., 1991. Fresh plant tissue (leaf) was frozen in liquid nitrogen then ground to a fine powder

using a pestle. 700µl Extraction Buffer (200mM Tris-HCl (pH7.5), 250mM NaCl, 25mM EDTA, 0.5% SDS) were added. The mixture was centrifuged for 5-10 mins at 13,000 rpm to pellet debris. The supernatant was transferred to a clean tube and an equal volume of isopropanol was added. Tubes were incubated at -20˚C overnight. The next day, tubes were centrifuged at 4˚C, at 13,000 rpm for 10 minutes, and the supernatant discarded. Pellets were washed with 70% (v/v) ethanol, centrifuged and the pellet was air-dried. Finally, the pellet was re-suspended in 50 µl of sterile water.

2.5 POLYMERASE CHAIN REACTION (PCR)

Genomic DNA was amplified using PCR. Generally, 25 µl PCR reactions were performed by adding 5µl 5X reaction buffer, 0.5 µl 10mM dNTPs, 1.25 µl forward primer, 1.25 µl reverse primer, 1µl DNA template (50-100 ng/µl), 0.25 µl Q5® high-fidelity DNA polymerase, and 15.75 µl of deionized water. Then PCR tubes were placed into a PCR machine and a PCR program run depending on the product size and annealing temperature. In general, PCR programs followed conditions similar to these: initial denaturation at 94ºC for 2 mins, 35 cycle at 94ºC for 30s following by the annealing for 30s and temperature depend on primers Tm, extension at 72 ºC 2 mins, final extension: 72 ºC for 10 mins, then hold at 4 ºC.

2.6 Gel electrophoresis

1% (w/v) agarose gel was prepared using 1X TBE buffer to run PCR product. The mixture was heated to dissolve the agarose then left to cool down. 5 µl of 10 mg/ml ethidium bromide was added to cooled but still molten gels poured into the gel mould and allowed to set. When solid, gels were moved to the gel electrophoresis tank. Before loading the PCR product, loading buffer was added to samples and gels were

generally run at 80 V for 1h. DNA migration was visualized under UV light to check the size of the DNA fragments run.

2.7 PCR purification

5 µl of PCR product was run on a gel to check product size. A PCR purification kit (GeneJET, Thermo Scientific) was used to purify the remaining of PCR product. Elution buffer from the kit was used to dilute the purified product, then stored in -20 ºC for further application.

2.8 DNA sequencing

PCR products and plasmid DNA were sent for sequencing to the Source Bioscience (www.sourcebioscience.com/services/genomics/sanger-sequencing-service/). Then the sequences were aligned by using Benchling software to analyse them.

2.9 GreenGate cloning

Constructs were cloned using GreenGate cloning system. GreenGate cloning is simple and effective because it uses only one type of IIS restriction endonuclease and contains six insert modules (plant promoter, N-terminal tag, coding sequence, C-terminal tag, plant terminator and plant resistance) which assemble in one destination vector (Lampropoulos et al., 2013). The DNA sequence of the gene of interest was cloned into plasmid using GreenGate method. BsaI-HF digestion was performed by adding 1µl BsaI-HF (NEB), 5µl CutSmart buffer, 0.3µl entry vector (pGGA000), 15µl gel purified product (56B2 DNA) and 28.5µl H_2O to make the volume up to 50µl. Then the digestion was incubated for 1 h at 37º C followed by incubation at 85ºC for 10 minutes to deactivate the enzyme. The digestion was purified by using the Qiagen PCR clean up. After that, Promega T4DNA ligase was used for ligation by adding 25 µl of purification, 3 µl T4 ligase buffer, 1 µl T4 DNA ligase AND 1 µl water to make the

volume up to 30 µl. Then the ligation was incubated in room temperature for 1 h followe by incubation at 70ºC for 10 minutes to deactivate the enzyme. 10µl of ligation was transformed into electro competent *E.coli* (*DH5α*) using heat shock transformation (section 2.11). Entry vectors were assembled with other GreenGate modules (N-TAG, CDS, C-TAG, terminator and resistance) and destination vector pDEAL (pGGZ003). Constructs were transformed into *Agrobacterium tumefaciens* (Strain GV3101; innate gentamicin, rifampicin, tetracycline resistance) via electroporation to be ready for floral transformations.

Table 2: primers that used for cloning sequence:

T7	GGTAATACGACTCACTATAGGGC
SP6	CACGAGCTATTTAGGTGACACTATA
pBGA004.1	ACCAGGTCTCGGGCTCTATGAATCGTGAAATGACGTCAAGCT
pBGA004.2 R	AACAGGTCTCTAAACCGGAAACGCCGTGGCTGAACC
CKX5conR	GCGATATAACCAGAAGAGGACG
CKX5conF	TCTGGGCTTACGTTAGCTCT

All primers are listed in Methods Supp. All plasmid maps were assembled on Benchling (www.benchling.com) and sequences checked by Sanger sequencing (www.sourcebioscience.com).

Table 3: component modules and completed assembled construct.

Construct	Destination	A Module (promoter)	B Module (N-Tag)	C Module (CDS)	D Module (C-Tag)	E Module (Terminator)	F Module (Resistance)	*In Planta* Resistance
prockx5m::GFP	pDEAL (pGGZ003)	pGGA_KA1H	pGGB003	pGGC025 (3xGFP)	pGGD002	RBCS (pGGE001)	pGGF007	Kan
pCKX5::GUS	pDEAL (pGGZ003)	pBGA004	pGGB003	pGGC051 (GUS)	pGGD002	RBCS (pGGE001)	pGGF007	Kan

2.10 CRISPR Cas9 using pKIR1.1 plasmid

2.10.1 Design gRNA

gRNAs were designed by using the website http://crispor.tefor.net/crispor.py.

Cas9 recognises and binds to PAM sequences on the gene; therefore, the gRNAs were designed near a PAM sequence. The system we are using recognises as PAM the NGG sequence. The gRNA is normally 20 bases long and needs specific overhangs to be added to primers to facilitate cloning into the vector.

2.10.2 Annealing the gRNA

The Annealing Buffer was prepared by adding 50 µl 20mM EDTA, 10 µl Tris pH8, 10 µl 5M NaCl, and 930 µl H_2O. Double stranded DNA incorporating the guideRNA with overhangs compatible for cloning into sites pKIR1.1 cut with AarI was created by adding 2.5µl of each primer to 45µl annealing buffer in PCR tubes. PCR tubes were

incubated in the PCR machine and using the following program: 5 min at 95ºC and 21ºC for 40 min, store at 4ºC until next step.

2.10.3 Digesting the pKIR1.1 plasmid

In order to clone the guide RNA into pKIR1.1 the vector was first linearised using *AarI* (Thermo Scientific). *AarI* cuts outside of its recognition sequence to leave four base pair overhangs. Unlike many restriction enzymes, the ability of *AarI* to recognise and cleave target sequences in the reaction mixture is significantly improved be the including the specific oligonucleotide supplied by the manufacture into digestion reactions. Therefore, digestion was prepared by adding 2 µl 10x Buffer, 2 µl plasmid (100-200ng), 0.4 µl 50x oligonucleotide, 15 µl – dH_20 and 0.6 µl *AaRI* enzyme. The plasmid was digested in a PCR machine at 37ºC for 16h followed by 20 min at 70ºC for inactivation of the enzyme.

2.10.4 Ligation of pKIR1.1 and gRNA using 3U T4 Ligase

The digestion of pKIR1.1 with *AarI* left the linearised plasmid with a 4 bp 3' TAAC overhang and a 4 bp 5' GTTT overhang. Primers for guide RNA were designed so that whilst the sequence over the guide RNA itself were complementary, each primer would contain a different overhang. This resulted in a double stranded product containing a 5' ATTG overhang (compatible with the 3' TAAC overhang from pKIR1.1) and a 3' CAAA overhang (compatible with the 5' GTTT overhang on pKIR1.1). These fragments could be ligated using a simple ligation reaction. Here, 1 µl of linearised plasmid, 1 µl insert (annealed gRNA primers), 2 µl 10x T4 Buffer, 15 µl - dH_20 and 1 µl of T4 Ligase(BioLab) were added. The ligation mixture was incubated at 22ºC 16 h then denatured for 10 min at 65ºC before transformation into *E.coli* cells (DH5α).

2.11 Transformation of *E. coli*

The heat shock method was used to transfer the plasmid DNA into *E.coli*. DH5α *E. coli* competent cells were thawed on ice, then 10 µl of plasmid was added to the cells. This was incubated on ice for 30 mins. Then, the mixture was placed at 42°C for 45s (heat shock), then immediately placed on ice for 2 min. 250 µl of LBD media was added, and then these tubes were incubated at 37°C shaker for 1 hour and 30 mins. Transformed bacteria were plated out onto agar plates containing the appropriate antibiotic then incubated at 37°C overnight.

2. 12 Plasmid extraction

Liquid cultures were prepared by picking single *E. coli* colonies from an agar plate. These were grown overnight with the appropriate antibiotic in 5 ml cultures in a 37 °C shaker. Plasmids were extracted using a mini-prep kit (GeneJET, Thermo Scientific), using the manufacturer's protocol.

2. 13 Transformation of Agrobacterium via Electroporation method

Plasmid DNA (30-50 ng/ µl) was introduced to the *Agrobacterium tumefaciens* strain GV3101 and transferred into a cold electroporation cuvette. Then the cold cuvette was electroporated using a Gene Pulser. Then 200 µl of LBD media was added to the cuvette and the bacteria/LBD mix moved to a 1.5 ml Eppendorf tube and incubated in a 28 ºC shaker for 2-3 hours, before being plated out on LB plates containing appropriate antibiotics.

2.14 Colony PCR

Colony PCRs was performed to confirm the transformation of plasmids into bacteria. Generally, 20 µl PCRs were set up by adding 4µl 5X reaction buffer, 0.8 µl $MgCl_2$, 0.4

µl dNTPs, 1 µl forward primer, 1 µl reverse primer, 0.2 µl DNA polymerase (Taq), 12.8 µl of deionized water, and picking a single colony from the plate and inoculating to each PCR tube. Tubes were placed into a thermo cycler using the following procotol : initial denaturation at 94ºC for 2 min, 35 cycle at 94ºC for 30s following by the annealing for 30s and temperature depend on primers Tm, extension at 72 ºC 1:30 min, final extension: 72 ºC for 10 min, hold at 4 ºC. Primers that used are Seq56B2F TGGTACCATATCGACCCACCA, Seg56B2R GGATGAGGTCACACGTGTGT, B-dummy-F GTATTCAGTCGACTGGTACC, and D-dummyR GCAGGGTACCAATTTACAGG.

2. 15 Floral transformation

Pre-cultures of *A. tumefaciens* harbouring the desired construct were prepared by picking confirmed single colonies from plates and inoculating 5-10ml of LB medium supplemented with the relevant antibiotics. Pre-cultures were incubated in a 28˚C shaker for 48hrs. Pre-culture were used to inoculate larger 500 ml cultures. These were grown with relevant antibiotics and incubated for 24 hours at 28ºC at 200 rpm. On the next day, cultures were centrifuged at 4000 rpm for 10 minutes to pellet the culture. The supernatant was discarded, and the pellet resuspended gently in 500 ml transformation buffer (5% sucrose, 0.05% Silwet L-77). *Arabidopsis* inflorescences were then immersed into the bacterial solution for 1 minute. Then plants were layed horizontally on tissue paper then covered with a plastic bag to maintain the humidity and left for 48h. The plants were grown and watered normally until seeds matured. Seed were harvested and sowing them on ½x MS media supplied with the appropriate selection marker to screen the growth.

2.16 Gene expression analysis

2.16.1 Plant growth

RNA was extracted from roots of 7 days old seedlings grown on ½x MS, either the whole roots or 2 mm sections cut from the root tip were used. Each sample consisted of a pool of 30 roots per replicates and 3 independent biological replicates were used for each.

2.16.2 RNA extraction and cDNA synthesis

Roots were frozen in liquid nitrogen then ground using a pestle. RNA was extracted using a Qiagen RNeasy Mini Kit following the instructions, including the optional on-column DNAse treatment. RNA concentration was measured by a NanoDropTM 1000 Spectrophotometer (Thermo Scientific), and RNA was subsequently stored at -80 °C. cDNA was synthesised using the RevertAid first strand cDNA synthesis kit (Thermo Scientific) following the manufacture's instructions and using the oligo (dT)18 primer: 1µl oligo (dT)18 primer was added to the total RNA (0.1 ng-5µg) then incubated at 65ºC for 5 min then chilled on ice. Then 5x reaction buffer, RiboLock RNase inhibitor, 10mM dNTPs and RevertAid M-MuL V RT were added and incubated at 42ºC for 60 min. cDNA was stored at -20 °C to use in qRT-PCR.

2.16.3 Quantitative Reverse Transcription Polymerase Chain Reaction (qRT-PCR)

Quantitative Reverse Transcription Polymerase Chain Reaction technique was used to measure the mRNA transcript levels. *CBP20* and UBC (house-keeping) genes were used to normalize the gene expression quantification. cDNA template was further diluted (1:10) dependant on the amount of RNA that used for cDNA synthesis. Gene expression was measured in cDNA samples using 5 µl of a fluorescent dye SYBR®

Green Master Mix (Bioline) and 0.1 µl of forward and reverse primers (10µM). The LightCycler®480 System (Roche, USA) was used initially and qTower 384G was used in subsequent assays. The programme conditions contain an initial denaturation at 95˚C for 10 minutes, repeated amplification cycles; 95˚C for 10s then 60˚C for 30s and finally a dissociation curve; 95 °C for 1 min, 60 °C for 30 s and 95 °C continuous. For each primer set, samples were ran as four technical replicates and three biological replicates were utilised.

2.17 GUS staining

Tissue was collected from plants, then cleared in 90% ice cold acetone for 1h on ice with gentle shaking. Acetone was removed with three washes in 0.05 M sodium phosphate buffer monobasic (100 mM, pH 7). Plant tissues were incubated in GUS staining solution (1 mm EDTA pH 8, 5 mm potassium ferricyanide, 5 mm potassium ferrocyanide, 0.1% Triton-X-100, 1 mg ml^{-1} X-gluc) in the dark at 37˚C until GUS expression is visible. Samples were then de-stained in 70% (v/v) ethanol.

2.18 Microscopy and Image capture

A. thaliana seedlings were grown on ½x MS agar plates for 5 days. Roots were stained prior to confocal microscopy in 25µg/ml propidium iodide (PI) to visualise the expression and root structure. Confocal microscopy was performed using a TCS SP5 II (Leica). Specimens were visualised using an Argon laser and GFP emission was detected between 493-548nm. Images were analysed by Fiji software.

2.19 Primary root length

Sterilized seeds were germinated on square Petri dishes (Greiner Bio-One Ltd., 120x 120x17 mm) contain half strength plant growth media (MS). The plates were stored at

4ºC for 48h then moved into growth cabinet (16h days at 23 ˚C). Root measurements were achieved using RootNav software.

2.20 Lateral root density (LRD)

The number of lateral roots was counted for each seedling (12 days old) germinated on 0.5 xMS. Then, the lateral root density was obtained by dividing the number of lateral roots by the primary root length.

2.21 Relative fluorescence measurements

The intensity or relative fluorescence was measured using ImageJ software. The image was imported into the software by pressing plugins then bio-format. Then, GFP intensity was measured by selecting specify width (100 pixel) and hight (500 pixel) around the area that produce signal for each image. Then, set the measurements to measure the mean value. After that, the means for 10 replicates for each line were calculated.

2.22 Vascular phenotype

Sterilization seeds of 56B2 and Col-0 were germinated on 0.5xMS plates. After five days seedlings were moved onto slides then chloral hydrate was added to clarify tissues. After 24h, the xylem phenotype was visualized by microscopy of 56B2 and Col-0 seedlings.

2.23 Statistical analysis

Data statistically was analysed using a Student T-test and one-way Analyses of Variances (ANOVA). If two group were compared Student T-test was performed, while if more than two groups were compared ANOVA followed by post hoc test was

performed. Small p-value ($P \leq 0.05$) indicated that there was a significant difference. Asterisks were used to indicate significant difference.

Chapter 3. Identification of novel genes regulating PIN7

This chapter contains work carried out by a previous PhD student and is necessary for providing the background for my work. In this chapter, I carried out the confocal microscopy for PIN7:GFP following cytokinin treatment, and the qRT-PCR for *CKX5*.

3.1 Overview

The core molecular module controlling vascular pattern has been uncovered, and mathematical simulations have shown that this is sufficient to generate realistic patterns in both *Arabidopsis* roots (de Rybel et al., 2014; el Showk 2015) and roots with more complex geometries (Mellor et al., 2019). However, there are several components that are not currently understood. One of these elements is the relationship between cytokinin and PIN class of auxin efflux transporters. We know that cytokinin regulates PINs in different ways, modulating both their transcription (Pernisová et al., 2009), as well as their subcellular localisation. This relationship between cytokinin and PINs is likely to be complex, as different PINs may be regulated in different ways. Here, this project focus on *PIN7*, as the spatial link between its expression and cytokinin signalling output is clearest. In this chapter, firstly the timing of this interaction is explored and asked how direct this is.

The subsequent sections (3.3 and 3.4) build on work done previously to identify novel factors regulating the expression of *PIN7*. Briefly, this had been investigated by using an EMS mutagenesis screen of the translational reporter *PIN7::PIN7:GFP*. This chapter will give a brief description of the forward genetic screening of reduced *PIN7::PIN7:GFP* expression that followed to identify the novel regulators of misexpression of *PIN7* in the root, as well as introduce one of the mutants that was selected for further analysis and is the subject of future chapters of this thesis.

3.2 Cytokinin regulates PIN7 transcription via an indirect mechanism.

The relationship between the expression of *PIN* genes and cytokinin has been well studied but has produced a complex web of regulations. For example, Pernisova´et al. (2009) looked at the expression of *PIN*s in hypocotyl explants using qRT-PCR and observed that each *PIN* responded differently to different levels of cytokinin. Some *PIN*s, such as *PIN2*, were strongly repressed by cytokinin, whilst others showed more complex relationships, with *PIN3* peaking at mid ranges (100 ng/mL) of cytokinin and *PIN6* being the most strongly induced. These effects were somewhat corroborated by looking at translational fusions between individual PIN proteins with GFP, suggesting a combined effect of cytokinin on both *PIN* transcriptional and post-transcriptional regulation. The exact relationships are likely to be tissue-specific as studies performed by Ruzička (2009) in the primary root meristem showed different results. Using fluorescent reporters in this work showed that PIN7 was the most strongly upregulated by CK; whilst PIN1 and PIN3 were slightly down-regulated. Dello Ioio et al. (2008) illustrate that the root meristem size is regulated by both auxin and cytokinin. They proved that cytokinin activates the Aux/IAA *SHY2*, which in turn inhibits the expression of *PIN*s in the transition zone; this is dependent on the transcription factor *ARR1*. Using qRT-PCR, they showed that the expression of *PIN1, PIN3* and *PIN7* was reduced significantly after 4h treatment of cytokinin (5 μM Zt). Analysis of translational reporter fusions for PIN1:GFP, PIN3:GFP and PIN7:GFP showed that the greatest reduction in signal was observed in the vascular tissue transition zone.

A similarly complex picture can be seen when considering vascular tissues in specific. Bishopp et al. (2011) studied the distribution of PIN1, 3, 4 and 7 proteins within the

stele. By looking at PIN expression in backgrounds affected in cytokinin signalling (*wol* and *cre1 ahk3*), they observed that cytokinin was required for the tissue specific expression of PIN3 and PIN7. In addition, cytokinin controlled the subcellular localisation of PIN1, as PIN1 was mis-localised in *wol* mutants. Collectively, they found that the correct radial distribution of PIN1, PIN3 and PIN7 is regulated by cytokinin signalling. Although the effect that cytokinin had on PIN7 was the most striking, as no signal of PIN7:GFP was detected in the meristem in *wol,* whilst PIN3 was still present albeit at a lower level. PIN7 was observed in smaller domain in *cre1 ahk3,* indicating a dose-dependent role for cytokinin in regulating PIN7.

Within the vasculature PIN7 is expressed highly within the procambial cells and phloem but is excluded from the xylem axis (Bishopp et al., 2011). This corresponds to expression in only cells with high cytokinin signalling output. When roots including PIN7 reporters were treated with cytokinin for 12h this expression pattern expanded radially to include the protoxylem cells (Bishopp et al., 2011a). This regulation occurs at the transcriptional level, as the transcriptional reporter gene *pPIN7::GFP:GUS* exhibited similar response to cytokinin as the translational reporter, *pPIN7::PIN7:GFP*. Collectively, these results show a tight link between cytokinin response and *PIN7* expression. However, the timing may be indirect effect, as there are no clear cytokinin response elements. Cytokinin response elements are type-B ARRs specific binding domains (5′-(A/G)GAT(T/C)-3′) which define a core binding motif for the targets of type-B ARRs genes (Sakai et al., 2000) and two component sensor *TCS* motifs (Müller and Sheen, 2008). The conserved DNA binding domain in the promoter of A-RRR type which is recognised by ARRs type-B was used in designing the *TCS* sensor.

3.2.1 PIN7 expression is expand after 12 h treatment of cytokinin

These data show a clear role for cytokinin in regulating *PIN7*, however it is unknown how direct this is. To address this, experiment similar to those above was ran, but at an enhanced temporal resolution to further dissect the timing. In this experiment *PIN7::PIN7:GFP* lines were treated with exogenous cytokinin (100 nM BA) at various time intervals. Five days old seedlings were incubated with 100 nM BA at 3, 6, 9 and 12 hr alongside mock (DMSO) controls. Seedlings were counterstained with propidium iodide, and both longitudinal images and cross sections were generating using a Leica SP5 confocal microscope. As previously published (Bishopp et al., 2011), it was observed that in all the mock treated lines PIN7 was expressed in two domains of intervening procambial cells flanking the xylem axis. In almost all cases (70/80 plants) a clear and readily discernible xylem axis could be seen (Figure 3.1 A-G) while in 10/80 the xylem axis could not be seen (Figure 3.1 H). As published, the expression pattern of PIN7 mirrored the domain of high cytokinin response. When it was looked at the lines which had been treated with cytokinin, no change was observed in PIN7 expression between (60/60) seedling that treat with cytokinin for 3, 6 and 9 hr and those not treated (Figure 3.1 A-C and E-G).

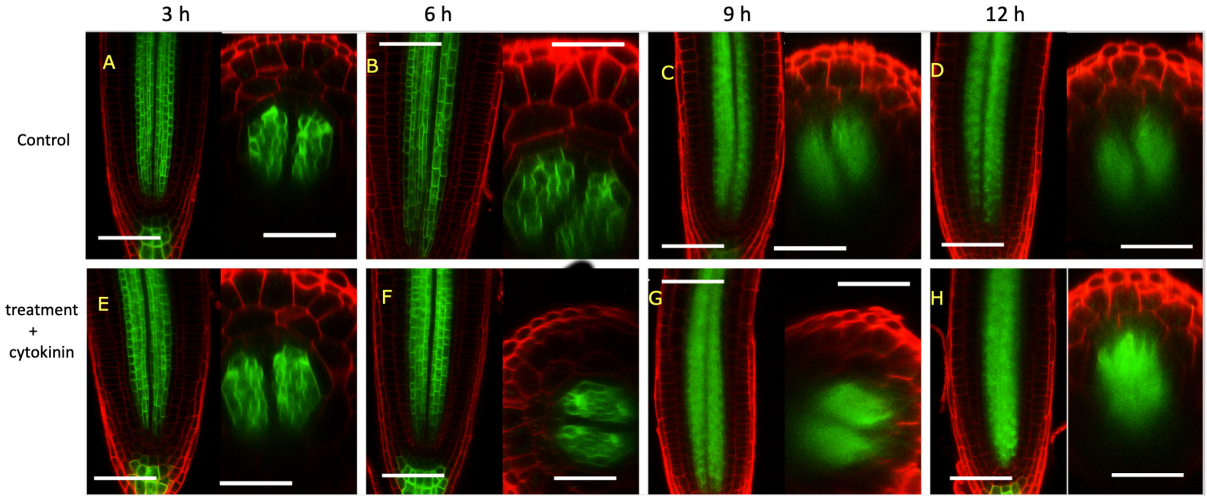

Figure 3.1: PIN7 expression is indirectly induced by cytokinin.

PIN7::PIN7:GFP seedlings were grown on agar plates for 5 days and then incubated with either 100 nM BA in liquid induction system for 3, 6,9 and 12 hrs or a mock DMSO control. Expression of PIN7:GFP was observed on a Leica SP5 microscope. In total 10 plants were analysed per treatment and a representative image for each treatment is shown in both a longitudinal orientation and in cross section. A-D) *PIN7:: PIN7:GFP* at 3, 6, 9 and 12 hrs, respectively, treated with a DMSO control in the liquid induction system. E-H) *PIN7:: PIN7:GFP* after 100 nM BA treatment at 3, 6, 9 and 12 hrs. H) PIN7 is largely responsive following 100nM BA treated for 12hrs and PIN7 domain expand to include the xylem axis. Note that the signal can be seen to expand into the xylem axis at 12h. Scale bar represents 50 µm. n=10.

However, after 12 hours of cytokinin treatment, *PIN7::PIN7:GFP* plants demonstrated a marked increase in the fluorescent signal and expansion of the signal into the xylem axis in 10/10 plants (Figure 3.1 D, H). These data suggests that the effect of cytokinin on *PIN7* is indirect. The observation that alterations in cytokinin response occurs only after 12 hr supports the theory that there may be more than one intermediate step between cytokinin response and *PIN7* activation, for example this could involve a simple transcriptional cascade.

3.3 Identification of novel mutants with altered PIN7 expression.

In order to identify factors upstream of *PIN7,* a previous PhD student had conducted a genetic screen. Dr Anthony Bishopp had performed an Ethyl methanesulfonate (EMS) mutagenesis of the translational reporter *PIN7::PIN7:GFP* in order to identify factors regulating PIN7 expression in the root tip. EMS is a chemical mutagen that has been shown to induce nucleotide transitions in a variety of species including *Arabidopsis* (Greene et al., 2003). This created a collection of randomly mutagenized lines.

Then, a forward genetic screen of these EMS mutagenised lines was performed by a previous PhD student to detect miss-expression/localisation of PIN7::PIN7:GFP in the

root tip. Five day old M2 seedlings were assessed by screening seedlings with a MZ10F (Leica) fluorescent screening microscope to identify plants with altered PIN7::PIN7:GFP expression (Figure 3.2*)*. Then, the phenotype for selected plants that showed the most reliable change in PIN7 was confirmed through confocal microscopy. From M2 screening approximately 169 mutants were identified across the 90 seed pools. Selected mutants were propagated to get M3 and the screening process were performed again to confirm the inheritance of the phenotype. The student then selected ~36 mutant M3 lines for further analysis.

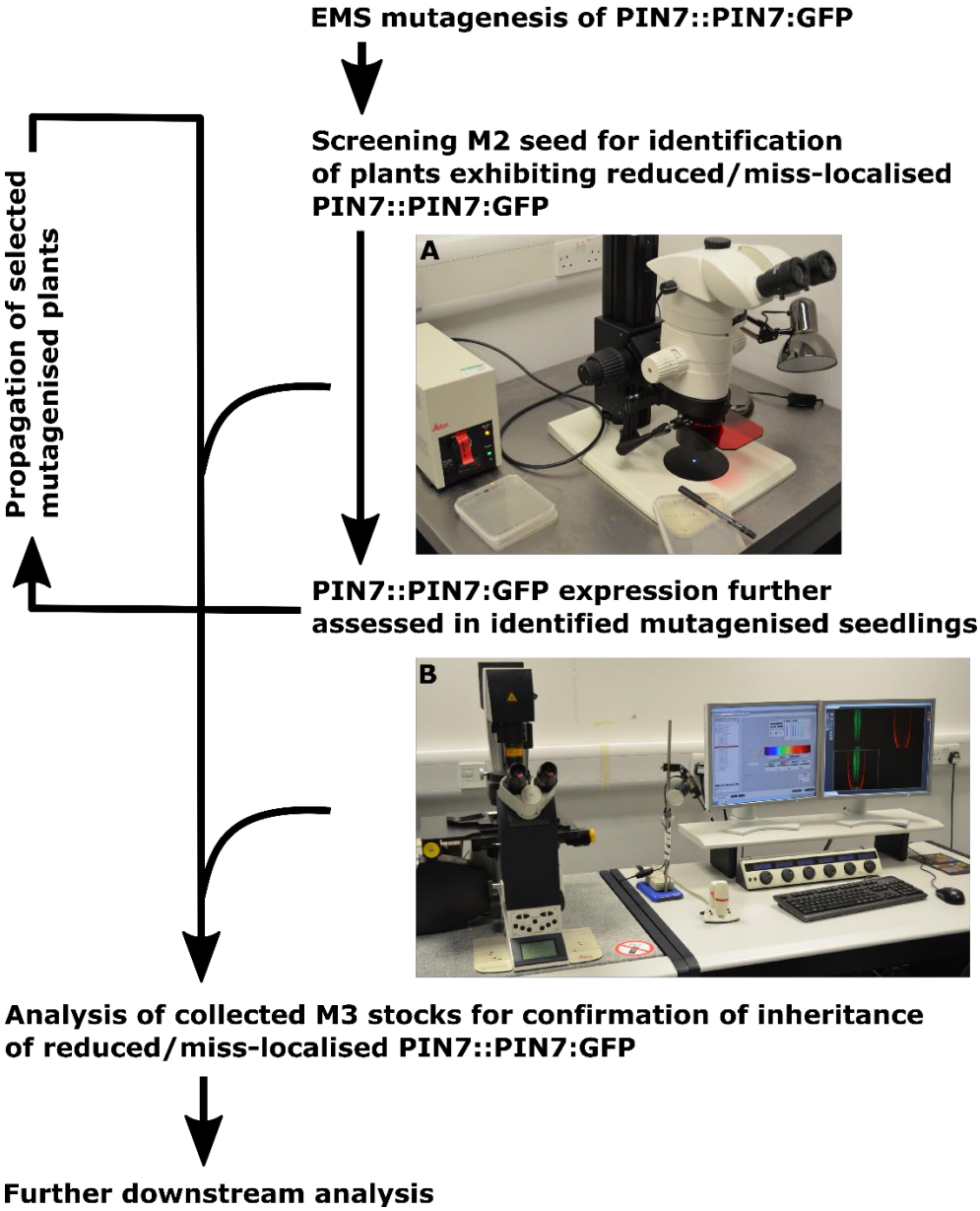

Figure 3.2: Flowchart illustrating the pipeline followed by a previous student to identify mutants caused with altered *PIN7* expression. Image produced by Ben Goodall, 2018.

As previous data supported a model in which the transcriptional control of *PIN7* is important in regulating vascular patterns, and any alterations in PIN7::PIN7:GFP imaged via microscopy may have resulted from either changes in the transcription or post-transcriptional regulation of *PIN7*, therefore the student used qRT-PCR to examine the transcriptional regulation of *PIN7*. He then selected lines with reduced endogenous of *PIN7* compared to Col-0 and *PIN7::PIN7:GFP* controls.

Through this process twelve M3 mutants that reduced *PIN7::PIN7:GFP* were confirmed. Selected homozygous M3 mutants plants were back-crossed to the parental non-mutagenized *PIN7::PIN7:GFP* for mapping-by-sequencing based on a strategy similar to those previously used (Hartwig et al., 2012; James et al., 2013). F2 generations that produced segregating mutant stocks in which only 25% of individuals exhibiting a reduction in PIN7 expression were taken further. This implies that an individual mutation causing decreased PIN7 is a recessive mutation. The EMS mutagenesis process will have generated multiple mutations in the genomes of the selected mutant lines. it was assumed that there is only one mutation per line underlying the PIN7 expression phenotype. In this case, only lines with the causative mutation will have 100% varied (mutagenic) read frequency compared to the reference genome in a back-crossed segregating population in which the reduced PIN7 phenotype is actively selected for, since all others are randomly selected out of segregation. Through this process 11 lines were sequenced via whole genome sequencing, and candidate genes were selected based on having a variant frequency of polymorphisms relate to Col-0 above 0.85. This process resulted in between 1-10 polymorphisms being identified within each line.

3.4 56B2 mutant

This shortlist of genes was then narrowed down based on expression of genes within the eFP Browser based on high resolution spatiotemporal map (Brady et al., 2007). This reduced the number of candidates. The original concept behind the screen was to identify either transcription factors or proteins with DNA binding properties. Although there were interesting candidates with diverse roles including defence, cell membrane composition, transport and ubiquitination, it was not immediately apparent how many of these would act as mediate the transcription of *PIN7*. One candidate that stood out was a mutation upstream of *CKX5* that was identified in the mutant named 56B2. This mutant had reduced levels of *PIN7*, with a PIN7 expression pattern resembling that of lines with low cytokinin signalling (Figure 3.3).

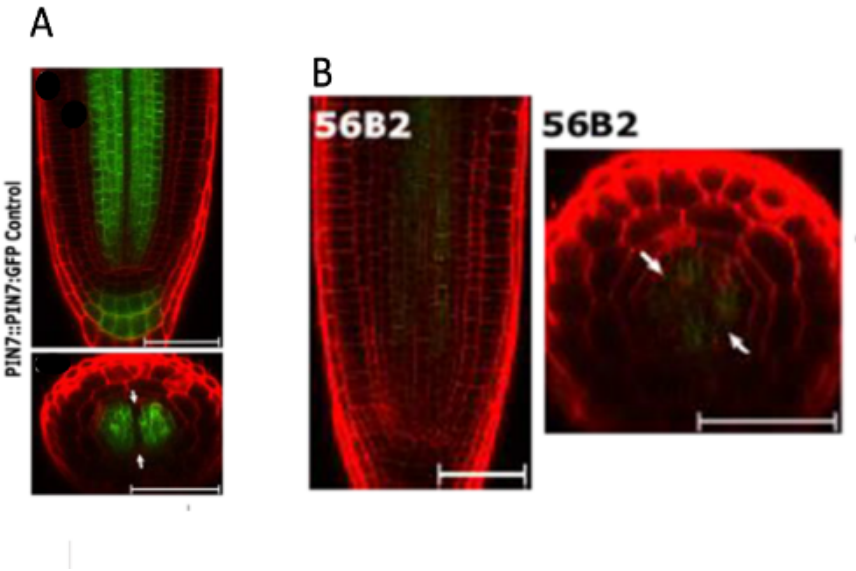

Figure 3.3: Expression of PIN7::PIN7:GFP is dramatically reduced in the 56B2 mutant.
A) Confocal images of the PIN7::PIN7:GFP control; *PIN7:: PIN7:GFP* showing PIN7 express in the procambium cells flanking xylem axis. B) PIN7::PIN7::GFP in the 56B2 mutant at significantly reduced levels. (Images taken from Goodall, 2018)

CKX5 is a member of cytokinin oxidase/dehydrogenases family of genes which catalyse the degradation of cytokinin (Werner et al. 2001). In *Arabidopsis*, there are 7

members of *CKX* genes (Werner et al., 2003). The level of active cytokinin is reduce by CKX proteins (Bartrina et al., 2011, Werner et al., 2001a). It has been known that the CKX proteins irreversibly cleave cytokinin by oxidative side-chain cleavage (Schmulling et al., 2003), and was known that *PIN7* levels are highly sensitive to cytokinin response in a quantitative way. Whilst *CKX5* was unlikely to be involved in the direct transcriptional regulation of *PIN7*, it was a strong candidate for the causal mutation behind the alterations in PIN7. It was predicted to be expressed in the correct tissue (Figure 3.4). The eFP browser is based on FACS sorted protoplast, and whilst there is congruence between the expression of many genes on the browser within *planta* experiment via *in situ* hybridization, or reporter lines this is not always the case. Therefore, whilst this is given confidence to explore *CKX5* further.

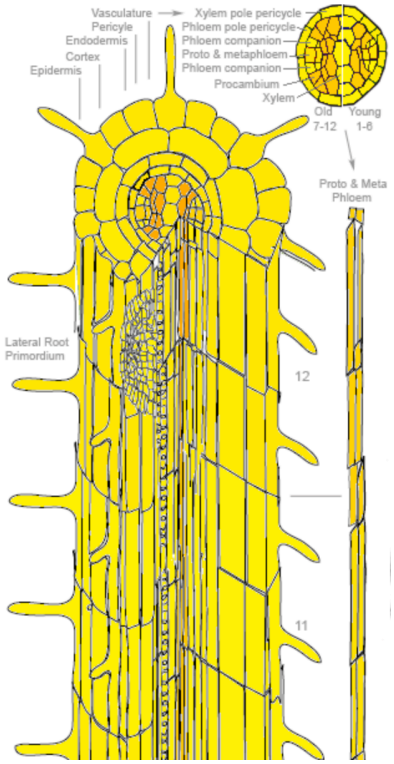

Figure 3.4: The expression profile of CKX5 from eFP Browser.
CKX5 express is expressed in the procambium cells; based on the spatiotemporal profile by Brady et al., 2007.

The 56B2 line contained a mutation in the promotor of *CKX5* on chromosome 1. This mutation resided in a region upstream of the transcriptional start site of *CKX5* in a poly(dA-dT) sequence and involved the substitution of a thymine to a guanine, thus breaking a continual chain of t residues (Figure 3.5).

Figure 3.5: Location of the mutation in the promoter of *CKX5*.

This sequence of AT1G75450 (*CKX5*) illustrated the position of mutation in the promoter on chromosome 1 of *CKX5* highlighted with red circle, where t (highlighted in blue) is substituted to g, the mutation is upstream of the ATG start codon. Start codon and stop codon are highlighted in blue. Primers that flanked the poly (dA-dT) are presented by the arrows and amplified amplicon size at 550bp. Orange sequence are exon, purple are intron, red are UTR.

The location of a mutation within a poly(dA-dT) sequence (also called T-tract) upstream of a gene of interest was interesting, since naturally occurring stretches of poly(dA-dT) sequences have previously been shown to act as upstream promoter elements to control expression; for example, the yeast *his3* gene contains a 17 bp region containing 15 thymine residues and deletion of this indicates it is required for constitutive expression (Struhl, 1985). Similar observations relating to the funerial importance of poly(dA-dT) tracts as upstream promoter elements for wild-type level transcription have also been made for *DED1* and *URA3* genes (Roy et al., 1990, Iyer and Struhl, 1995, Struhl, 1985).

DNA T-tracts are enriched in eukaryotic genomes (including *Arabidopsis*) but not in prokaryotes (Dechering et al., 1998). It is likely that the role of poly(dA-dT) tracts on gene transcription is not due to binding of specific transcription factors, but due to their ability to alter the intrinsic structure of DNA. *In-vitro* analyses have shown that poly(dA-dT) tracts confer an unusual structure on the DNA in which it is more straight and rigid with a shorter helical repeat of 10 bp per turn (Nelson et al., 1987). It was therefore proposed that poly(dA-dT) tracts affect nucleosome stability and enhance binding of transcription factors to nearby sequences (Iyer and Struhl, 1995). This was further supported by research showing that poly(dA-dT) tracts are not folded in nucleosomes (Suter et al., 2000). More recent, *in-vivo* analysis has shown that nucleosomes are strongly depleted from poly(dA-dT) tracts (Yuan et al., 2005, Field et al., 2008). As nucleosomes prevent the DNA enwrapped within them from interacting with other proteins, decreasing nucleosome occupancy will increase accessibility of the DNA within this region. This is likely to affect DNA accessibility over much larger regions (Segal and Widom, 2009). More recent analyses suggest that this mechanistic

causation of nucleosome depletion over poly(dA-dT) traits is more complex. Current data suggests that structural changes will have only a modest role in nucleosome incorporation, with a more active mechanism such as the ATP dependent chromatin remodeler RSC actively displacing nucleosomes away from poly(dA-dT) sequences (Barnes and Korber, 2021).

Whilst the mechanism of poly(dA-dT) tracts in gene transcription is not understood, there is a strong correlation with DNA accessibility. In the 56B2 mutant, in which we see a mutation in a similar sequence, this raises the possibility that this may affect expression of *CKX5*, and through modulation of cytokinin affect transcription of *PIN7*. Therefore, we predict that like in yeast these poly (dA-dT) tracts may function to alter the level of gene transcription – in this case for *CKX5*.

Although the above suggests that that the presence of an intact poly (dA-dT) tract would boost transcription by increasing DNA accessibility, we reasoned that if motifs around the poly (dA-dT) site were involved in transcriptional repression this could result in the opposite effect. In this scenario, increased *CKX5* activity would result in lower cytokinin levels and be compatible with the decrease in PIN7. To test this, a qRT-PCR was performed to measure the levels of *CKX5* mRNA in 56B2 versus wild-type.

The level of *CKX5* mRNA in root tips of 56B2 and WT was measured for 3 biological replicates. RNA was extracted from 7 days old seedling by excising 2mm roots tip from 30 plants for each biological replicates. The cDNA was synthesised, and qRT-PCR performed using primers specific to *CKX5* and the housekeeping gene UBC. These

experiments demonstrated that there was a significant increase in *CKX5* mRNA in the 56B2 line (Figure 3.6) [See Footnote 1].

This is compatible with our hypothesis that decreased cytoknin levels were responsible for the alteration in *PIN7* expression seen in 56B2. Furthermore, the fundamental understanding of the role of poly (dA-dT) tracts in plants is very limited and this appeared to provide an elegant example of how such a system could modulate gene expression in *Arabidopsis*.

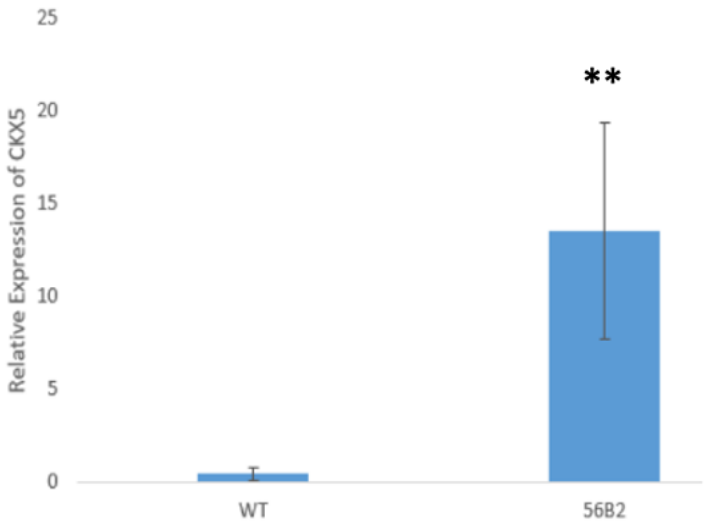

Figure 3.6: *CKX5* mRNA is significantly higher in 56B2 compared with Col-0.
The level of *CKX5* mRNA is measured in the root tip of 56B2 and wild-type by qRT-PCR. 2mm of root tips was excised from 30 seedling (7 days old) to extract the RNA for each biological replicates. Student T-test reveal that significant difference between Col-0 and 56B2 in the level of CKX5 transcription. **=P ≤0.01. Error bars=SD.

[1] Footnote. At the time of the experiment these results led me to pursue the idea that *CKX5* levels were increased in the 56B2 mutant. Later results in this thesis, encouraged me to challenge this and the experiment was repeated later. This gave a different result in which there was little change in *CKX5* levels between 56B2 and wild-type.

3.5 Discussion

This project aims to explore factors mediating the crosstalk between cytokinin and PIN7. Since this has previously been shown to be one half of a key regulatory network controlling vascular pattern (Bishopp et al., 2011). Previous data had shown that cytokinin promotes the transcription of *PIN7* and that this was likely to be via an indirect mechanism. To better resolve the kinetics of this the expression of the *PIN7::PIN7:GFP* translational marker was followed after induction with cytokinin. The results were similar to those previously observed in that after 12h of cytokinin treatment, it was observed that PIN7 was present throughout the root including the xylem axis. The experiment was included additional timepoints (3, 6 and 9 hours) and no changes of PIN7 expression was observed within these times. These finding agrees with a previous study which showed that cytokinin enhance the expression of *PIN7* indirectly (Bishopp et al., 2011). However, findings were obtained from this project extend these by including a greater number of timepoints. These data suggest a very indirect regulation, that could potentially involve the many intermediate components.

There are several potential ways to identify factors downstream of cytokinin that may regulate *PIN7*. These include using a transcriptomic approach to identify factors downstream of cytokinin, using a yeast one hybrid approach to identify factors that bind to the *PIN7* promoter, and identifying mutants with altered *PIN7* expression. Whilst there is considerable value in performing experiments such as these in parallel, it was decided to focus on the candidate genes produced by a mutagenesis screen as this had already been performed in the lab and the material was ready to go.

Here, an EMS mutation screen was previously conducted to identify novel factors regulate *PIN7* expression. In total, twelve mutants had been sequenced, and candidates identified in genes potentially affecting *PIN7* transcription. From the polymorphisms observed, there were no mutations in genes associated with transcriptional activity. In addition, for many genes it was not immediately apparent about how related to *PIN7* transcription. However, one of the strongest candidates was in the 56B2 line and was found in the promoter of the *CKX5* gene. It was reasoned that this would be a good place to focus, as there was a strong link with cytokinin and therefore this was considered to be good candidate.

Given the role of the CKX proteins, it seemed feasible that enhanced expression of CKX5 would reduce the levels of cytokinin within the root. Given that, it is well documented that the transcription of *PIN7* is cytokinin-inducible (Bishopp et al., 2011); it was predicted that plants with reduced levels of cytokinin would result in lower levels of *PIN7* level, similar to how the original 56B2 line was screened. To explore this hypothesis, qRT-PCR was performed in wild-type versus 56B2 and observed that the *CKX5* mRNA was increased relative to wild-type. Therefore, the phenotype of 56B2 will be study to attempt to understand the mutation and the affect that might overexpression of CKX5 cause in the root and shoot in next chapter (4). It is essential to be mindful of the fact that 56B2 was proposed to be an overexpression mutation so it could not be complemented by adding a version of the gene under its own promoter. Instead, it could be analysed by either expression of a 56B2- like CKX5 construct in WT, or knock out of *CKX5* in 56B2, which will be discussed in chapter 6.

Some of the other candidates identified within the screen that have not been associated with either *PIN7* or cytokinin may provide novel mechanistic insights and identify the role of new components in vascular patterning. However, it was thought

that *CKX5* represents a good starting point with which to pursue other targets. This is because *CKX5* is known to modulate cytokinin levels, is expressed in the procambial tissues and reducing cytokinin signalling in these cells would have an effect on *PIN7* transcription. This works will therefore improve our understanding of the tissue-specific homeostasis of cytokinin. Therefore, initially it was decided to investigate *CKX5* then move to other interesting and novel candidates that regulators *PIN7* transcription.

Chapter 4: Characterising the phenotype of 56B2

4.1 Overview

The previous chapter illustrated that mutation 56B2 induced by EMS mutagenesis was found to reduce the expression of *PIN7::PIN7:GFP* in the root tip. The strongest candidate for mutation 56B2 is in the promoter of *CKX5* in the poly (dA-dT) tract. This mutation led to overexpression of *CKX5,* a member of cytokinin oxidase/dehydrogenases family of genes which catalyse the degradation of cytokinin (Werner et al. 2001). These enzymes play a vital role to control cytokinin level in plant tissues. Previous research showed that elevated *CKX* levels reduced the endogenous levels of cytokinin, which in turn restricted growth of the shoot and promoted growth of the root (Werner et al., 2003). The formation of new rosette leaves was delayed, and leaf expansion was reduced in *35S:AtCKX1* and *35S:AtCKX3* transgenic plants. In terms of reproductive development, the onset of flowering was delayed in transgenic *CKX1* and *CKX3* lines (Werner et al., 2003). Moreover, transgenic plants siliques produce less seeds than wild type. However, the root length in transgenic plants over-expressing *CKX1* and *CKX3* was greater than wild type, and the formation of lateral root enhanced (Werner et al., 2003). Bartrina et al, (2011) investigated the function of *CKXs* genes by studying *ckx3-1 ckx5-2* double mutant, which abolished the expression of the respective genes. It was reported that the levels of the biologically active trans-zeatin and trans-zeatin riboside were higher in inflorescences of *ckx3 ckx5* mutants compared with the wild type. *ckx3 ckx5* mutants form larger inflorescence meristems owing to the increase in the number of meristematic cells. They found that the *ckx3 ckx5* mutant produced significantly more flowers and siliques than the wild type. In addition, the total seed yield of *ckx3 ckx5* mutants was found to be increased by 55% compared with the wild type (Bartrina et al, 2011).

Given the role of the CKX proteins, it seems highly feasible that overexpression of *CKX5* would reduce the levels of cytokinin within the root. Given that, it is well documented that the transcription of *PIN7* is cytokinin-inducible (Bishopp et al., 2011); we would predict that plants with reduced levels of cytokinin would result in lower levels of PIN7 expression, similar to how the original 56B2 line was screened.

In addition to regulating *PIN7*, cytokinins regulate many aspects of plant growth and development such as root growth, maintenance of apical dominance and leaf senescence (Mok and Mok, 1994). Given the diverse roles for *CKXs* in general and *CKX5* in particular, It was reasoned that over-expression of this gene would not only affect *PIN7* expression but may affect other developmental genes. In order to explore this possibility, phenotypes were studied relating to both shoot and root development in 56B2. In particular, phenotypes related to cytokinin were selected, as this would further explore the relationship between the 56B2 mutant and the most likely underlying candidate gene, *CKX5*.

4-2 Root phenotyping in 56B2

Roots are crucial for the plant as they are responsible for absorbing water and nutrients, anchorage of the plant body, and storage of nutrients (Takatsuka and Umeda, 2014). Roots system comprise of two types of roots: the primary root and secondary roots, such as lateral root.

The root meristem in *Arabidopsis* is an excellent system to study how the balance between cell division and differentiation is crucial for organ size and development.

Therefore, various traits for root development and growth were investigated in the 56B2 line.

4-2-1 The 56B2 mutant shows similar root growth to wild-type

As both auxin and cytokinin control many root traits including root length (Skoog and Miller, 1957), the root length in a simple mutant was compared versus wild-type in this experiment. Previous analyses have shown that plants with lower levels of cytokinin have increased root length; for example, reduced cytokinin levels by overexpression of *CKX* family genes increased the root length (Werner et al., 2003). This study over-expressed four *CKXs; CKX1, CKX2, CKX3* and *CKX4*. Although they did not specifically look at *CKX5,* the results for over-expression of each of these CKXs showed increased root growth. It would seem reasonable to predict that over-expression of *CKX5* may produce a similar result. For some of the lines the increase in root length was modest, but for others it was increased by 50 to 90%.

To examine the length of the primary root in 56B2 compared with WT, plants were grown on vertical 0.5x MS plates under 16h days. To minimize plate-to-plate variation, both mutant and wild type were grown on the same plate. In this experimental set up, it had three plates with one row of wild-type at the top and one row of 56B2 at the bottom. Plates were kept vertically in the growth chamber, and the root lengths were imaged at 3, 6, 9 and 12 days using the imaging robot. The length of primary roots was measured using RootNav software (Pound et al., 2013).

There was no significant change in total root length between 56B2 and Col-0 under my growth conditions (Figure 4.1). However, these measurements of root length reflect both cell division (i.e., meristematic activity) and root elongation. Therefore, to explore this more thoroughly, other ways of measuring growth were explored.

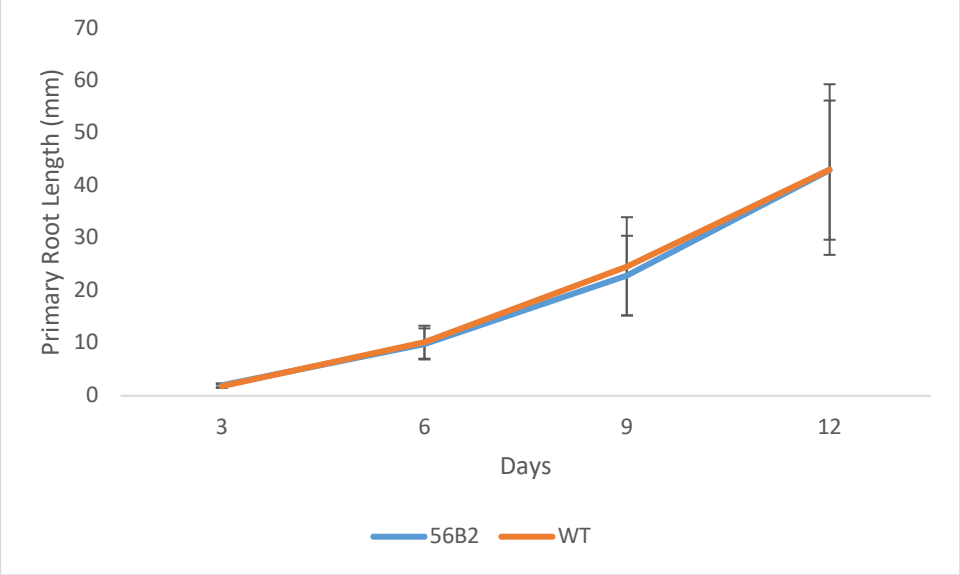

Figure 4.1: Primary root length is unaltered in 56B2.

The primary root length of 3, 6, 9 and 12 days old seedlings for 56B2 and WT (Col-0) were measured for 12 roots using RootNav software. Plants were grown vertically on 0.5x MS agar plants under long day conditions. A students' t-test confirms no significant difference in means of the two samples. Error bars are SD, n=12 roots.

4-2-2 The 56B2 mutant has a similar meristem size to wild-type

The production of new cells, their differentiation, and elongation determine the root growth (Růžička et al., 2009). New cells are generated in a zone of active division, termed the meristem. Elongation occurs in the elongation zone, and finally cells reach maturity in the meristem zone (Dolan et al., 1993). The phytohormone cytokinin regulates the root meristem activity by controlling the balance between cell division and elongation. Published studies showed that increasing the cytokinin level by exogenous treatment results in a reduction of the root meristem size and therefore reduces root growth (Ioio et al., 2007). This Ioio et al. (2007) study followed the development of the root meristem in different *Arabidopsis* ecotypes (Col-0 & Ws) upon application of different exogenous cytokinins and cytokinin concentrations (0.1 µM dihydrozeatin, 1 µM kinetin, 0.1 µM 6-benzylaminopurine and 0.02 µM transzeatin). In

untreated plants, after five days germination meristem reaches its final size and does not increase further, when a fixed number of about 30 cells is established in the meristem as the rate of cell division. At this stage the rate of cell division is equal to the rate at which cells enter the elongation-differentiation zone (Ioio et al., 2007). In plants treated with exogenous cytokinin, the meristem size was decreased (Ioio et al., 2007). The point at which different cell types start to elongate alters with respect to distance from the QC. Because of this, cortical cells are commonly used to define the meristem. The size of the meristem can therefore be measured either as the total number of cells were counted immediately above the QC up until to the first cortex cell becomes elongated, or as a distance (in μm) for the same space. Additional information links cytokinin to root meristem size, as reducing the cytokinin level by overexpressing CYTOKININ OXIDASE/DEHYDROGENASE (*CKX*) results in plants with longer root meristems (Werner et al., 2003). This study shows that there is a greater primary root length of *35S:AtCKX1* seedlings than that of the wild type. In this study, the authors used a different method for determining meristem size, in which they visualised the domain in which the division marker CycB1: GUS was present. These data suggest that the growth in *35S:AtCKX1* roots is enhanced because of the increasing number of dividing cells in the RAM (Werner et al., 2003).

To explore whether there is any alteration in the size of the root apical meristem, the root meristem in 56B2 and Col-0 was measured. Plants were grown on vertical 0.5x MS plants under 16h days. To measure the meristem size in these lines, five-day old seedlings (12 replicates for each line) were stained with propidium iodide to visualise the plasma membrane and imaged them on SP5 confocal microscope. Then, the number of cortical cells were counted from start of the division zone (just above the

QC) until the first cell in the elongation zone. The start of the elongation zone was defined as the first cortical cell that was longer than it was wide.

The size of the root apical meristem of 56B2 was found to be similar to that of Col-0 (Figure 4.2). In both cases, the average number of cortical cells in the meristem zone was found to be between 26 and 27 cells. Previous research showed that cytokinins control meristem size by acting in a restricted region of the root meristem (transition zone TZ), which is the border between division and elongation zones, and shifting the position of transition zone (TZ), by controlling the rate of meristematic cell differentiation. It was known that increasing levels of *CKX1* results in increased meristem size (Ioio et al., 2007). Collectively both these assays show that the 56B2 mutant does not have an observable effect on cell division or root growth under the conditions of my experiment. This maybe because the level of cytokinin in 56B2 is not as low as in the other *CKX* over expressing lines, it could be that the 56B2 line shows alterations in cytokinin levels in different tissues, or it could be that *CKX5* binds and degrades different cytokinin isoforms to the main ones that regulate root size.

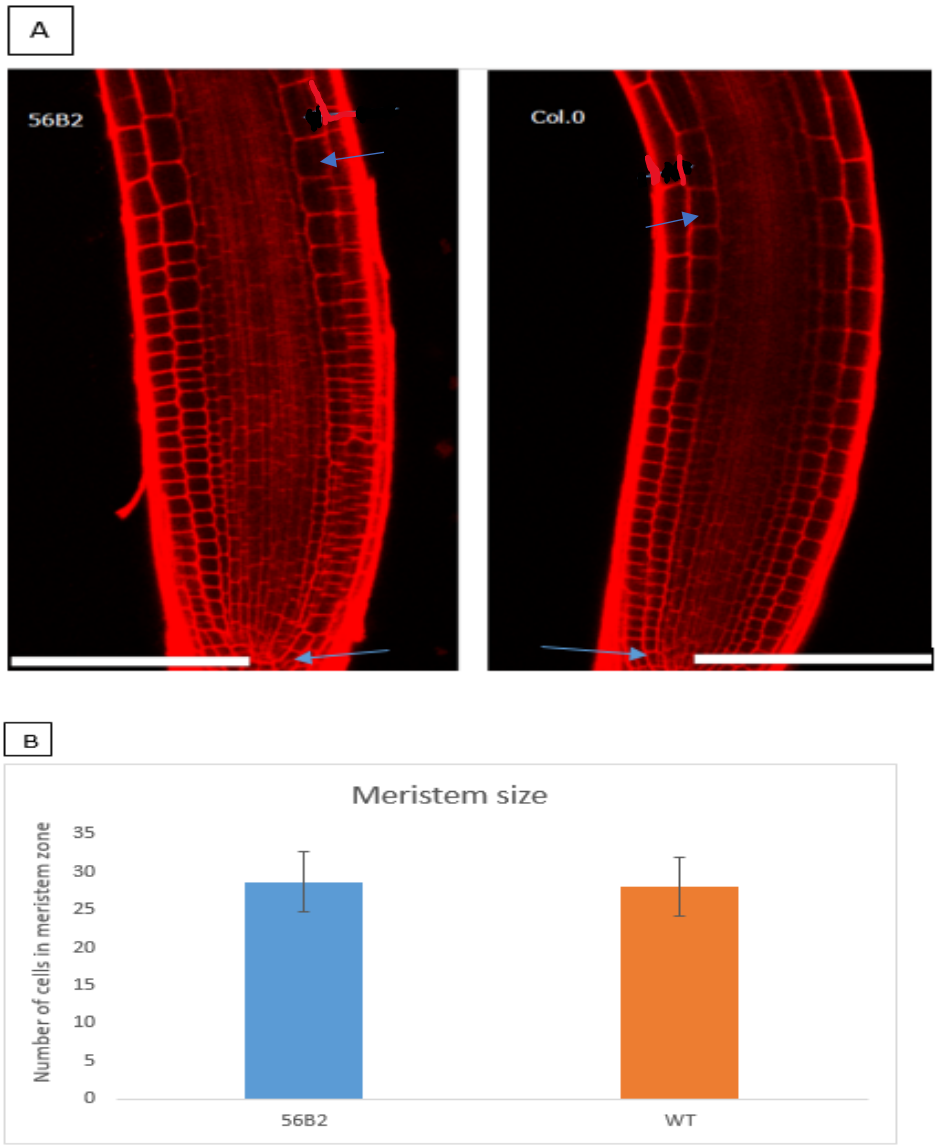

Figure 4.2: Meristem size is unaltered in 56B2.

The meristem size of 56B2 compared to WT (Col-0). Meristem size was determined by counting the number of cortical cells in the division zone, with the elongation zone defined as starting at the first cortical cell that was longer than it was wide (A). Twelve roots for each line were imaged using confocal microscopy (SP5) after staining the plasma membranes with propidium iodide. B) The number of cortex cells in the meristem zone are similar in 56B2 and WT. A students' T-test was used and there was no significant difference between the mean values, Error bars represent SD, n=12. Arrows indicate the first cell above QC and first cortical cells in the elongation zone.

4-2-3 The 56B2 mutant shows an increase lateral root density.

Lateral root branching help plants to explore the soil to obtain water and nutrients. Lateral root formation and development has been well studied in *A*. *thaliana*. It has been known for decades that cytokinin inhibits the formation of lateral roots (Böttger, 1974). Studies reported that reduced the level of cytokinin by overexpression the gene encoding the cytokinin-degrading enzyme cytokinin oxidase (*CKX*), enhances root branching (Werner et al., 2003). Furthermore, loss-of-function cytokinin receptor, *ahk2 ahk3* double mutants exhibit increased root branching (Riefler et al., 2006) . In addition, lateral root density is strongly increased in the double and triple mutants *ipt3 5*, *ipt3 7*, and *ipt3 5 7* (Chang et al., 2013). It was found that cytokinin promotes the degradation of PIN proteins and modulates the trafficking of polar auxin transport during lateral root organogenesis (Marhavý et al., 2011, Marhavý et al., 2014). These results indicate that cytokinin deficiency enhances lateral root initiation and development.

To explore whether the 56B2 mutant resulted in differential formation of lateral roots, the number of emerged lateral roots in 56B2 was quantified and compared these to WT and calculated lateral root density by counting the emerged lateral roots, then divided by the primary root length. This experiment was conducted twice.

The first time this experiment was performed, the lateral root density for 12 roots of 56B2 and Col-0 were quantified for plants that were 12 days old. In this experiment, a greater number of emerged lateral roots in 56B2 was observed. To test whether this result was statistically significant, a students' t-test was performed. Although there was no statistically significant difference between lateral root densities in 56B2 and Col-0

in the first experiment (figure 4.3 A), this difference encouraged to repeat the experiment with a greater number of replicates. In the second time of this experiment, the number of replicates were increased to 27 roots for both mutant and wild-type samples there was a significant difference between 56B2 and Col-0 (figure 4.3 B). This observation is in similar to that seen in other lines in which cytokinin levels have been altered, such as the results discussed earlier by Werner et al, (2003) which showed that transgenic plants overexpressing *CKX1* and *CKX3* promoted the lateral root formation.

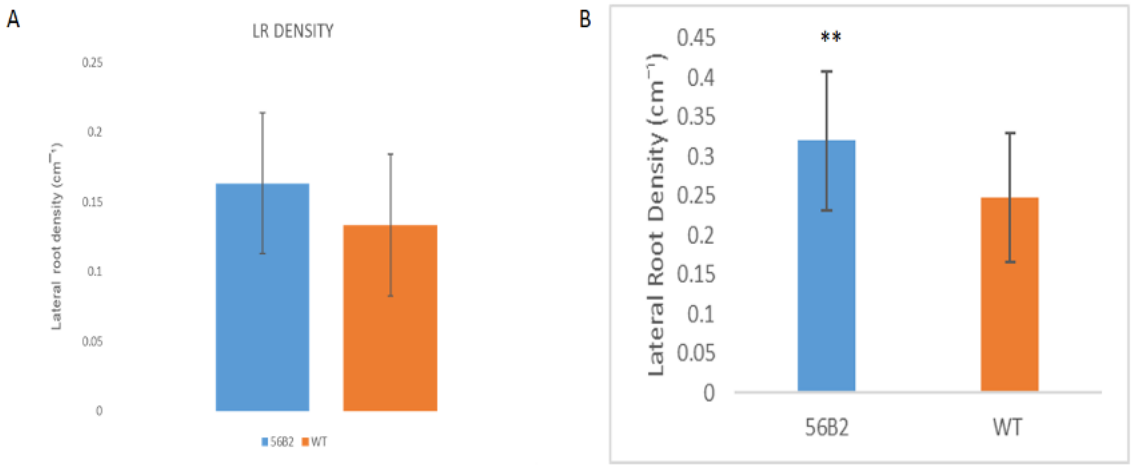

Figure 4.3: Lateral root emergence is enhanced in 56B2.

Emerged lateral roots were counted and compared to primary root length. A) Twelve replicates were used for each sample. A T.test demonstrates that there are no statistical differences between the means for both samples. B) The experiment repeated with 27 replicates for each sample. A T.test validates that there is a significant difference between 56B2 and Col-0. C) 56B2 and Col-0 seedling at 12 days old grown on 0.5 MS. Error bars represent SD. **= $p \leq 0.01$. n=12.

4-2-4 The 56B2 mutant is more resistant to exogenous cytokinin than WT.

The previous results suggest a role for *CKX5* in regulating lateral root formation, but do not show an effect of *CKX5* on the growth of the primary root. This is not in line with the fact that the original 56B2 mutant was identified due to alterations in the level of *PIN7* in the primary root; therefore, it would be expected that if the changes in *PIN7* are due to elevated expression of *CKX5*, then we should also see differences in other aspects of primary root growth. As well as being necessary for root growth, it has been found that the application of exogenous cytokinin has a strong effect on root size by decreasing the number of dividing cells and the size of the meristem rather than by reducing the rate of cell division (Beemster and Baskin, 2000). There have been a number of cases where mutants affecting cytokinin levels and/or signalling do not exhibit a phenotype comparing to the WT but are more resistant or sensitive to low/moderate levels of exogenous cytokinin. For example, there is little difference in the elongation in root elongation between wild-type and that of mutants in the cytokinin receptor CRE1 under normal or low levels of cytokinin (Higuchi et al., 2004). However, at higher levels – such as 100 or even 1000 ng/ml 6-benzyladenine (BA) – there is a marked reduction in the sensitivity to cytokinin (Higuchi et al., 2004).

Therefore, It can be reasoned that by studying the response to exogenous cytokinins, subtle phenotypes masked by measuring just root length alone might be tease out. To investigate the effect that cytokinins had on supressing root length for 56B2, the root length experiments were repeated this time for plants that were grown in medium supplemented with different concentration of cytokinin. After cooling 0.5xMS medium, the appropriate amount of cytokinin (BA) was added to make the final concentration

(25, 50, and 100 nM). As cytokinin was dissolved in DMSO, this was added to the no cytokinin control. Sterilised seeds were sown onto plates and kept vertically under 16 h days in the growth chamber. As before, wild type and mutant seeds were grown on the same plate. In the experiment set up, 4 plates for each concentration had been prepared; two plates with one row of WT at the top and one row of 56B2 at the bottom, and two plates have 56B2 in the top and WT in the bottom. This removed any positional bias, if for example plants at the bottom of the plate were further away from the lights.

Plates were imaged at 3, 6, 9 and 12 days and the root length were measured using RootNav software (Pound et al., 2013). The experiment was performed twice to increase the number of replicates. In the first replicate, twelve seedlings were analysed, and it was found that 56B2 plants were more resistant to cytokinin, but the differences were subtle. However, when this was examined more closely using a students' T-test only a few of the data points were considered statistically significant. There was, however, a significant difference in the primary root length at 6 days in 25nm cytokinin between 56B2 and WT (Figure 4.4 A).

The experiment was repeated in the same condition but increased the number of replicates, it was performed with 25 plants. This time, it was found that statistically significant difference in 50nM cytokinin at 6, 9 and 12-days old seedlings and in 25nM cytokinin in 9 and 12-days old plants. For example, at 25 and 50 nM BA 56B2 roots are 2 mm longer than Col-0 at days 9 and 12 (Figure 4.4 C). Moreover, the primary root length of 12 days old seedling of 56B2 had a significant difference comparing to WT (Col-0) in 100nM CK (Figure 4.4 C), as 56B2 roots are about 1 mm longer than Col-0 roots.

Collectively these results show that 56B2 seedlings were more resistant to exogenous cytokinin over a wide range of concentrations. There is significant reduction in the sensitivity of cytokinin at the later time periods, after 9 or 12 days (Figure 4.4C). 56B2 roots at 6, 9 and 12 days old significantly resistant to 50nM of cytokinin compared to Col-0, as 56B2 roots are 2 mm longer than Col-0 at days 9 and 12 (Figure 4.4 C). Moreover, at high concentration of cytokinin (100nM) 56B2 more tolerance than Col-0 at 12 days old seedlings (Figure 4.4 C). These results are consistent with the hypothesis that the phenotypes associated with 56B2 are due to it being an over-expressor of *CKX*. Elevated levels of *CKX* may deplete the pool of exogenous cytokinin and therefore we could expect plants to be more resistant to cytokinin application. It is also worth noting, that even though the number of replicates were increased for the control plants without cytokinin, there was no observable change in root length between 56B2 and Col-0.

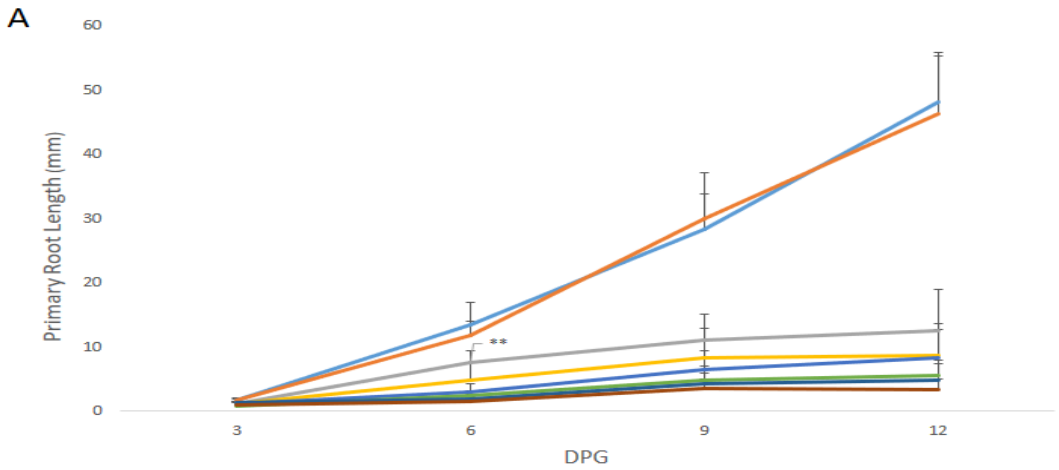

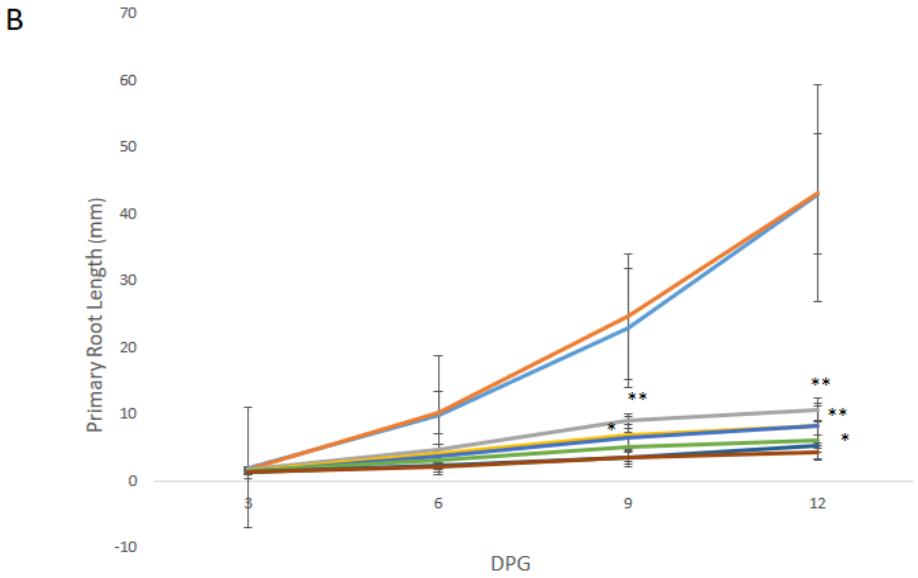

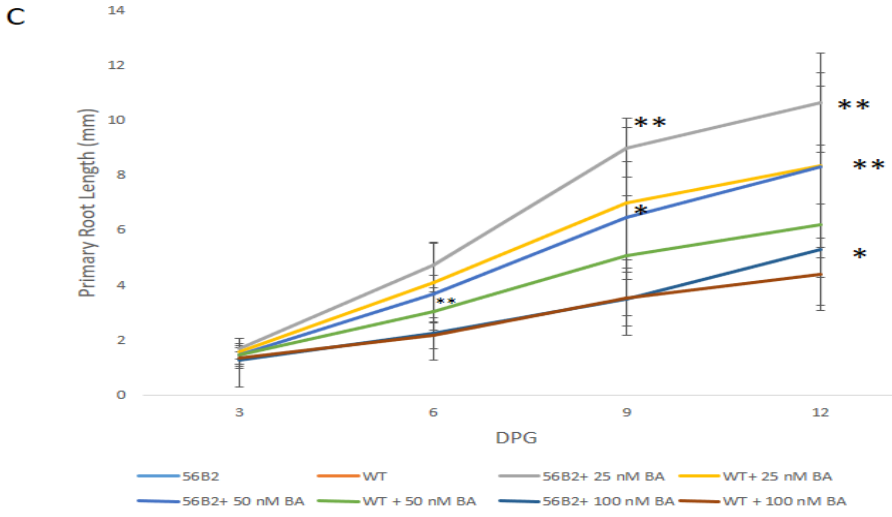

Figure 4,4: 56B2 is resistant to exogenous cytokinin with respect to root elongation.
56B2 and Col-0 seedlings were grown with different concentration of cytokinin (25 nM BA, 50 nM BA, and 100 nM BA) for 3, 6, 9 and 12 days. The experiment was performed twice (panels A and B), with each experiment showing similar results. In the first experiment (A) only 12 roots were used, n=12. This number of replicates was increased to 25 in the second experiment (B). A students' T-test comparing growth in Col-0 versus 56B2 showed only a statistically significant difference in growth at 6 days old in 25nM in experiment A. Increasing the sample size to 25 increased the statistical power and a Students' T-test subsequently showed difference between the means of 56B2 and Col-0 in 25 nM,50nm and 100 nM BA at 6, 9 and 12 days old. Due to large differences in root length, graph B was re-scaled to show only the cytokinin treatments and the same data is shown in graph C. These statistics are summarised in the table below. **=p≤0.01, *=p≤0.05. Error Bars=SD. n=12 (in A), n=25 (B).

4-2-5 56B2 has a similar vascular pattern to wild-type

The vascular pattern of *Arabidopsis* consists of a single xylem axis flanked by two phloem poles and procambium. The xylem axis contains two types of cells: protoxylem at the outer and metaxylem cells in the centre. Cytokinin inhibit the differentiation of procambium to protoxylem (Yokoyama et al., 2007). Previous study reveal that plants that reduced the cytokinin level by overexpression of *CKX2* decreased the number of cells in the vascular bundle and all vascular cells specified as protoxylem (Werner et al., 2001b).

To explore whether 56B2 had a vascular phenotype, both 56B2 and Col-0 seeds were grown after sterilization on 0.5xMS plates. After 5 days germination the seedlings were transferred into slides and chloral hydrate was added to clarify tissues. After 24h, the xylem was visualized for 20 seedlings for 56B2 and Col-0 using a microscope.

there were not any differences observed in xylem pattern between 56B2 and WT (Figure 4.5). It was particularly focused on the protoxylem phenotype as either gaps in protoxylem or ectopic protoxylem files had been reported for cytokinin signalling mutants.

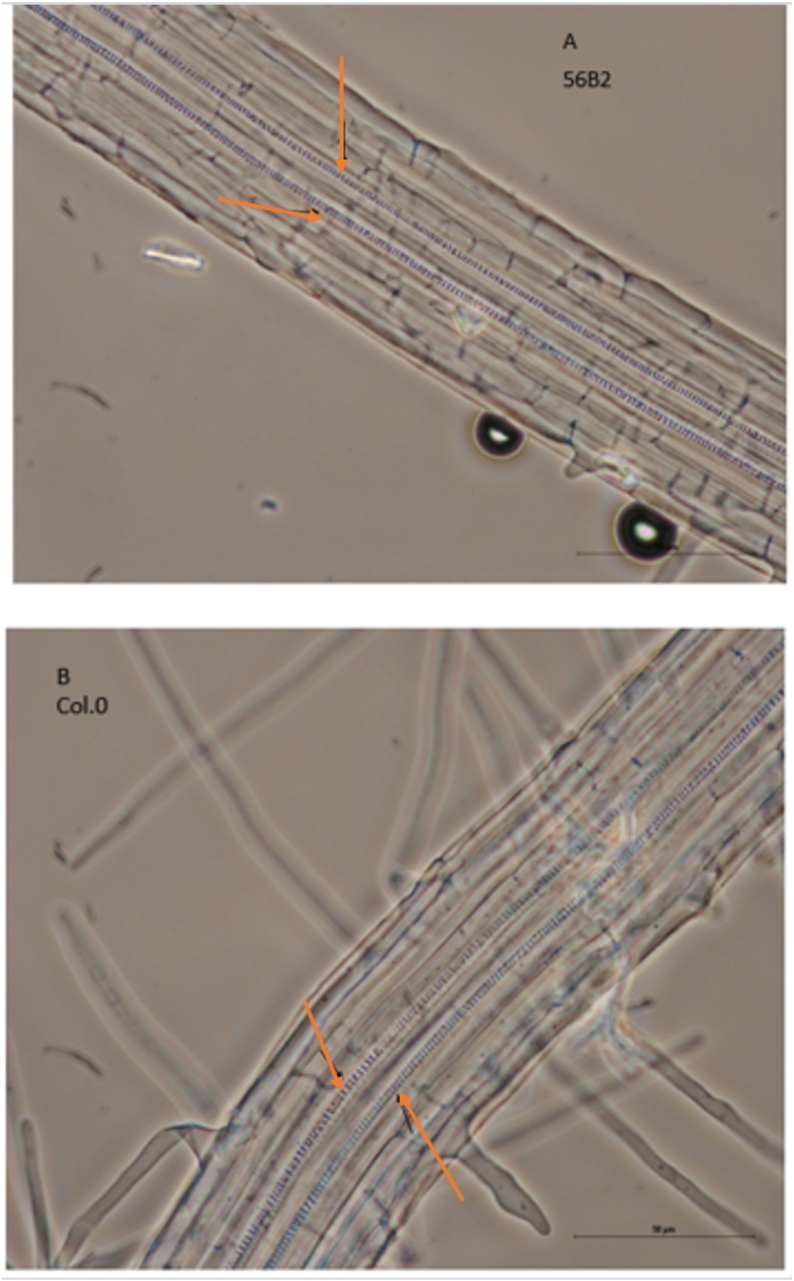

Figure 4.5: 56B2 has similar continuity of protoxylem files as Col-0.

20 roots of 5 days old seedlings visualized under the microscope to investigate the xylem in 56B2 (A) and Col-0 (B). Here, the protoxylem was visualised. No breaks or additional protoxylem files were observed in any of 20 wild-type or 20 56B2 mutant plants. Arrows show protoxylem files. Scale bar=50 μm. n=20.

4-3 56B2 shows altered shoot development.

The previous sections (4-2) examined the phenotypes of 56B2 in the root and attempted to link these to cytokinin, as qRT-PCR had revealed that *CKX5* was elevated in root meristems in this line. Although it is not known whether this mutant shows elevated *CKX5* in shoots, it is well known that cytokinin regulate multiple aspects of shoot development. Cytokinin is a negative regulator of root growth and lateral root formation, whereas it promotes the activity of shoot apical meristem. Published data reveal retardation in the shoot development when cytokinin level is decreased, for example the size and activity of the shoot apical meristem is decreased when cytokinin levels are reduced by overexpression of *CKX* family genes (Werner et al., 2003). Specifically, these in these lines the formation of new rosette leaves is delayed, and the size of leaves is reduced. Also, compared with wild-type, *35S:AtCKX1* and *35S:AtCKX3* show delayed onset of flowering by up to 5 weeks, contained more axillary branches, but formed thin inflorescence stems containing very few flowers (Werner et al., 2003).

In addition, it is known that modulating cytokinin levels in the root can affect development in the shoot. For example, grafting wild-type stocks onto cytokinin deficient scions can rescue many of the cytokinin-related phenotypes in the shoot (Matsumoto-Kitano et al., 2008). Therefore, even if *CKX5* was not expressed at elevated levels in the shoot, there may still be phenotypes visible in the shoot due to alterations of cytokinin levels in the roots. Therefore, shoot phenotypes associated with 56B2 also was considered. It had been chosen to study traits such as leaf area, number of primary inflorescence stems, number of secondary stems, number of branches on the secondary stem and number of siliques on the main inflorescence

because they easily visualize. This would allow me to explore whether the activity of shoot meristem and reproductive development is affected in 56B2.

4-3-1 Effect of 56B2 on leaf development

The number and size of cells in the leaf determined the leaf size, and are determined by two biological processes: cell division and cell expansion (Donnelly et al., 1999). Moreover, leaf size is affected indirectly by the time of the transition between cell division and cell expansion (Gonzalez et al., 2012). Auxin allows cells to enter the cell cycle (Stals & Inze, 2001), while cytokinin delays the onset of cell expansion and differentiation to extend the period of cell division (Wu et al., 2021). As cytokinin stimulates cell expansion, plants treated with cytokinin often produce larger leaves (Skalák et al., 2019, Efroni et al., 2013). Degradation the cytokinins by upregulation of *CKX3* brought the onset of cell expansion forward (Skalák et al., 2019). Conversely, plants that are affected in cytokinin signalling (such as the *crf1,2,5* triple mutant) show highly reduced cotyledon sizes (Rashotte et al., 2006).

Although there are several ways to visualise the activity of the shoot meristem
In the first instance, leaf number was followed as more active meristems are likely to produce more leaves. The leaf number was performed by counting the leaves for 5 plants of 56B2 and Col-0 after 25 days germination. Figure (4.6 A) shows that there are more rosette leaves in 56B2 than Col-0. The average number of rosette leaves for each plant in 56B2 is 14 ±1.17, compared with 12 ±2.1 leaves in wild type. The T-test showed no significant difference. However, the number of replicates is very low, and this may mask subtle differences between 56B2 and Col-0.

At the same time, leaf area was considered due to the role that cytokinin plays in regulating leaf size. The leaf area in 56B2 and Col-0 was measured using ImageJ by

harvesting the rosettes leaves for five plants of 56B2 and Col-0 after 25 days germination. Plants were grown in soil under long day conditions (16h days). There was not a statistically significant difference in the leaf area between 56B2 and Col-0 (Figure 4.6 B). The first leaves for all plants of Col-0 comparing with first leaves in all 5 plants of 56B2, the same for all leaves, then the average and SD was calculated and T.test was performed.

The data from this experiment indicates a change in the leaf number as 56B2 produced more leaves comparing to Col-0. This could be investigated further by increasing the number of replicates from 5 plants to 20 plants that would increase the statistical power which may be enough to determine whether this is due to the phenotypic difference between these two genotypes.

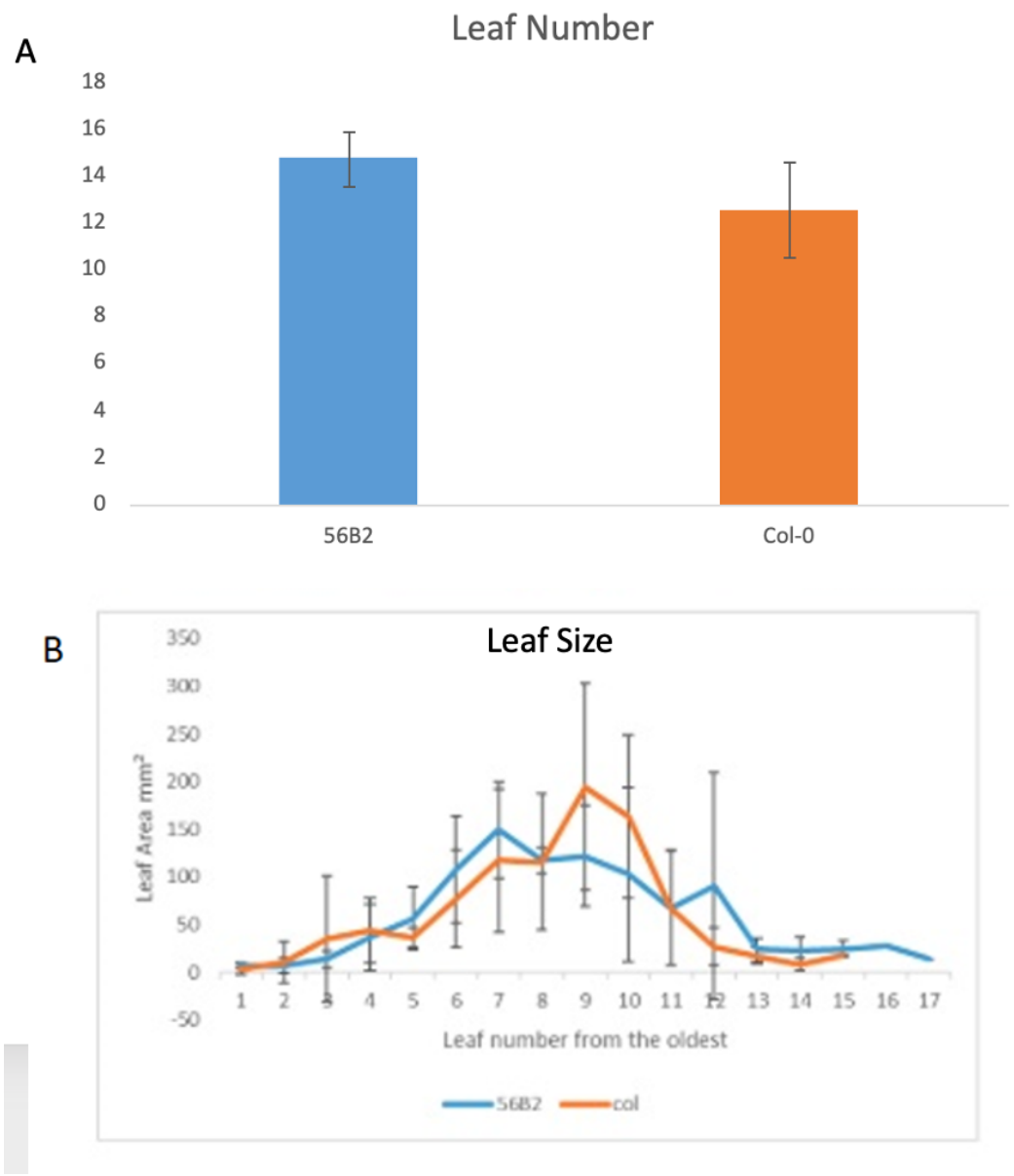

Figure 4.6: 56B2 has greater leaves than Col-0 but no significant difference in the leaf area between them. Rosettes were harvested 25 days after germination. Leaves from five plants per genotype analysed using Fiji image J software. A- shows that the number of leaves in 56B2 was greater than in Col-0, the T.test shows no statistical difference. B- The size of leaf area in mm² for both 56B2 and Col-0. Leaves are arranged from the youngest, each row present leaves for one plant. A T-test demonstrate that there is no difference in the leaf size between 56B2 and Col.0. Plants were grown in soil under long day condition (16h day) - Error bars= SD. n= 5 plants.

4-3-2 Shoot architecture of 56B2

Cytokinin promotes shoot branching, and direct application of cytokinin to axillary buds enhances outgrowth (Sachs and Thimann, 1964). The level of endogenous cytokinin is increased in and around axillary buds during growth initiation (Li et al., 1995). Müller et al. (2015) investigated the effect of *IPT* loss-of-function on branching, and found that *ipt1, ipt3, ipt5* and *ipt7* single mutant plants produced fewer branches than wild type.

This section focuses on quantifying the number of primary and secondary stems, the number of branches on the secondary stem and siliques number in the main inflorescence. All of these observations were conducted when the first siliques had dried, and flowering was completed at 45 days after germination. Plants were grown in soil under long day condition and 14 plants were observed for each 56B2 and Col-0.

There were no differences observed between 56B2 and Col-0 for any of the phenotypes investigated (figure 4.7). Under long day condition, the onset of flowering in 56B2 was unaffected compared with that in wild type. Moreover, after the initiation of flowering 56B2 had the same number of axillary branches as wild type. However, Werner et al, (2003) showed a shoot response when the cytokinin level decreased through *CKX* genes overexpression. For example, the onset of flowering was delayed by up to 5 weeks in *35S:AtCKX1* and *35S:AtCKX3* transgenic plants compared with the wild type, whereas it was unaffected in *CKX2* and *CKX4* over-expressors.

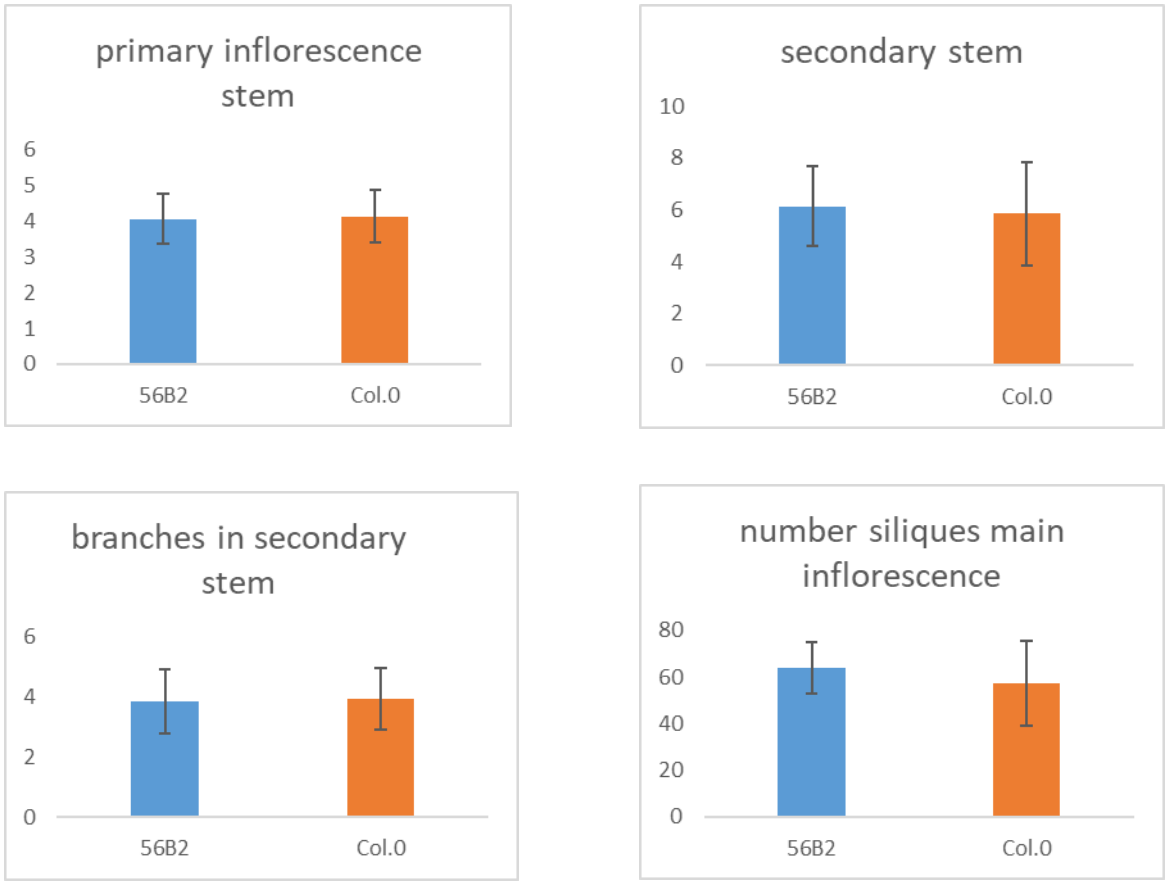

Figure 4.7: Shoot architecture is unaltered in 56B2.

Shoot phenotyping was conducted for 14 plants per genotype as the first siliques had dried and flowering was near completion at 45 days after germination. Results show that there are no different between Col-0 and 56B2 in the shoot including inflorescences, numbers of siliques on the main inflorescence, secondary stem and branches on the secondary stem when a T-test was applied. Plants were grown in soil under long day conditions. Error bars=SD. n- 14.

4.4 Discussion:

The 56B2 line contained multiple mutations, the mutation frequency depends on the concentration of EMS that is used in mutagenesis and the mutation load the 56B2 cannot be known, however other EMS populations have been estimated to carry 1 mutation every 89 kb (Martín et al., 2009). Mutations enriched in *PIN7* segregating lines are shown in table 1. However, the strongest candidate gene in 56B2 controlling

the regulation of *PIN7* was *CKX5*. As screening did not produce mutation in transcription factors so other candidates did not give clear link to *PIN7* transcription while *CKX5* link *PIN7* by modulating cytokinin which induce PIN7 indirectly. As cytokinin regulates many processes of development, it is feasible that any gene regulating cytokinin levels may show pleotropic phenotypes in a number of downstream pathways. Therefore, a detailed analysis of 56B2 phenotype during both root and shoot development was performed.

The first roles that has been investigated was related to root growth. Here, both total root length as well as meristem size was examined. In both cases the 56B2 root phenotype was not different from Col-0. Although it has been shown that reduction in cytokinin levels causes changes in both root length and root meristem size, the fact that we do not see phenotypes in these lines may be due to a number of reasons:

Firstly, *CKX5* might be expressed in a particular subset of cells where it directs a very localised degradation of cytokinin. Confocal images of the pCKX5 transcriptional reporter showed expression through procambial cells flanking xylem axis (see next chapter), so it might catalyse the degradation of cytokinin in the root meristem not in the TZ. Ioio et al. (2007) had shown that cytokinin signalling specifically at the transition zone-controlled meristem size. For example, they showed that expressing CKX1 in the TZ increased meristem size. Whilst no change in the size of meristem was detected when CKX1 was fused to promoter active only in the root meristem.

Secondly, different members of the *Arabidopsis* cytokinin oxidase have different subcellular localizations. For example, a recent report shows that CKX1 is a membrane localized protein located mostly on the ER (Niemann et

al., 2018). This contrasts to a previous report showing that CKX1 and 3 are targeted to vacuoles, and CKX2 to the ER (Werner et al. 2003). CKX7 is targeted to the cytosol (Köllmer et al., 2014), whilst CKX4, 5 and 6 are predicted to be targeted to the apoplast based on a hydrophobic N-terminal signal peptide (Frebort et al., 2011; Gajdosova et al., 2011). This may expose different enzymes to slightly different pools of cytokinin.

- Thirdly, it was found that *CKX1*, *CKX5* and *CKX7* isoforms preferentially degrade cisZ type (Gajdošová et al., 2011, Köllmer et al. 2014), although *CKX5* also degrades transZ. In most cases *cis*-zeatin (cisZ) is considered to be a weakly active form of cytokinin (Gajdošová et al., 2011), but it may have specific roles and therefore show phenotypes in specific processes.

To address the above issues, the sensitivity to cytokinin was focused on this chapter. In this assay plants were treated with the synthetic cytokinin benzyl-adenine. It has been observed that the 56B2 mutant was more resistant to exogenously applied cytokinin in a root elongation assay, particularly at the later time points. This data supports the idea that a cytokinin oxidase is over-expressed in this line. Given the fact that *CKX5* has a high affinity towards cis-zeatin and isopentyl-adenine (Gajdošová et al., 2011), one possible way to pursue this further would be to repeat this assay for different isoforms. This may help elucidate a specific role for *CKX5*, that may separate it from the other apoplastic CKXs.

Cytokinins exist in multiple molecular forms and the most important compounds are iP and tZ (Sakakibara, 2006). The majority of *Arabidopsis* cytokinins come from Z-derived metabolites, which have a concentration that is approximately twofold higher than that of iP derivatives (Werner et al., 2003). The concentration of phytohormones can be quantified using mass spectrometry technology. Based on the numerous forms

of cytokinin, it can be estimated that concentration may vary between different tissues and cell types. Antoniadi et al., 2015 quantified cytokinins in specific cell populations of the *Arabidopsis* root apex. To analyse the cytokinin metabolite content in different cell types a combination of fluorescence activated cell sorting and ultra-high-performance liquid chromatography- tandem mass spectrometry was used (Antoniadi et al., 2015). Using this method, they estimated cytokinin metabolites concentration between (3×10^{-21} and 100×10^{-21} mol per cell) in a single cell. Furthermore, The affinity of cytokinin receptors to their ligand are in the range of 1-40 nM (Lomin et al., 2015). Therefore, different concentrations of cytokinin (25, 50 and 100 nM) were used in a cytokinin sensitivity assay described in this chapter.

There is a strong linked between cytokinin and lateral root formation. For example, reducing the level of cytokinin by the overexpression of cytokinin-degrading enzyme cytokinin oxidase (*CKX*) promotes both root growth and branching (Werner et al., 2001, 2003). Furthermore, it was found that *Arabidopsis CKX5* gene (chapter 5) is expressed in LRPs. Therefore, it was hypothesised that 56B2 may have a lateral root phenotype.

Lateral roots form from founder pericycle cells, and initiate development through an 8 stages process to produce emerged roots (Malamy and Benfey, 1997). In this case, the processes of lateral root initiation and emergence did not separate, and only visualised emerged lateral roots. Even though cytokinin has been implemented in both processes, results cannot separate between the two. Increased lateral root density in 56B2 was observed. This is consistent with published experiments which show over-expression of CKXs (Werner et al., 2003). The role of CKXs in LR organogenesis could be further investigated by looking and potentially staging LR primordia rather than just

emerged roots. This would provide greater insight into which stages of development are affected.

The bisymmetric pattern of root vascular tissue in the *Arabidopsis* root contains single xylem axis consisting of protoxylem and metaxylem in the middle surrounded by two phloem pole and intervening procambial cells. The maintenance of this diarch vascular pattern caused by the mutually inhibitory interaction between auxin and cytokinin (Bishopp et al., 2011a). An essential element within this network is the role that cytokinin plays in directing *PIN7* expression (Bishopp et al., 2011a). Therefore, this prompted to investigate xylem patterning in 56B2. A xylem phenotype in either 56B2 or Col-0 plants did not observe. This is perhaps not surprising as vascular patterning is very robust to alterations in cytokinin due largely to in-built genetic redundancy, and loss-of-function mutations in either PINs or cytokinin signalling rarely show vascular phenotypes.

56B2 plants do not display a significant change in the leaf size than that in wild type plants. However, 56B2 plants produce more leaves than wild type plants. Previous studies have shown that cytokinin promotes meristem maintenance (Wu et al., 2021). Therefore, one might expect that reduction in cytokinins levels might increase the number of leaves. This could be explored further by examining *CKX5* expression in the SAM.

In conclusion, this chapter better sought to understand the processes affected by the 56B2 mutant. It was hypothesised that if the PIN7 phenotype was due to upregulation of *CKX5* then this mutant may also show pleotropic phenotypes in processes in which cytokinin plays a role. A suite of phenotypes in both the root and shoot known to be

affected by cytokinin were examined. These analyses revealed that 56B2 has additional roles in lateral root formation and in controlling leaf number. Furthermore, the mutant is resistant to exogenously applied cytokinin in a root elongation assay. As these phenotypes are consistent with lines with reduced cytokinin, it supports the idea of 56B2 showing elevation of *CKX5* and confirms the value in understanding how a mutation in the promoter can have this effect. Given that 56B2 affected some but not all cytokinin-mediated processes, this suggests that there might be a certain amount of tissue-specificity. This will be examined in subsequent chapters.

Chapter 5: Defining the spatial regulation of CKX5

5.1 Overview

Chapter 4 investigated potential phenotypes associated with 56B2 and found alterations in LR density, in cytokinin response (via a root elongation assay) and in leaf number, although leaf size was not significantly changed. One candidate gene that may underlie these phenotypes is *CKX5*. Therefore, studying spatial expression pattern of CKX5 *in planta* may provide insight into whether the pattern of CKX5 expression is consistent with the phenotypes observed in 56B2. If the alterations in *CKX5* levels are behind these phenotypes, it would be predicted to see overlap in the expression of CKX5 and the tissues affected. For example, it would be predicted to see expression in both primary and lateral roots, as well as in the shoot apical meristem.

The analysis of plant gene expression pattern is vital to understand its function in plant development and cell differentiation (De Ruijter et al., 2003). Techniques such as *in-situ* hybridisation provides spatial data on gene expression, and use of reporters have been proved to be useful tools to study gene expression in transgenic plants (Jiang and Gill, 2006). Reporter genes such as β-glucuronidase (GUS) and green fluorescent protein (GFP) have been commonly used for spatiotemporal expression profiles. Consequently, two reporter gene systems (GUS and GFP) were used in this chapter driven with the promoter of *CKX5* to observe the expression pattern of CKX5 in *planta*, and to compare with phenotypes that have been observed in 56B2.

5.2 Understanding the spatial regulation of *CKX5* using a GUS reporter.

First GUS reporter was chosen to develop because this is a useful tool to examine expression patterns on a whole plant scale. In 1987, Jefferson et al. developed a new reporter gene system for analysing gene expression in transformed plants using the *E.coli* β-glucuronidase gene, *uidA* which encode β-Glucuronidase (GUS). GUS gene activity converts a colourless substrate (X-Gluc) into two indoxyl derivatives which oxidatively dimerize to generate a blue pigment that can be visualised readily using conventional microscopy (De Ruijter et al., 2003, Dedow et al., 2022). This assay is rapid, cheap and highly sensitive (Jefferson et al., 1987).

Often plant tissues can be challenging for fluorescence microscopy due to the thickness of the material, and the opacity of organs (De Ruijter et al., 2003). For example, chlorophyll in leaves makes fluorescent proteins difficult to observe, as the emission spectra often overlap with chlorophyll (De Ruijter et al., 2003). However, GFP has been imaged successfully in the SAM (Gordon et al., 2009). This requires a long working distance objective, which our microscopes do not have. GUS offers an alternative, as plants can be cleared to reveal signal deeper within the tissue. In addition, plants can be imaged using a wide-field or whole mount approach. This provides a good way to visualize the expression patterns of genes at a whole plant level but lacks the detailed cell type specificity of fluorescent proteins.

Figure 5.1: Schematic diagram showing the *proCKX5::GUS* assembled using GreenGate.

GreenGate assembly based on six modules, which are the *CKX5* promoter in the A module, pGGB003 (B-dummy), pGGC051 (GUS) in the C module, pGGD002 (D-dummy), RBCS terminator, and pGGF007 providing kanamycin resistant. Empty "dummy" modules were used in the B and D position. This was assembled with the pDEAL destination vector (Kuempers et al., 2022). Benchling software was used to generate the plasmid map (Benchling, 2018).

A destination plasmid that would have the GUS reporter downstream of the *CKX5* promoter was designed. The GreenGate system (Lampropoulos et al., 2013) was used because it is effective and simple (Figure 5.1). To create this construct an existing A module that contained the *CKX5* promoter was recombined with a C module containing the GUS (β- glucuronidase) gene, an E module containing the RBCS terminator and an F module containing the kanamycin gene that provided antibiotic selection into the pGGZ003 destination vector (Lampropoulos et al., 2013). The entry module with the *CKX5* promoter was sequenced prior to assembly to verify that it was correct. Assembly of the destination vector first checked via colony PCR. Here,

primers that amplified fragment between B & D dummy boxes were used (essentially the GUS gene). The predicted size of this fragment is 1814 bp, and this was visualised by gel electrophoresis (Figure 5.2). Sanger sequencing was performed using two primers to check the junctions with the destination vector; one located within the vector sequencing into the *CKX5* promoter and the other sequencing into the kanamycin resistance gene. This plasmid contained a piece of transfer DNA flanked by left and right boarders containing a tdTomato reporter driven by the UBQ10 promoter staining plasma membranes, the *proCKX5::GUS* gene and the *35S::KanR* gene for *in-planta* selection.

The *proCKX5::GUS* plasmid was then transformed into *Agrobacteria* subsequently into *Arabidopsis* using floral dipping. T0 seeds for *proCKX5::GUS* construct were collected and plated out on kanamycin to select the primary transformants, then eight independent T1 lines were moved to soil for seed propagation.

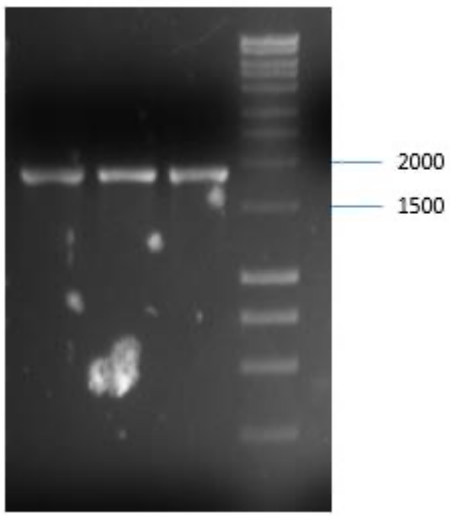

Figure 5.2: A gel taken from a colony PCR verifying that the cloning was successful.

1%(w:v) agarose electrophoresis gel run at 80 A for 1h. Colonies have an amplicon corresponding to the size expected for *proCKX5:GUS* using B dummy forward and D dummy reverse primers. These primers amplified fragment at nearly 1800bp. Hyper ladder 1kb was used as a marker.

Independent lines of T2 were then cleared and stained to detect GUS activities in 7-day old seedlings. Seedlings of transgenic lines containing the *CKX5 promoter::GUS* showed that GUS was detected in the root tip, lateral root primordia, and the shoot meristem (Figure 5.3). These data show that CKX5 is expressed in many of the tissues in which phenotypes were observed in 56B2 in the chapter 4. Previous publications showed that CKX5 expression in the shoot was localized at the base of the youngest emerging leaves and in the rib zone of the axillary meristems (Werner et al., 2003). In root, it was expressed in the vascular cylinder within the apical meristem of primary root and in the centre of lateral root primordia (Werner et al., 2003). Data gain from GUS reporter which showed that CKX5 express in root tip, LRP and shoot meristem were consistent with these findings and show the suitability of the promoter fragment that was used in this experiment. These findings paved the way for more detailed cell-type specific analysis using fluorescent reporters (GFP).

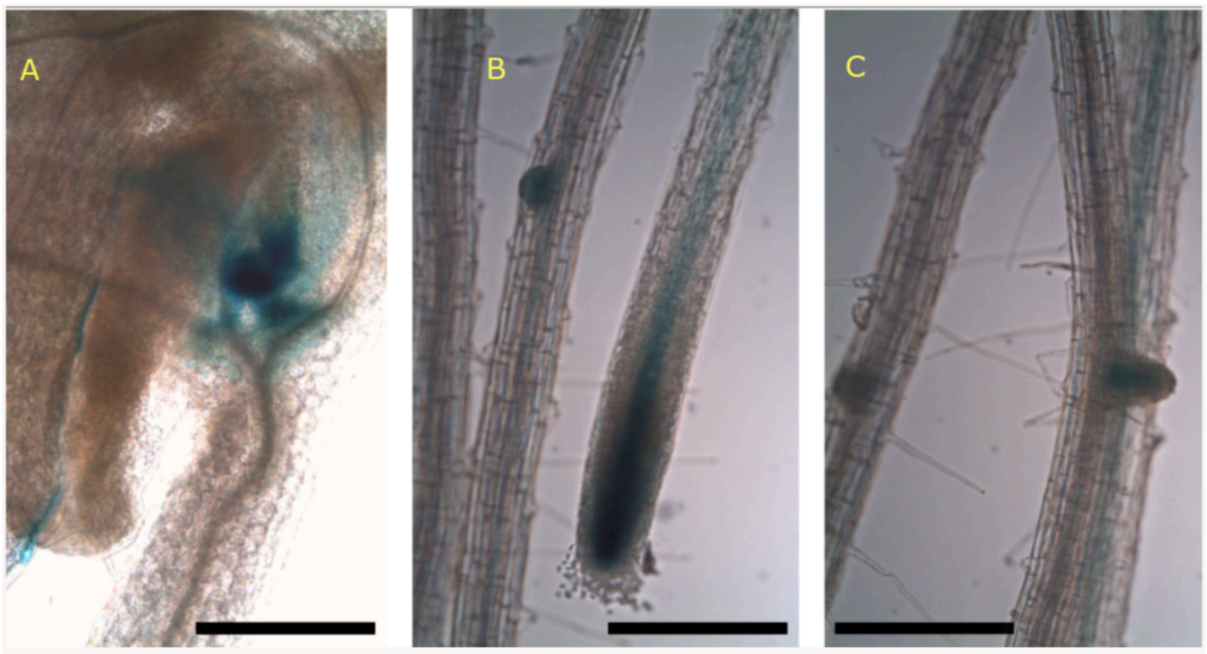

Figure 5.3: CKX5 is expressed in the root and shoot apical meristem.
Images show the expression pattern of CKX5 using GUS reporter in the *Arabidopsis*. CKX5 is expressed in the shoot meristem (A), in the root tip (B) and in the lateral root primordium (C). Plants are 7 days old, and images are taken from transgenic T2 plants stained with GUS to detect the expression of CKX5 in *planta*. Scale bar=50 μm.

5.3 CKX5 is expressed in the procambium cells

The previous section using the GUS reporter showed that CKX5 is expressed within the root tip. Whilst the GUS reporter gives a general idea where *CKX5* is expressed, without performing plastic sections it lacks the specificity to determine the exact cell types. Therefore, a GFP reporter was used to more precisely probe where CKX5 is expressed in the root tip. This construct uses the green fluorescent protein (GFP) from the cnidarian jellyfish *Aequorea victoria* which has been placed under the control of the *CKX5* promotor. The emission of green fluorescence from GFP required blue or UV light and oxygen only but no other exogenous substrates (Chalfie et al., 1994). Fluorescence can easily be visualized via fluorescence microscopy or confocal microscope using the Argon laser.

A previous student built the construct *proCKX5::GFP* using Greengate cloning. The promotor of *CKX5* in an A module was fused into GFP in a C module. However, the expression in plants was analysed in this thesis. The expression pattern of CKX5 in the root tip was visualized by confocal using 5 days old seedling after staining with PI. It was observed that CKX5 is expressed in the procambial cells flanking xylem axis (Figure 5.4). This mirrors the pattern of both high cytokinin signalling output and PIN7 (Bishopp et al., 2011). This means CKX5 and PIN7 expression are largely overlapping and occur in cells with maximum cytokinin signalling output.

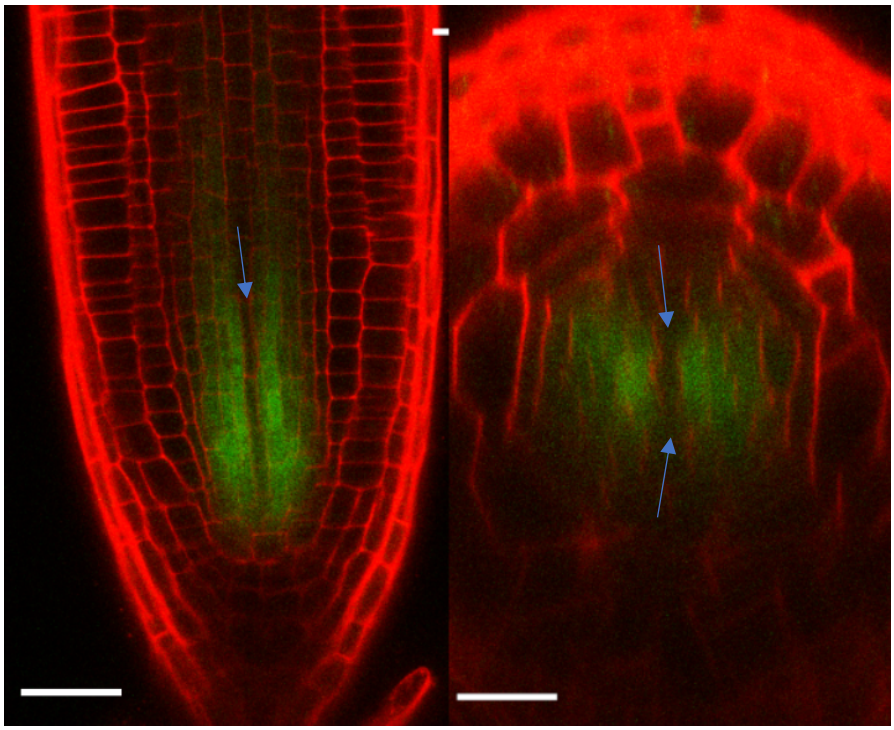

Figure 5.4: CKX5 is expressed in the procambial cells flanking xylem axis**.**
Confocal images show the expression pattern of CKX5 using a GFP reporter in the *Arabidopsis* root. Five days old seedling are imaged. Scale bar= 50µm. Arrows indicate the xylem axis.

5.4. Is *CKX5* expression regulated by different hormonal signals?

PIN7 and CKX5 are expressed in overlapping domains where cytokinin responses are high in cambium cells flanking the xylem axis. It is well documented that cytokinin induces *PIN7* expression (Bishopp et al., 2011) and cytokinin signalling and homeostasis is known to be controlled partly through the activation of both cytokinin signalling inhibitors such as AHP6 and enzymes involved in cytokinin degradation such as (CKXs) (Mähönen et al., 2006). This raises the question, could *CKX5* be induced by cytokinin to feedback on cytokinin levels? To test this, an experiment to determine the effect of exogenous cytokinin on *CKX5* expression in a time resolved manner was conducted. The aim was to investigate the alterations in the expression pattern/levels when plants treated with cytokinin at multiple time points.

Five days old seedlings were incubated with 100 nM BA at 0h, 3h, and 6h. Seedlings were then stained with PI prior and visualised by confocal microscopy. As before, at the 0h timepoint, the expression of CKX5 was observed in the procambium cells flanking the xylem axis. After 3h treatment with BA, the signal of fluorescent seems to be stronger comparing with untreated plants (Figure 5.5 A &C), although the level of the signal did not quantify. After 6h cytokinin treatment, the CKX signal increased and the expression domain expanded into the xylem axis (Figure 5.5 D). Under this time point the control (untreated line) showed clear exclusion of CKX5 from the xylem axis (Figure 5.5 B).

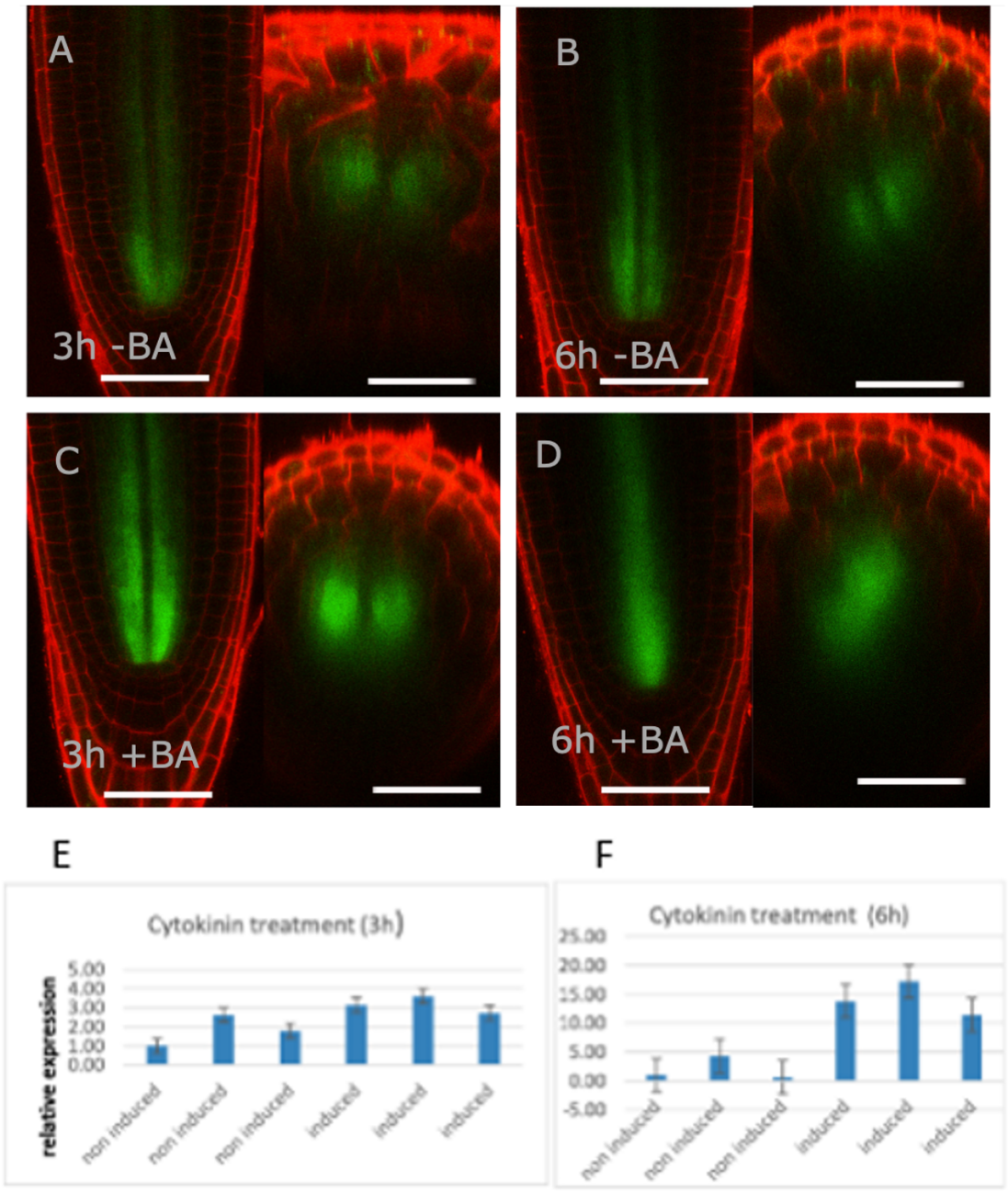

Figure 5.5: *CKX5* expression is induced by cytokinin.

5 days old seedling of *proCKX5::GFP* were treated with 100 nM BA in a liquid induction system for 3 and 6 hrs. A-D) Confocal microscopy images shows the expression pattern of *proCKX5::GFP* with and without cytokinin treatment. A-B) *proCKX5::GFP* at 3 and 6 hrs as a control in liquid induction system. C-D) *proCKX5::GFP* after 100nM BA treatment at 3 and 6 hrs, respectively. Images display that *CKX5* largely responsive following 100nM BA treated for 6h, scale bar 50 µm, n=10. E & F show measurement of *CKX5* mRNA levels by qRT-PCR. Three independent biological samples were used for mock treatments, and three biological samples were treated with 100 nM BA for the time indicated on the graph. In each case plants were grown on agar plates for 7 days. For each replicate, 30 plants were moved to liquid MS containing +/- cyktokinin (100 nM BA), and kept in the growth chamber. Around 30 root tips (2 mm) were excised and used for RNA extraction. qRT-PCR values are normalised against the first un-treated replicate. It confirms that *CKX5* mRNA is upregulated after 6h incubation with BA. Error bar=SD.

In addition to looking at the spatial pattern of CKX5 expression using GFP, it was followed by measuring the levels of *CKX5* mRNA using qRT-PCR after treatment with BA. The level of *CKX5* mRNA in the root tip was measured for 3 biological replicates for each of *proCKX5::GFP* seedling with and without cytokinin for 3 and 6h. The root tip of 30 seedlings were excised for each biological replicate, and each replicate represented an independent transgenic line. There is a slight increase in the transcription level of *CKX5* after 3h treatment with cytokinin (Figure 5.5 E) which corroborated with the observations of *proCKX5::GFP* made using confocal microscopy. The qRT-PCR analysis revealed that the transcription of *CKX5* is upregulated and the expression increase (between 10-15 fold) after 6h treatment (Figure 5.5 F), which seems in part due to the expansion of the CKX5 domain from procambial cells into the xylem axis.

Collectively, these results show that *CKX5* transcription is also regulated by cytokinin, consistent with published microarray datasets of genes that are differentially expressed following cytokinin treatment (Bhargava et al. 2013). In order to identify genes that respond to cytokinin Bhargava et al. (2013) created the “Golden List” which contains 226 genes identified as cytokinin responsive. The golden list established by using a meta-analysis of 13-microarray experiments of cytokinin treated *Arabidopsis* seedlings and containing genes were > 1.5-fold differentially regulated in 40% of the experiments. Theses microarrays found that tissue from seedlings, shoot and root induced by zeatin and BA. Then, a RNA-seq experiment was used verified most of the genes identified from microarray data. RNA-seq was performed using seedlings that were treated with 5 nM BA for 12 min. *CKX5* was identified as one of the cytokinin metabolism genes in this list.

5.5 Discussion:

Two reporter constructs were designed to study the expression pattern of CKX5 in the plants. First construct carried GUS gene under the promoter of *CKX5* which give broad idea about the expression in whole plants. Second construct aims to provide cell type specificity by using the fluorescent protein GFP fused to the promoter of *CKX5*. Analysis of the expression of CKX5 via the reporter marker showed that CKX5 expressed in the shoot meristem, LRP and root tip mainly in the procambium cells which consistent to the phenotype that observed in 56B2 in chapter 4.

Previous data investigating CKX5 expression included data from bioinformatics resources. The eFP Browser gives an indication of the expression profile of various genes based on the work of Brady et al. (2007). Brady et al. (2007) combined fluorescence activated cell sorting and microarray expression profiles of different tissue types and developmental zones to provide a spatial map of gene expression. The eFP browser shows that expression for CKX5 was found in the procambial cells (Figure 3.4). More recently, researchers have made use of single cell sequencing approaches to document expression of genes. Resources such as scRNA-seq dataset show that CKX5 is most abundant in procambium cells (Figure 5.6) (Wendrich et al., 2020). The expression was investigated via reporter genes and confocal microscopy imaging and show that CKX5 is expressed in procambial cells flanking the xylem axis where the highest cytokinin response was found. This is broadly in agreement with data shown in single cell/ cell type gene expression profiling.

A

B

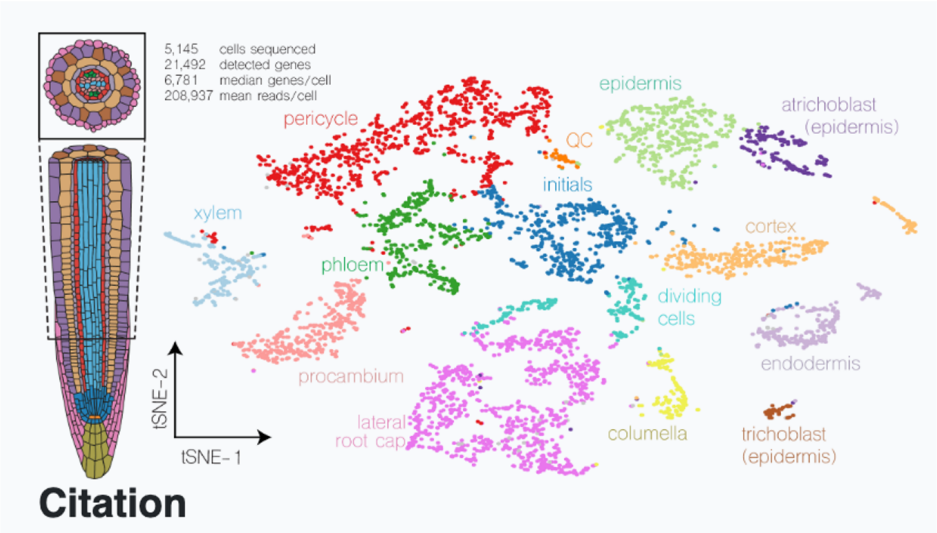

Figure 5.6: Expression of CKX5 in the *Arabidopsis* root meristem cell using scRNA-seq.

Panel A: distribution of cells containing *CKX5* mRNA are shown in blue. B) The panel below shows clustering of different cell populations. In this dataset CKX5 is found in procambium, phloem and some initial cells. There is also some expression within a subset of cells that are classified as xylem. Image taken from (Yang et al., 2021b).

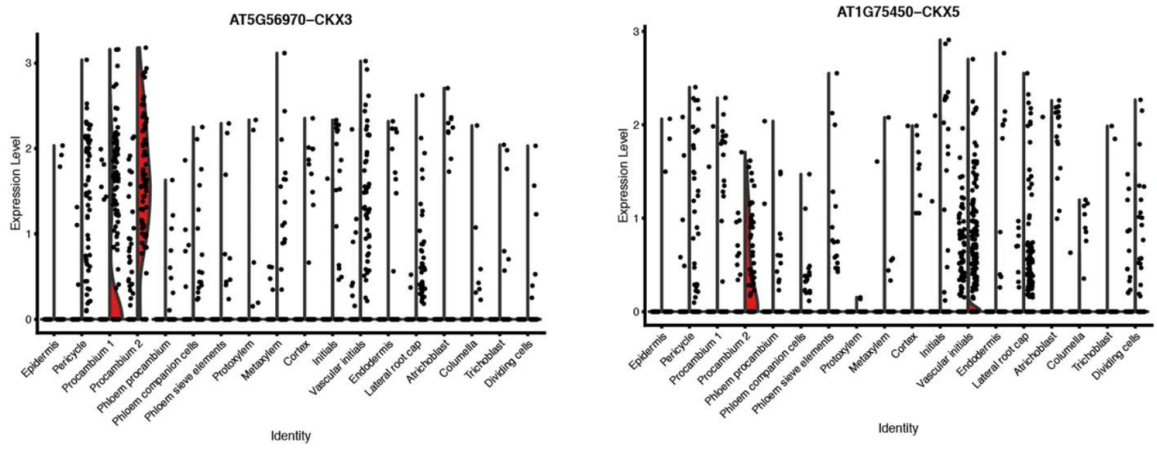

Figure 5.7: Expression of CKX3 and CKX5 in root meristem cells at cytokinin treatment based on scRNA-seq dataset.

The expression of *CKX5* and CKX3 normalized by the cell type and presented as violin plots shows the expression in mock and cytokinin treatment. Left side mock, right is cytokinin treated. In the procambium 1 and 2 cells there is an increase significantly in the expression level of CKX3 when the cytokinin treatment (in red), and the expression of CKX5 increase slightly after treatment with cytokinin (in red). The expression was measured after treatment with 10 µM BA for 3h. Graph from (Yang et al., 2021b).

Single cell sequencing data also exists for cytokinin treated data (Yang et al., 2021b). Yang et al (2021) reveal the expression of CKX3 and CKX5 in different cell type after treatment with cytokinin (Figure 5.7). These data were analysed and can see that CKX3 induced rapidly and CKX5 is induced slightly in the procambium cells in response to treatment with 10 µM BA for 3h comparing to untreated with cytokinin, (Figure 5.7). These data support the results in this chapter showing that *CKX5* transcription is upregulated slightly after treatment with 100 µM BA for 3h and increased rapidly after 6h treatment. Result in this chapter showed that after incubation with cytokinin (100 µM BA) CKX5 expression pattern expands into the xylem in 6 h but not 3 h treatments. This expansion into the xylem axis was not seen in the single cell sequencing results (Yang et al., 2021); however, it is important to note that they followed the expression of mRNA after only 3h treatment with cytokinin. Collectively,

this observations support previous studies indicating that cytokinin could be able to balance its level by enhancing the expression of cytokinin oxidases (Rashotte et al., 2003, Lee et al., 2007). Moreover, data on this work and others suggest that *CKX* genes also dampen the function of cytokinin by providing feedback mechanism (Kieber and Schaller, 2018).

To investigate the expression of CKX5 in the whole plant, a GUS reporter was generated. The expression of CKX5 in 7-day old seedlings was examined, and observed expression in the root tip, similar to the GFP reporter. Moreover, the expression was detected in lateral root primordia at the emergence stage. Expression, or enhanced expression of CKX5 in 56B2 could explain the effect of lateral root density shown in chapter 4. Furthermore, chapter 4 shows that 56B2 produced more leaves than WT. In this chapter CKX5 expression was observed in the shoot meristem. Therefore, enhanced expression of CKX5 in the shoot meristem could mean that perturbation of *CKX5* leads to a phenotype in with increased the number of leaves. The overall expression pattern of CKX5 in similar tissues to those where phenotypes exhibited was prompted to focus on the effect that the 56B2 mutant may have on *CKX5* levels in chapter 6. Using the reporter marker in this chapter suggest that introduce GFP reporter to both 56B2 and WT and compare the level of GFP between these lines in chapter 6.

Chapter 6: Confirming the molecular identity of 56B2

6.1 Overview:

Chapters 4 and 5 explored the phenotype of the 56B2 mutant and characterised the expression pattern of CKX5 in plants. This chapter aims to investigate the possibility that a polymorphism in the *CKX5* promoter caused local changes in CKX5 expression and was responsible for the both the phenotypes observed in results chapter 4 and the decrease in *PIN7* expression level. The 56B2 mutant shows increases the density of lateral root, the root become more resistant to cytokinin with respect to WT and there is an increase the number of leaves. These findings are all consistent with altered cytokinin response and support a model in which the mutation in the *CKX5* promoter of 56B2 leads to elevated CKX5, which reduces the pool of bioactive cytokinin and ultimately gives rise to the root and shoot phenotypes described.

This chapter tests the theory that elevated CKX5 expression is causal for the reduced PIN7 expression phenotype in 56B2 in two ways. Firstly, comparing transgenic reporter lines carrying the endogenous *CKX5* promoter versus those carrying a polymorphism in the promoter to 56B2 (called $CKX5_{mut}$) may reveal changes in either the level or the spatial expression pattern of CKX5 (Figure 6.1 A). Although the transcription factors acting upstream of *CKX5* are unknown, it would be predicted that expression of *CKX5* mutant would phenocopy 56B2 that means levels of GFP would be higher in the $CKX5_{mut}$ lines. Secondly, it was attempted to use the CRISR/Cas9 system to knockout *CKX5* in 56B2 to demonstrate the causality between *CKX5* and *PIN7.* The hypothesis here was that if elevation in *CKX5* expression in 56B2 was causal for the reduction in *PIN7*, then an intragenic suppressor in *CKX5* would reverse this. In this scenario, the 56B2 mutation would continue to produce overexpression of

CKX5, but if *CKX5* was mutated by CRISPR/Cas9, this could produce a non-functional CKX5 protein, and the levels of *PIN7* would increase close to that of the wild-type level (or more precisely equal to that of a *ckx5* loss of function mutant) (Figure 6.1 B).

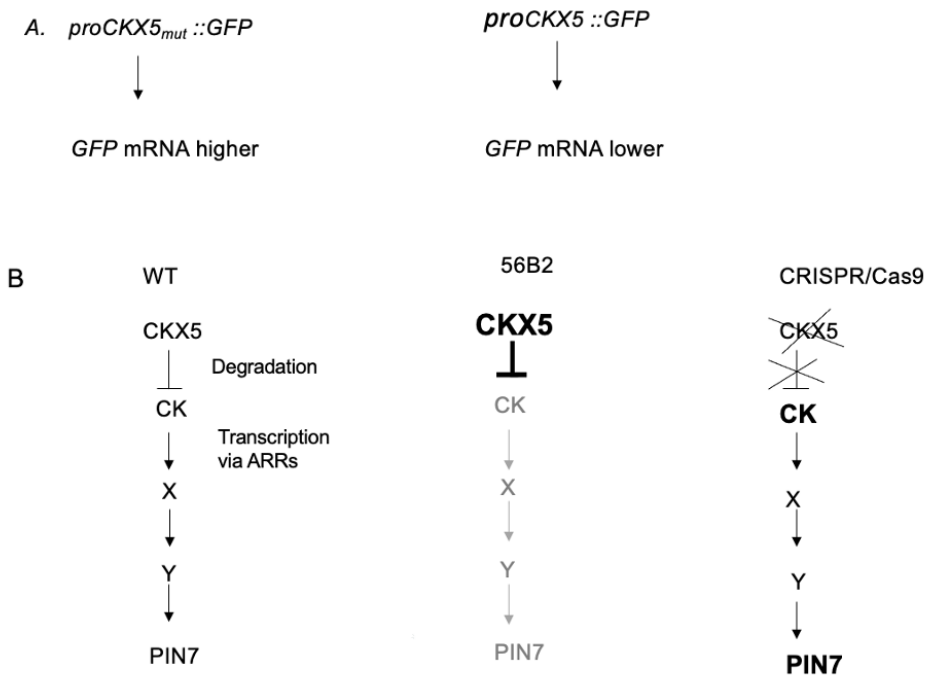

Figure 6.1: Schematic shows the two ways that used in this chapter to test the theory increasing *CKX5* expression may lead to reduce *PIN7* expression. A- Comparing transgenic lines that carrying a polymorphism in the promoter of 56B2 called (proCKX5$_{mut}$) and endogenous *CKX5* promoter called (proCKX5), the level of *GFP* predicted would be higher in the CKX5$_{mut}$ lines. B- the hypothesis for this project state that the 56B2 mutant increase the amount of *CKX5* transcription and causes elevated mRNA levels (shown in bold). This would result in higher levels of the CKX5 resulting in greater catabolism of cytokinin (shown in grey). If the CKX5 cDNA was targeted with CRISPR guides specifically in the 56B2, this would generate a range of novel mutations within CKX5 in the 56B2 background. Then strong loss-of-function could be selected (i.e alleles creating either frameshifts or premature stop codons). In these cases, it would be predicted that the transcription of CKX5 would still be high (due to the polymorphism in the 56B2 promoter) but the protein expressed would be non-functional and therefore not degrade cytokinin. If the reduction in PIN7 expression in 56B2 was directly caused by increased CKX5 transcription it would predict that the reduced PIN7 phenotype would be absent from the 56B2 CRISPR knockout due to it overexpressing a non-functional CKX5.

6.2 The role of the 56B2 mutation in determining expression levels of *CKX5*

To explore the role a 56B2-like mutation would have on modulating CKX5 expression, a construct in which the *CKX5* promoter was amplified from 56B2 DNA was designed and called proCKX5$_{mut}$. Like the first construct (proCKX5::GFP), this contained 1.2 kb of *CKX5* sequence upstream of the transcription initiation codon. This was fused to GFP in the same way to make *proCKX5$_{mut}$::GFP*. The two constructs differed only in the 1bp polymorphism in the poly (dA-dT) tract present in the 56B2 mutant.

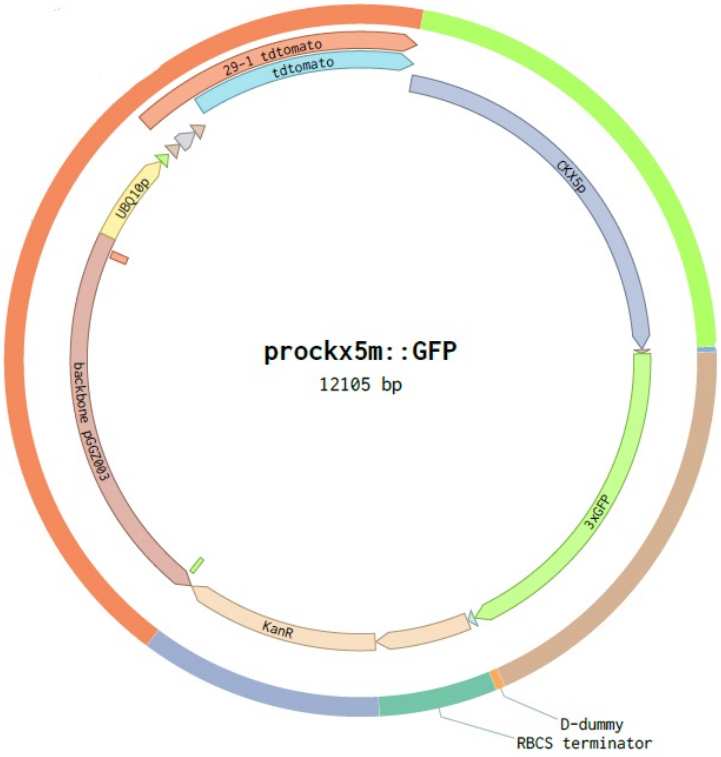

Figure 6.2: Schematic diagram showing the *prockx5m::GFP* construct.

GreenGate cloning consist of six modules, which are *ckx5m* promoter in A module, pGGB003 (B-dummy), 3xGFP in C module, pGGD002 (D-dummy), pGGE001 (RBCS)terminator, pGGF007 kanamycin resistant assemble with the destination vector pDEAL (Kümpers et al., 2022). Benchling software was used to generate the diagram (Benchling, 2018).

GreenGate cloning was used to build this construct (Figure 6.2). The promoter of 56B2 was amplified via PCR, and combined into an A module plasmid. The proCKX5$_{mut}$ A module was combined with the GFP C module, the RBCS terminator as the E module and the kanamycine resistance gene in F module to provide antibiotic selection into the pDEAL destination vector (Lampropoulos et al., 2013). As before, empty modules were used in B and D positions. To ensure that the promoter was correct, the A module was sequenced prior to assembly, then the junctions of other modules after assembly into the destination vector. As before, this plasmid contained a piece of transfer DNA flanked by left and right boarders containing a tdTomato reporter driven by the UBQ10 promoter staining plasma membranes, the *proCKX5 $_{mut}$::GFP* gene and the *35S::KanR* gene for *in-planta* selection.

The final vector was transformed into *Agrobacterium tumeficens* and then transformed to Col-0 *Arabidopsis* plants via floral dipping. The T0 seeds were plated out on ½x MS with kanamycin (50 µg/ml) plates to select the primary transformants. In the first round of transformation, around five plants were resistant to kanamycin, however, when visualized under the screening microscope the roots did not have GFP expression. Consequently, the dipping was repeated using the same construct which transformed into *A. tumefaciens* (GV3101). This time individual *A. tumefaciens* contained the plasmid was checked using colony PCR (Figure 6.3). Primers that amplified a fragment of *CKX5* promoter were used and saw that two of the *A. tumefaciens* colonies contained the correct insert. *prockx5m::GFP* in *A. tumefaciens* transformants , lane 5 and 6 (figure 6.3) had the correct plasmid because there is a band that is approximately 544 bp size, which was expected. Surprisingly, the B and

D dummy primers used in the previous chapter for amplifying the GUS gene did not work here. This may be because the 3xGFP is larger than GUS and the PCR extension time may not have been sufficient (Figure 6.3 1-3). Therefore, the colony in lane 5 was used for subsequent liquid culture and floral dipping. After that, T0 seeds were plated out with kanamycin and the first transformants were moved to soil to get T1 seeds. Six independent lines of *prockx5m::GFP* and seven independent lines of *proCKX5::GFP* were sown out and moved to soil to collect T2. T2 plants were sown out on Kan plates to test for single insertion lines based on segregation of Kan resistant versus Kan sensitive lines. Lines that had a ratio of close to 3:1 resistant: sensitive were selected. These lines were moved to soil, the progeny collected. After that, T3 seeds were selected from populations that were all resistant to Kan. This yielded 4 lines for *proCKX5mut::GFP* and 2 lines for *proCKX5::GFP*. Homozygous lines were then plated out on 1⁄2 xMS and confocal microscopy (Leica SP5) and qRT-PCR were used to visualize the expression pattern and to measure the mRNA of *GFP*, respectively.

It had been hypothesized either that if a mutation in the poly (dA-dT) tract enhanced the expression of *CKX5*, then expression levels would be higher in *prockx5m::GFP* than *proCKX5::GFP* when the expression was visualized via confocal microscopy or when measuring *GFP* transcript abundance with qRT- PCR. There is great variability in the expression of transgenes in independent transgenic lines, depending on the insert number and position, for this reason it was important to look at as many independent transgenic lines as possible.

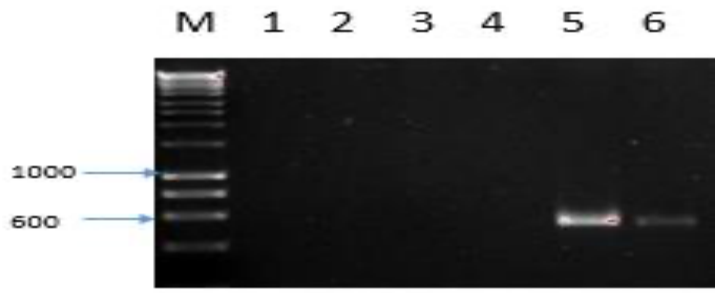

Figure 6.3: Colony PCR for 3 independent colonies of *A.tumefaciens* transferred with *prockx5m::GFP* using two set of primers.

Lanes 1-3 show 3 colonies of *Agrobacterium* using B dummy forward and D dummy reverse primers. These primers amplified fragment at nearly 2200bp. Lanes 4-6 show the same 3 colonies using different primer seq56B2 primers, theses primers were designed to amplify *CKX5* and the predicted size=544bp. Lanes 5 and 6 produce an amplicon of the predicted size (544 bp). PCR products were run on 1% (w:v) agarose gel at 80v for 1h. Hyper ladder 1kb was used as a marker.

The expression of GFP was analysed in the root tip for two independent lines of *proCKX5::GFP* and four independent lines of *prockx5m::GFP* using confocal microscopy (Figure 6.4). Firstly, it was looked at the expression pattern at a tissue level. It was found that *proCKX5::GFP* and *prockx5m::GFP* were similarly expressing CKX5 through the procambial cells. This expression pattern was similar to those described previously by bioinformatic tools such as eFP browser and single cell approaches (Figure 3.4 & 5.6). After ascertaining that there were no differences in the overall expression patterns, GFP signal was measured.

The pixel intensity of the fluorescence in the green channel was quantified for all independent lines (10 roots each). By using ImageJ software, the image was converted into pixel to measure the fluorescent signal as described in section 2.22 (chapter 2). These results reveal that the intensity of GFP in the lines that contain the WT promotor was higher than the lines containing the 56B2 promoter significantly

different– the opposite of the prediction. To test significance, an Anova test with a post-test T-test was applied. The Anova was significant and the post-test T-test indicate that the intensity in *proCKX5::GFP* lines was significantly higher than three out of the four lines of *prockx5m::GFP* lines (5-6 , 10-3 and 11-5) (Figure 6.4 G).

Whilst side-by-side comparison of GFP is a useful tool to investigate qualitative spatial differences, it is not always the most suitable to investigate quantitative differences. To better quantify levels of transcription, *GFP* mRNA was measured for the independent lines via qRT-PCR using primers within GFP. The RNA for 7 days old seedling was extracted from the whole roots of 30 plants in each sample (independent lines). Then cDNA was synthesised, and the qRT-PCR was run. This showed that the mRNA levels of one out of the two *proCKX5::GFP* lines was higher than *prockx5m::GFP* lines (Figure 6.4 H). This result was interesting as the *GFP* mRNA levels do not correlate well with the measurement of fluorescence. Especially *proCKX5::GFP* line 4-7 showed the highest fluorescence, but the levels of *GFP* mRNA were similar to those of the *proCKX5mut* lines. These differences could be due to a variety of reasons. One possibility relates to the fact that these approaches quantify CKX5 in different spatial domains. The root tips used in the microscopy represent only a few hundred micrometres close to the root tip. It is not possible to dissect such fine tissue for qRT-PCR, and so these will offer a consensus of CKX5 over a much larger area. This may also reflect differences in the mRNA or protein stability in the different transgenic lines.

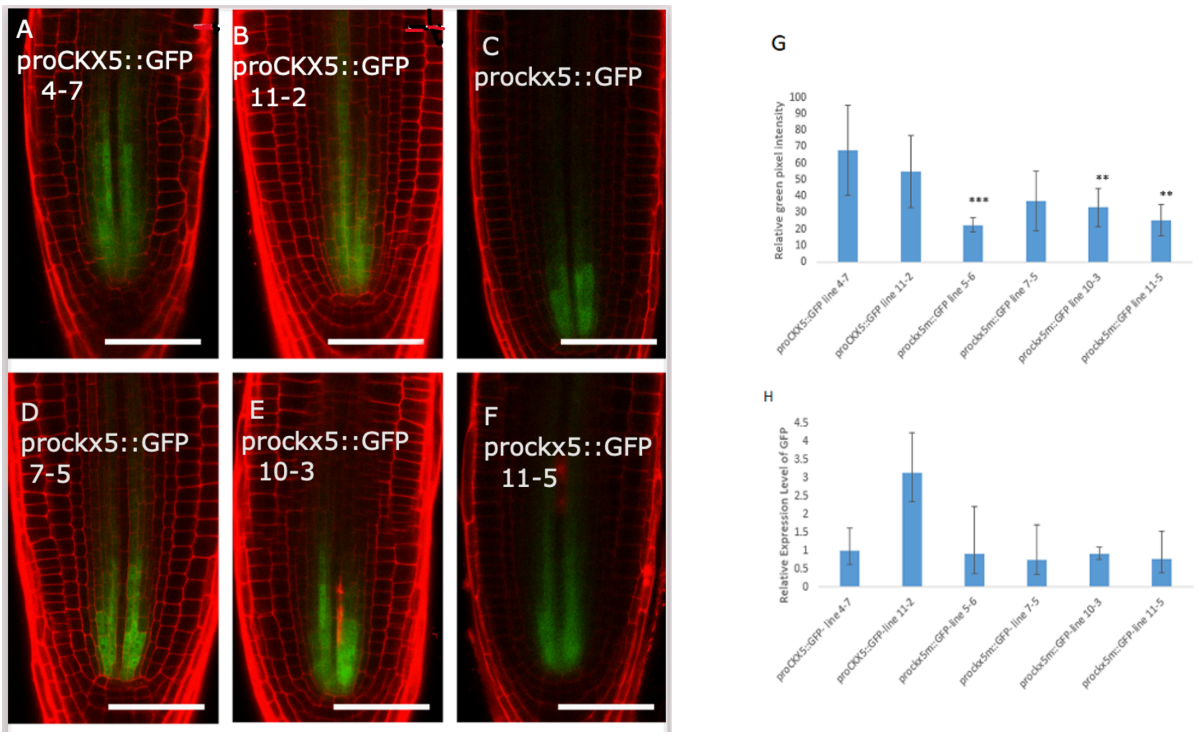

Figure 6.4: The prockx5m does not increase transcription relative to the proCKX5 promoter .

A & B show confocal images for 5 days old plants of 2 homozygous independent lines for *proCKX5::GFP* . C-F confocal images for 5 days old plants of 4 homozygous independents lines for *prockx5m::GFP* . G shows the intensity of GFP fluorescence averaged over 10 roots for each line. The intensity is significantly lower in 3 lines 5-6,10-3 and 11-5 without an intact poly (dA-dT) tract promoter. H shows the levels of GFP mRNA measured via qRT-PCR. The RNA for 7 days old plants was extracted from the whole root approximately 30 plants for each. It shows that transcription of GFP is higher in one of the lines that contained the intact poly (dA-dT) tract promoter. Anova and post-test t-test was performed. **=P≤0.01, ***=P≤0.001 . Error bars=SD,n=10, scale bar 50μm.

Overall, it had been predicted that the levels of GFP fluorescence or mRNA would be higher in the prockx5m line than the proCKX5 line. This was based on the observation that *CKX5* levels were higher in 56B2 than Col-0. This was investigated in a number of independent transgenic lines using two techniques (quantifying fluorescence and qRT-PCR). This proved not to be the case as 3 out of four lines of *prockx5m::GFP* is significantly lower the intensity of GFP, as well as one line of *proCKX5::GFP* increased the level of *GFP* mRNA . In fact, although the number of independent lines were quite

low, quantification of fluorescence suggested the opposite, in that there were higher levels of GFP in plants with the poly (dA-dT) tract intact. Taken alone this result would suggest that the poly (dA-dT) tract has a role in boosting expression of CKX5, a role more similar to what has been observed in the regulation of other genes. However, this would require analysis of more independent lines to test.

In order to fully analyse these results, there are a number of factors that need to be taken into account. These results are based on a relatively small number of independent transgenic lines. It would be important to see if the trend seen in Figure 6.*4* G was continued if a greater number of transgenic lines were used. Ideally it would be better to look at at least five independent lines for both constructs. One other important issue is to consider whether the constructs inserted within these plants are bound around heterochromatin in the same way, as the inserts will be located at different positions within the genome. One way round this would be instead of looking at different transgenes to explore the role of the poly (dA-dT) tract,but would be to look at natural accessions of *Arabidopsis* to see if there is variability within this region, and this is something that I will explore within the final chapter.

6.3 Is elevated CKX5 behind the altered PIN7 expression in 56B2.

Does regulation of *CKX5* directly lead to alterations in PIN7 expression? In chapters 4 & 5, a hypothesis was presented in which the reduction in PIN7 expression could be attributed to the mutation in the *CKX5* promoter in the 56B2 mutant, and this chapter was aimed to test it. Mutagenesis by EMS results in many genetic lesions and it is possible that the effect on PIN7 expression in 56B2 is caused by an a yet unidentified mutation. To demonstrate causality, it was planned to use a CRISPR/CAS9 approach to knockout the *CKX5* gene in line 56B2. It is important to note that this experiment

was started before the results of the previous experiment were obtained in which the expression of *CKX5* versus *CKX5mut* promoters driving GFP was compared. In this experiment, guide RNA was designed to target exons within the *CKX5* gene. The rationale behind this was to create an intragenic knockout in the 56B2 line. Here it had been predicted that levels of *CKX5* transcript may still elevated in the 56B2 line, but if this transcript was rendered non-functional via CRISPR editing, the elevated *CKX5* would not affect cytokinin levels and therebefore *PIN7* expression. If such an intragenic suppressor reverted levels of *PIN7* close to that of wild-type (or more precisely equivalent to that of a loss-of-function *ckx5* mutant), then it could be more confident that the altered *PIN7* expression in 56B2 was a direct outcome of *CKX5* activity in 56B2.

One of the most effective genome editing technologies developed in recent years is CRISPR-Cas9 and this has been used for genetic engineering in various organisms including plants. The CRISPR/Cas9 (CRISPR-associated 9) system involves two components, the Cas9 protein and a single guide RNA (sgRNA) (Jinek et al., 2012). Cas9 allows sgRNA to scan along DNA looking for a target sequence that matches with the 20 bp of the 5′ sequence of sgRNA with protospacer adjacent motif (PAM) sequence (NGG), then a double-strand break (DSB) is induced at the target site by the Cas9–sgRNA complex (Tsutsui & Higashiyama, 2016).

In the plant, various factors determine the success of CRISPR/Cas 9 system such as the efficiency of the vector, the design of gRNA and transformation method (Bernard et al., 2019). The attempts to produce CRISPR/Cas9 knockouts took part in two stages. In the first stage constructs designed and built by a former student was used

(detailed in this section 6.3). I then designed and built my own CRISPR/Cas9 constructs (next section 6.4).

The former student designed guide RNAs to introduce polymorphisms within exonic regions in *CKX5* and had introduced these into both *PIN7::PIN7:GFP* and 56B2 lines. Guide RNAs are located in the first exon (figure 6.5 A). As CRISPR/Cas9 gene editing often produces small insertions or deletions, there is a high chance of producing null alleles.

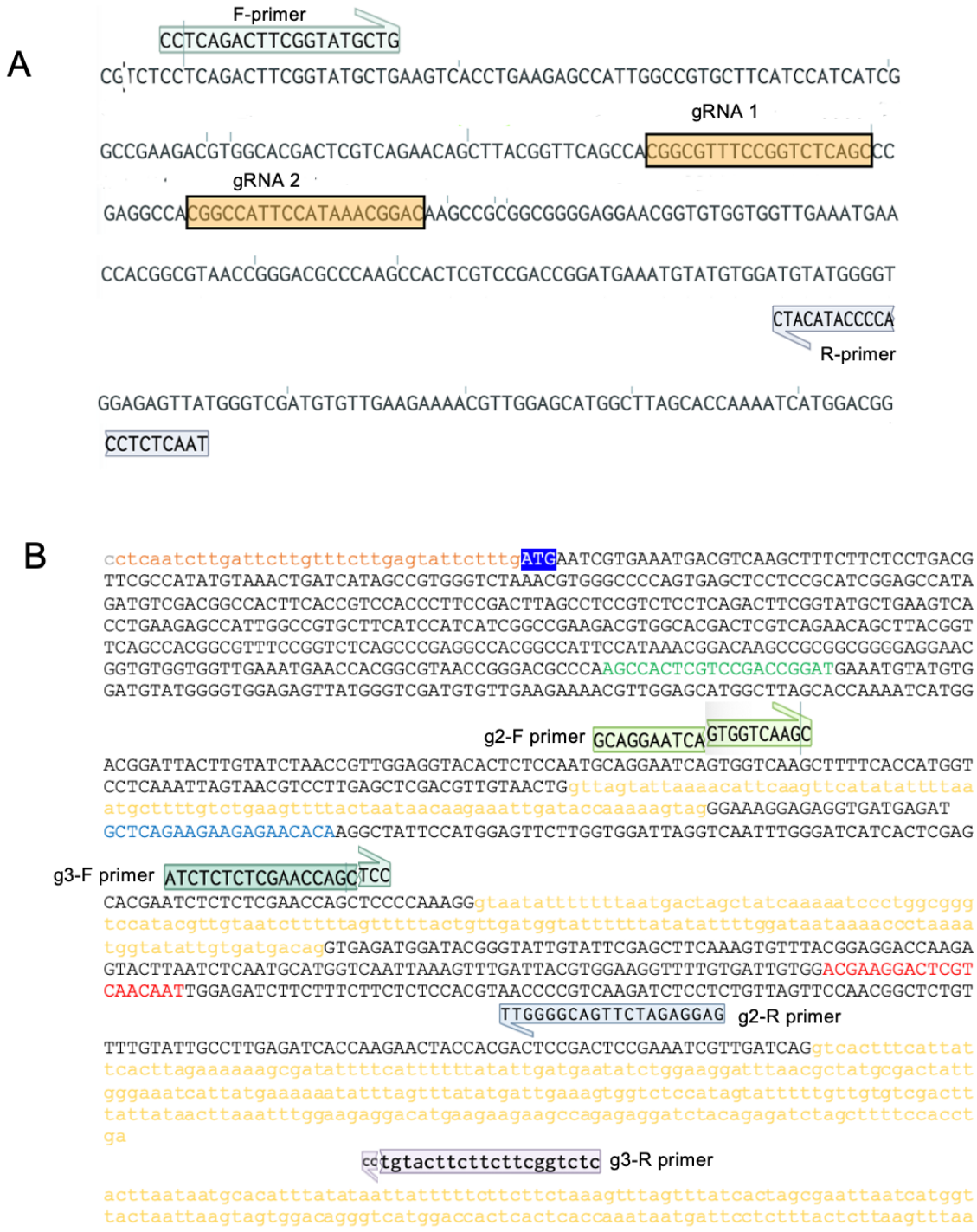

Figure 6.5: Location of gRNAs in *CKX5*.
A. Image shows the location of guide RNAs in the first exon of *CKX5* which were designed to guide Cas-9 in CRISPR-CAS9 approach. Orange blocks indicate the first gRNA and the second gRNA respectively. Green arrows indicate the forward primer and blue arrow indicate the reverse primer which amplified amplicon size 272 bp. B- image shows gRNAs that were designed in different exons of *CKX5.* Green sequence indicate gRNA in the first exon, blue sequence indicate gRNA in the second exon and red sequence indicate gRNA in the third exon. Black sequence indicates exons, yellow sequence indicate intron, orange sequence in the first row indicates the promoter and blue block indicate start codon. Green arrows indicate the forward primer and grey arrow indicate the reverse primer for gRNA in third exon.

The previous student had transformed *PIN7::PIN7:GFP* but not the 56B2 line with these constructs, but had not selected primary transformants or taken this work further. I transformed the 56B2 line using the same construct, and selected T1 transgenic plants for both 56B2 and *PIN7::PIN7:GFP* were selected using antibiotic basta resistance gene (PTT, 10 µg/ml).

DNA for T2 plants was extracted, 35 WT plants (15 putatively guide 1 and 20 putatively g2) as well as 10 56B2 plants (3 putatively with guide 1 and 7 with g2). PCR were performed for the DNA from 45 plants (T2) to amplify a 272 bp fragment flanking the PAM site (Figure 6.5 A). After that, PCR products were sent for Sanger sequencing via Source Bioscience (https://www.sourcebioscience.com/). These were aligned with reference gene using benchling (https://www.benchling.com/), but the sequence was wild type.

In order to understand why this gene-editing did not work, it was asked if the construct was correctly incorporated within the plants. To do this, another PCR was performed using primers to amplify the Cas9 gene that produced amplicon size 514bp. When the PCR was run none of the CRIPSR lines introduced into *PIN7::PIN7:GFP* produced a band of the correct size. That means that there was a likely to be a problem with the transformation, and it is possible that true transformants did not picked.

6-4 Designing and building a CRISPR/CAS9 construct using pKIR1.1 plasmid

Rather than continuing to trouble shoot this process, other options were considered for producing new CRISPR lines. A recent paper had shown that driving Cas-9 under a germline- specific promoter has been shown to increase the efficiency of CRISPR/Cas-9 in *Arabidopsis* (Miki et al., 2018). This approach had been used

successfully by a colleague in my lab to create a spectrum of mutations in the AHP4 gene. Therefore, it was decided to use the same highly efficient CRISPR/Cas9 vector (pKAMA- ITACHI Red (pKIR) vector). Also, rather than using the same guide RNAs that had not worked previously, new guide RNAs were designed that utilize PAM sites in different exons (Figure 6.5 B).

Tsutsui & Higashiyam (2016) created a new CRISPR/Cas9 vector that is highly efficient for *A. thaliana*, termed pKIR. They used the promoter of a gene expressed from an early embryonic stage to express Cas9, *RIBOSOMAL PROTEIN S5 A* (*RPS5A*) (Weijers et al. 2001), as its promoter is constitutively active in egg cells (Maruyama et al. 2013). Expression of Cas9 continuously from egg cells produces high efficiency mutation induction already in the T1 generation. Moreover, they created non-destructive method to select Cas9-free plants by using pFAST-R (Shimada et al. 2010) backbone vector with an expression cassette of OLE1–TagRFP (red fluorescent protein) that exhibits red fluorescence in seeds. This has several advantages, not only does it allow selection of primary transformants without antibiotics, but it also facilitates subsequent selection of plants without the Cas9 insertion.

Various sgRNAs were prepared for different target sequence of *CKX5* in exon 1, 2 and 3 (Figure 6.5 B). It was decided not to solely produce guide RNA in exon 1, based on unpublished work by a collaborator had created CRISPR mutants for his gene of interest. For his gene of interest (undisclosed here as his work is unpublished), He recovered several miss-sense mutants within the first intron. Despite the fact that knockouts in this gene had previously been shown to have a strong phenotype, all the miss-sense mutations that he uncovered in the first exon were phenotypic. He later

showed that this was due to the usage of an alternative translational start site that skipped over much of the first exon (data unpublished).

As Cas9 recognises and binds to PAM sequences found in the gene, gRNA was designed near a PAM sequence. The pKIR system recognises the NGG sequence as a PAM, and suitable gRNAs were designed using the CRISPOR website http://crispor.tefor.net/crispor.py The important domains in CKX proteins are FAD-binding and cytokinin-binding domains (Dabravolski and Isayenkov, 2021). The FAD binding domain is present in many catalytic enzymes. Therefore, it was ensured that one guide RNA was located within each domain.

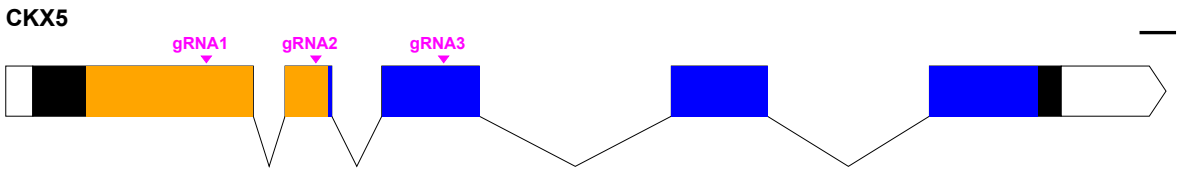

Figure 6.6: Schematic showing the intron exon structure of *CKX5*. Exons are shown with solid shading, and introns with a black line. 5 and 3' UTR regions are shown in white. The FAD-binding domains is shown in orange and the cytokinin dehydrogenase domains in blue. Location of three guideRNA shown in pink. The locations of each component were mapped in Benchling with the final figure being made using WormWeb. The scale bar is 100 bp.

Cloning sgRNAs in the pKIR system is easy and quick. pKIR1.1 has two restriction enzyme sites (*Aar*I) between the U6.26 promoter and sgRNA scaffold. Digestion of the pKIR1.1 plasmid with the *Aar*I enzyme forms four base overhangs, so sequence with complementary overhangs can be inserted into this site. The complete vector can be created by annealing two 23 bp primers with the correct overhangs for subcloning into pKIR-1. Firstly, the two guide RNA primers were annealed. pKIR1-1 was then cut using the *AaRI* enzyme. This enzyme cuts outside of the recognition site, and leaves sticky

ends that the annealed primers can be ligated to. This construct was then be transformed into chemically competent cells (DH5μ) by heat shock and colonies selected. This procedure was followed and found colonies in plates that contain gRNAs for exon 2 and 3, but did not contain colonies for the gRNA for first exon. Therefore, it was decided only to continue with these two guides. These colonies were then grown in 5 ml cultures, and the plasmids were extracted and sequenced to confirm incorporation of the guides. After checking the sequences, it was found that gRNA was correctly inserted in the correct site between *AarI* site in both constructs. Then, the plasmid contain gRNA in exon 2 was transformed into *A. tumefaciens* and transformed into plants (*PIN7::PIN7:GFP* & 56B2) by floral dipping.

Firstly, T0 seeds were identified using the Leica MZ10F dissecting microscope to identify primary transformants. These were easily identifiable as they had strong red fluorescence in the seed. Primary transformant seeds were sown out to generate T1 plants. DNA was extracted from 35 plants and PCR was run using primers that designed flanking the PAM site. After that, PCR products were sent to the sequence using Sanger sequencing via Source Bioscience (https://www.sourcebioscience.com/). There was no change in the sequences when they aligned with *CKX5*. So, then was decided to use the gRNA in exon 3 and transformed it to *A. tumefaciens* then to the *PIN7::PIN7:GFP* & 56B2 lines.

T0 seeds were screened via screening microscopy to select seeds expressing the red seed coat marker. Primary transformants were plated out on 1/2 MS plates to generate T1 plants and keep in growth chamber under long day conditions. DNA were extracted from 15 *PIN7::PIN7:GFP* plants and 20 56B2 plants. PCR were performed using primers flanking the PAM site that amplified 640 bp. Purified PCR product send to

sequence by Source Bioscience. The sequences did not reveal any lines with altered *CKX5* sequence.

Due to a combination of time constraints and results of other experiments (see also next chapter) challenging our hypothesis that mutations within the *CKX5* promoter were responsible for the observed changes in PIN7, these constructs were not taken further.

6.5 Discussion

Two independent approaches were designed to investigate the relationship between the 56B2 mutant and *CKX5* expression and test the hypothesis that changes in the expression of *CKX5* led to alterations in the levels of *PIN7*. The first approach involved comparing the expression of GFP when driven under either the *CKX5* or the *CKX5mut* promoter. Here, two independent homozygous lines for pro*CKX5::GFP* and four independent homozygous lines for pro*CKX5mut::GFP* were tested. These were visualised via confocal microscopy to explore changes in gene expression, and then the intensity of fluorescence and quantity of *GFP* mRNA was measured. Measurements of fluorescence revealed that expression in the lines pro*CKX5::GFP* that contain the promoter with the intact poly (dA-dT) tract was higher than three out of four of the lines pro*CKX5mut::GFP* without intact poly (dA-dT) tract. This was opposite to our initial theory. However, to be certain this would require analysis of a greater number of primary transformants. Whilst microscopy analysis considered only expression at the root tip, qRT-PCR was used on whole root samples and measured *GFP* mRNA across a wider spatial range. There was a surprising disagreement

between the two datasets, indicating that these results might be affected by stability of either the mRNA or the GFP protein. However, despite these variations, the hypothesis suggests that mutations in the poly (dA-dT) tract made the DNA more accessible to transcription factors that led to over expression, is not yet supported by this experiment.

It has been know that transgenic insertion events are known to occur at random and often in multiple places through the genome (Gelvin, 2003, Gelvin, 2017). It is therefore possible that in the previous transgenics the construct was inserted in regions with a different epigenetic context. It is known that the epigenetic landscape surrounding t-DNA insertions can be complex. For example, Jupe et al. (2019) investigated the genome structure surrounding four *Arabidopsis* T-DNA transformed plants. They identified multiple inserts, including, in one line, seven genomic changes including three insertion events, an inversion, an inverted translocation in the chromosome, and a swap between chromosome arm ends by using a combination of long-read sequencing and DNA visualizing tools. They also reported changes in chromosome marks including trimethylation of H3K4 and H3K27. Therefore, examining changes within the poly (dA-dT) tract within *CKX5* within its native context may provide a more accurate picture of the role that it may play on transcription (next chapter).

In this project it was also attempted to validate the causality between *CKX5* and *PIN7* through producing intragenic mutations in the 56B2 line within the *CKX5* gene. Two approaches were used, one based on constructs built by a previous student, and one based on constructs that I designed and built. Although CRISPR/Cas9 has been successfully used to generate gene-modified mutations plants in *A. thaliana*, there

some problems that have yet to be resolved (Tsutsui & Higashiyama, 2016). For example, non-specific cleavages (off-target mutations) can occur during genome editing, so the specificity of CRISPR/Cas9 have to overcome this (Osakabe et al. 2016). This was addressed by using software to design the guide RNA. The problem in this project was lack of expected mutations in the gene of interest. Tsutsui & Higashiyama developed highly efficient CRISPR/Cas9 vector for *A. thaliana*, pKAMA-ITACHI Red (pKIR). Their results suggest that the pKIR system is a powerful molecular tool for genome engineering in *Arabidopsis*. However, using this vector didn't work in this case in creating knockouts within the *CKX5 gene*. While one of my colleagues used the same construct with another gene, AHP4, and reported that 1:5- 1:10 T2 plants were mutant. These included a number of single nucleotide changes as well as some larger (ca.33 bp) deletions. It might be because the packaging of the chromatin around the gRNA sites in *CKX5* did not allow the Cas9 protein to access in this case.

Chapter 7. Does variation within the *CKX5* promoter contribute to phenotypic diversity in natural populations?

7.1 Overview:

Chapter 6 examined the effect that a polymorphism in the poly(dA-dT) tract within the *CKX5* promoter has on expression of GFP by studying independent lines of pro*CKX5mut::GFP* and pro*CKX5::GFP*. The results showed that this did not result in elevated GFP expression. Another independent avenue with which to explore the relationship between the poly(dA-dT) tract and *CKX5* expression is to exploit the enormous pool of diversity present in natural accessions of *Arabidopsis*. This would enable to firstly investigate whether this region of the promoter is conserved across diverse *Arabidopsis* accessions. If sequence variation is present within the poly(dA-dT) tract, this will secondly provide ideal germplasm with which to confirm or challenge our hypothesis that this region influences *CKX5* transcription.

Investigating the role of the poly(dA-dT) tract within natural accessions provides a number of potential advantages over solely using transgenic plants. Within the natural accessions the poly(dA-dT) tract will be in its native genomic context. If there are variations within this, then the biogeography of these alleles can be considered, and this may provide insights into any functional benefit that the sequence region may confer.

It is known that DNA accessibility to transcription factors is affected by the positioning and post-translational modification of nucleosomes. Therefore, looking at the DNA within the native *CKX5* promoter will be an improvement on analysing transgenics. This is because the native DNA contains all DNA and chromatin modifications. This is not necessarily the case with transgenes.

With current advances in both whole genome sequencing and the wide repertoire of available databases, it is highly feasible to search natural accessions for specific polymorphisms. Along with other scientists, Weigel & Mott (2009) began a longstanding project to describe whole genome sequence variation of 1001 accessions of *A. thaliana*. The 1001 Genomes Project provides full genome sequences for 1,135 natural *Arabidopsis* accessions (Alonso-Blanco et al., 2016). This project involves ecotypes collected from different parts of the world, with the aim of understanding how the genetic variation within the individuals of the same species translates into the pool of phenotypic and environmental diversity biology present in nature (Ferrero-Serrano and Assmann, 2019).

In this chapter, the 1001 genome project data was used to identify natural accessions that were either similar to our wild-type (Col-0) or our mutant (56B2), i.e. those with either an intact poly (dA-dT) tract upstream of *CKX5* and or those without. Seeds were ordered from NASC for these lines. Firstly, the promoter region of these lines was re-sequenced to confirm the sequence over the poly (dA-dT) tract. Then, the expression level of *CKX5* and *PIN7* mRNA was measured to test the hypothesis that the poly (dA-dT) tract altered *CKX5* expression. Finally, phenotypes of these lines were observed to investigate whether the phenotypes observed in 56B2 were present in lines with similar polymorphisms.

7.2 Identifying polymorphisms in the *CKX5* promoter in natural accessions.

To examine whether regulation of *CKX5* via the poly (dA-dT) tract may have a role that perturbation of cytokinin levels in natural populations, we looked for polymorphisms in the *CKX5* promoter using data from the 1001 genome project. To

search the 1001 genome database, we started with a region of genomic sequence on Chromosome 1 corresponding to the *CKX5* promoter (Chromosome 1 2831912-28319229), that contained the 17 A's in a row. Within the promoter there was considerable sequence variation, however using the web interface, there was not a clear way to search for intact versus non-intact poly (dA-dT) tracts. To investigate this further, Dr.Rahul Bohosale (university of Nottingham) used a programme that he had developed for a previous project. This programme scans for specific motifs in upstream of genes. He used the poly (dA-dT) tract (17 As bp) as a motif search and exported a file with the found motifs from each of the genomes within the database. He then calculated an alignment score between the input motif (Gmotif) and the Found Motif (Fmotif). In this case a 100% score meant that the motif was intact. Additionally, he exported data for each motif incorporating #Ns (Number of N's (ambiguous nucleotide) found in the motif), #As (Number of A's found in the motif) and #O (Number of other nucleotides (T, G, C's) found in the motif). He also exported basic information, such as the accession name, the location in which it was collected and the name of the collector.

Immediately apparent from this is that the quality of the genome sequences in this region was not high. Of the 1135 genomes available, 1099 had at least one N within this motif. This analysis identified 154 ecotypes in which all 17 nucleotides in the motif query were ambiguous, and a further 194 in which five or more of the nucleotides were ambiguous. These ecotypes were discounted from the analyses and focused on the ones in which the poly (dA-dT) tract was best resolved. We then assembled two lists of ecotypes; one that shows at least one non-ambiguous mismatch with GMotif (#O) (235 ecotypes), and one that contains no non-ambiguous mutations (552 ecotypes), potentially with a complete poly (dA-dT) tract. If it is assumed that there is no bias in

the quality of the sequence related to the continuity of the poly (dA-dT) tract, this suggests that the majority of accessions may be like Col-0 in containing a poly (dA-dT) tract within the *CKX5* promoter. If only sequences without any ambiguity were accepted, a scenario in which only one ecotype has an intact poly (dA-dT) tract and 35 do not was presented. Based on these findings, it was attempted to select a series of accessions with an intact poly (dA-dT) tract and another series without an intact poly (dA-dT) tract. This would then be used to study whether the expression of *CKX5* is different in these lines. Due to the high level of sequence ambiguity, some ecotypes that contained an N within this sequence were selected. The rationale behind this was that the ambiguous nucleotides might be A, and represent an intact poly (dA-dT) tract, but this would only be determined via further sequencing. Where possible pairs of ecotypes (one potentially with and one potentially without an intact poly (dA-dT) tract) from the same geographical region were chosen. With this logic, 12 ecotypes were selected.

7.3 Geographical distribution of mutations within the poly (dA-dT) tract of *CKX5*

The 1001 genome project provides information about where the natural accession was collected from. It was exploited to look for distribution of the lines identified with and without the poly (dA-dT) tract. The category of ecotypes was first considered that show at least one nucleotide mismatch within the poly (dA-dT) tract. It was noticed that these were mainly distributed in Europe and North America.

Google map shows the locations of the natural accessions that have the same polymorphism as 56B2 (without an intact poly (dA-dT)) in Europe (Figure 7.1). The poly (dA-dT) tract for these accessions has other nucleotide in the sequence. It reveals

that the natural accessions distribute in most countries such as Sweden, Spain, France and Czechia. It is illustrated from the map that Sweden has many, but there are some in other places too. Majority of ecotypes in 1001 genome project from Sweden (22%), Spain (20%) and USA (18.75 %) according to the information provided by Dr. Rahul Bohosale.

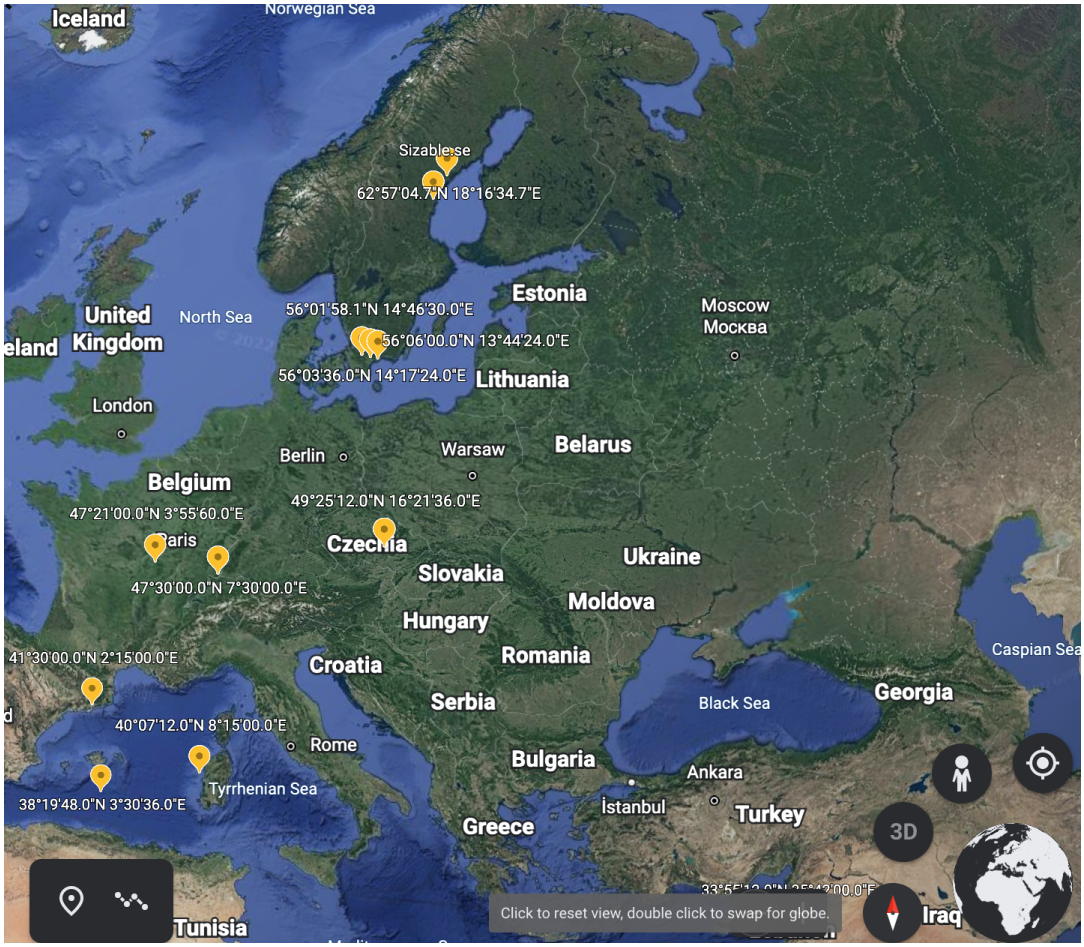

Figure 7.1: Location of selected natural accessions on the map.

Google map illustrates the location of 11 natural accessions without intact poly (dA-dT) tract similar to 56B2 in Europe.

Given the widespread locations of lines that have similar polymorphisms to 56B2 suggests that variation within the poly (dA-dT) tract is well mixed within the local population. There is no clear association with either a particular area, or an immediate link to a specific climate that may be present if the variation was associated with a local adaptation. That raise the question what does the effect this polymorphism in the poly (dA-dT) has on growth and development? Studying these lines will give better understanding if the poly (dA-dT) tract controls the expression of CKX5 in *planta*. To attempt to answer this question a number of these accession were ordered from ecotypes collected in Spain, Sweden, Bulgaria, and Slovakia.

7.4 Genotyping analysis of natural population lines.

Twelve natural accessions lines were selected and ordered from NASC (table 4). Due to the high level of sequence ambiguity the first task was to verify the sequences provided by the 1001 Genome Project and resolve the ambiguous bases.

Table 4: Selected ecotypes from 1001 genome project. The table illustrates the name of the accession, their location (country) and the sequence of the poly (dA-dT) tract in the promoter within the *CKX5* based re-sequencing. The ability of plants to produce flowers and seeds to germinate is listed.

Accession	Location	confirmed by resequencing	Germination	Flowering
Kardz-1	BUL	AAAAAAAAAAAAAAAA	Some	Yes
Kardz-2	BUL	AAACAAAAAAAAAAAA	yes	Yes
Bela-4	SVK	AAACAAAAAAAAAGAA	no	N/A
Bela-2	SVK	AAACAAAAAAAAAA--	yes	Yes
Hov1-7	SWE	AAACAAAAAAAAAAAA	no	N/A
Hov1-10	SWE	AAACAAAAAAAAAAAA	Yes	Yes
Nyl-2	SWE	AAACAAAAAAAAAAAA	Yes/little	Yes
Nyl-7	SWE	AAACAAAAAAAAAAAA	Yes/little	Yes
Fja1-2	SWE	AAACAAAAAAAAACAAA	No	N/A
Fja1-5	SWE	CAAACAAAAAAAAAAA	No	N/A
IP-Lch-0	ESP	AAACAAAAAAAAAANN	Yes	Yes
IP-Lam-0	ESP	AAACAAAAAAAAAGAA	yes	Yes

Seeds were sown out on ½x MS and plates, kept in dark for 2 days, then moved to the growth chamber under long day condition (16h days) for 14 days before being moved to soil. DNA was extracted from leaves for all the natural accessions, with two plants sampled for each ecotype, except Kardz-1 – where 5 plants were selected, and 7 plants of Kardz-2 were selected. A region of the *CKX5* promoter flanking the poly (dA-dT) tract was amplified via PCR to produce a 550 bp fragment (Figure 7.2). This fragment was purified and sent to be sequenced to ask if that they matched the sequence annotated on the 1001 genome project.

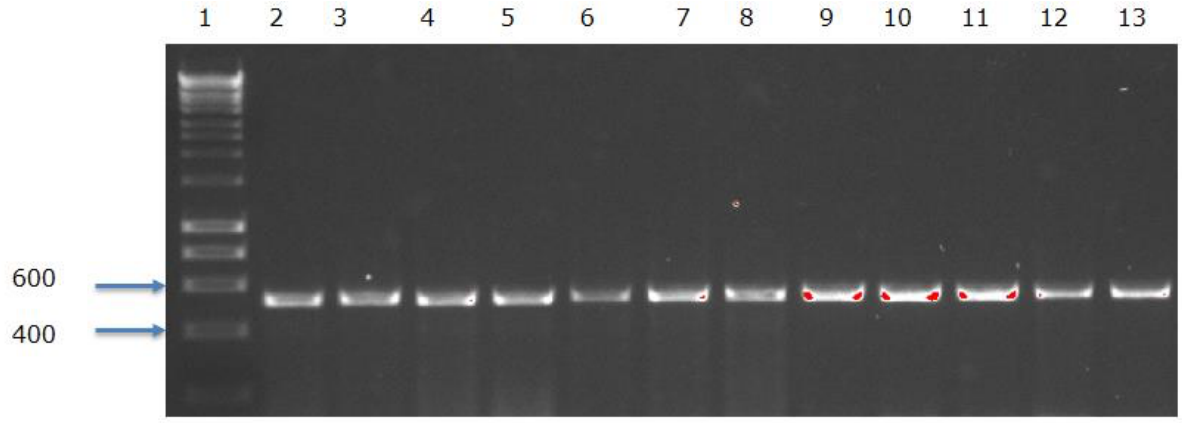

Figure 7.2: PCR was performed for natural accessions to amplify a *pCKX5* fragment of 550 bp.

1%(w:v) agarose electrophoresis gel run at 80 A for 1h. Lanes from 2-13 illustrate PCR products from one replicate from each of the natural accession lines. A product was amplified from every accession at 550 bp. Lane 1 is hyper ladder 1kb which used as a marker. Lane 2= Nyl-7, 3= Kardz-1,4= Bela-2,5= Bela-4, 6= Kardz-2, 7= Fja1-2, 8=Fja1-5, 9= Hov1-10, 10= Hov1-7, 11= IP-Lam-0, 12= IP-Lch-0, 13= Nyl-2.

Ecotype sequences were aligned with the Col-0 sequence using the Benchling website. Despite the fact that 6 accessions were selected that were thought would have an intact poly (dA-dT) tract, and 6 which were predicted would not, it was found that 11 out of 12 accessions have a polymorphism in the poly (dA-dT) tract, and only

one ecotype has an intact poly (dA-dT) tract. This was a surprise as it differed so radically from the sequences within the database.

Of particular interest was the Kardz-1 and Kardz-2 alleles. Like Col-0, Kardz-1 has 17 A in the promoter of *CKX5,* while like 56B2, Kardz-2 showed a substation of the fourth A to C. Coincidentally, this was exactly the same polymorphism as seen in 56B2. It was fascinating to note that exactly the same change that happened via chemical mutagenesis, could be observed in natural environment. Interestingly, most of natural populations that were sequenced have C instead of the fourth A (table 4). Therefore, Kardz-1 and Kardz-2 were selected for further study due to their similarity to Col-0 and 56B2 respectively. *CKX5* and *PIN7* expression as well as the phenotypes seen in 56B2 were studied.

Kardz lines had been collected from Bulgaria which is located in South East Europe. The Kardz plant has a large rosette with numerous and narrow leaves. The flowering time delay comparing to Col-0, as Kardz plant starts flowering after more than 50 days while Col-0 completes the life cycle within 8 weeks (https://www.arabidopsis.org). The seeds of Kardz were donated as part of 1001 Genomes project by Bergelson laboratory at the University of Chicago (USA) (https://www.arabidopsis.org).

Whilst Col-0 and many other ecotypes grow well in our growth facilities, this is not the case for all the natural accessions. In some cases, the accessions may be biennial, in other cases it may require specific conditions such as day length in order to induce flowering. Growing these natural accessions was complex, involving both germination and flowering.

Seeds from NASC were sterilised, sown on ½x MS then plates keep at 4 ^{o}C for 2 days then moved to the growth chamber. However, not all seeds germinate. The plant that germinated were all moved to soil. In all of these lines flowering was delayed and took more than 3 months. Many *Arabidopsis* accessions require a period of vernalization to accelerate flowering (Henderson and Dean, 2004). This is not well documented for every accession, and it might that this is the case for these lines. I tried an alternative approach to induce flowering and sprayed all plants with GA. This approach stimulates some lines to produce flowers and then seeds, but not in all. Even where the accessions flowered, the number of seeds that produced was much fewer than in Col-0, and even in the next generation, some problems had faced with seed either germinating poorly or not at all. It was found that keeping plates in dark and cold for one week rather than the two days used for Col-0 helped to overcome seed dormancy and enhance germination.

7.5 Phenotypic analysis

To investigate whether the polymorphism within the poly (dA-dT) tract resulted in a phenotype similar to those observed in 56B2, Kardz-1 to Kardz-2 was compared using similar assays to those used in chapter 2 and considered both the shoot and the root. It has been mainly focused on studying leaf development and primary root length in the presence and absence of cytokinin, because 56B2 and Col-0 differed in these phenotypes.

7.5.1 Leaf development is altered in the Kardz lines.

Chapter 4, shoot phenotyping of 56B2 and Col-0 was performed. It was found that 56B2 produced more leaves than Col-0. If the alterations in leaf production in 56B2

were due to the polymorphism in the *CKX5* promoter, it was predicted that a difference in leaf number between Kardz-1 and Kardz-2 would be seen. In this scenario, like WT, Kardz-1 would show fewer leaves than Kardz-2, which is like 56B2. Therefore, similar experiments to those in chapter 4 were performed and measured the leaf number and leaf area in the two lines.

The leaf area for Kardz-1 and Kardz-2 was measured for 5 plants each with rosette leaves harvested 25 days after germination. As before, plants were grown in soil under long day conditions and ImageJ was used to measure the leaf area.

In this assay Kardz-2 was found to have significantly more leaves than Kardz-1 (Figure 7.3 A). The average number of leaves in Kardz-2 is 14 ± 1.1 and 10 ± 0.74 leaves in Kardz-1. This result was very similar to results shown in Chapter 4, in which 56B2 had a greater number of leaves than Col-0, although they were not significantly different.

Next leaf size was considered. The first eight leaves of Kardz-1 and Kardz-2 are of similar size. However, at this time point subsequent leaves in Kardz-1 are all small, whereas Kardz-2 continues to produce big leaves (Figure 7.3 B). A student T-test revealed that there is a significant difference in the size of leaf 9^{th} and 10^{th} leaf in Kardz-2 compared with Kardz-1.

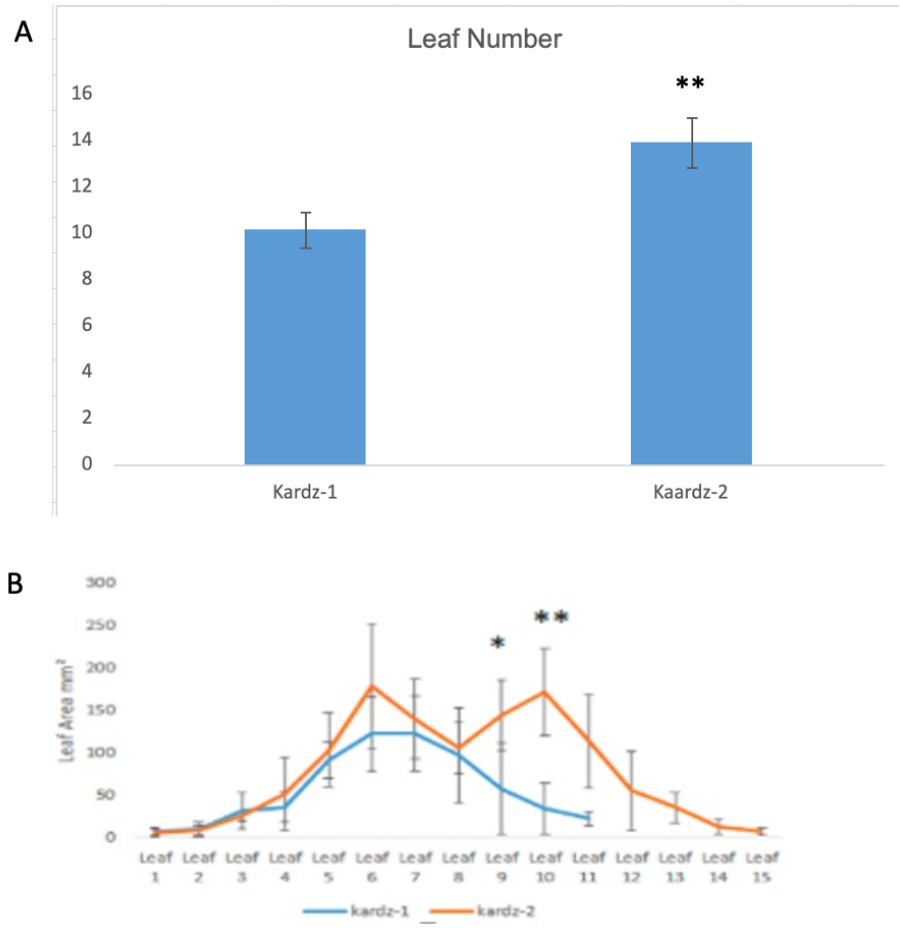

Figure 7.3: Kardz-2 has more and larger leaves than Kardz-1.
Rosettes were harvested 25 days after germination. Leaves from five plants per genotype analysed using Fiji image J software. A&B- shows that number of leaves in Kardz-2 (B) is more than Kardz-1 (A), T.test shows that number of leaves in the Kardz-2 is significantly more than Kardz-1 ($P < 0.01$). Leaves are arranged from the youngest. Each row presents the leaves for one plant. C shows the size of leaf area in mm² for Kardz-1 and Kardz-2. A T-test reveals that leaf 9 and 10 in Kardz-2 is larger than Kardz-1. Plants were grown in soil under long day condition (16h day) - **=p≤0.01,*=p≤0.05. Error bars= SD. n= 5 plants.

7.5.2 Investigating primary root length in Kardz lines.

In chapter 4, the effect of cytokinin on primary root length have been studied by growing plants (56B2 and Col-0) in medium supplemented with BA at different concentrations. It was found that 56B2 roots were more resistant than Col-0 to cytokinin over wide range of concentrations, especially at later time points (9 and 12 days). Therefore, a similar experiment was set up to measure the root length for Kardz-

1 & Kardz-2. Based on the behaviour of 56B2 and Col-0, it was predicted that Kardz-2 would be more resistant to the cytokinin than Kardz-1.

The experimental set up was identical to that have made previously for 56B2 and Col-0 (chapter 3). The appropriate amount of cytokinin (BA) was added to 0.5 x MS medium after cooling it to make the final concentration (25, 50 and 100 nM). Sterilized seeds were plated out into 4 plates for each concentration and kept vertically under 16h days in the growth chamber. Kardz-1 and Kardz-2 were grown in the same plates in different rows. For each concentration of cytokinin, 2 plates were prepared with Kardz-1 in the top row and Kardz-2 in the bottom row, and two plates have Kardz-2 in the top row while Kardz-1 was in the bottom.

Primary root length for Kardz1 and Kardz-2 was measured at 3, 6, 9 and 12 days using the RootNav software (Pound et al., 2013). The experiment was repeated twice as Kardz-1 seed had low germinate rates. From the previous experiment with low number of replicates present, a significant difference between 56B2 and Col-0 was only seen in one concentration (25 nM) at 6 days only, however increasing the number of replicates showed that 56B2 was resistant to cytokinin across a range of concentrations (25, 50 and 100 nM). However, the poor germination meant led to investigate only 8 seedlings for each line (Kardz-1 & Kardz-2). This occurred despite keeping plates at 4° C for 7 days to promote germination.

In the absence of cytokinin the primary root in Kardz-2 is longer than Kardz-1, with significant differences observed at 3,6 and 12 days (Figure 7.4 A). This is a different from the comparison between 56B2 and Col-0 where root length without cytokinin was similar. This may be due to differences in the genome unrelated to *CKX5*. Interestingly, Kardz-2 has the longest root among any samples of Col-0, 56B2 and Kardz-1 with root length about 60 mm in 12 days old seedlings.

Furthermore, Kardz-2 seedlings were more resistant to cytokinin than Kardz-1 (Figure 7.4 B). For example, at 25 and 50 nM BA Kardz-2 root longer that Kardz-1 root by about 3 mm at 9 and 12 days. However, when this examined more closely using students' T-test only few of the data were considered statistically significant. It shows that a significant difference in the root length within 3 days old among all the concentrations range between Kardz-2 and Kardz-1 plants. This result is similar to the first results seen in 56B2 and Col-0 in experiments with lower number of replicates when the statistical test showed significant differences in the root length at only a few time points. However, when the replicates number increased, it was found significant difference of root length between 56B2 and Col-0 in 25, 50 and 100 nM of cytokinin at 6,9 and 12 days. Increasing the sample number might would increase the statistical power and therefore the smaller differences in the cytokinin response between Kardz-2 and Kardz-1 might be more apparent. It might be given result similar to 56B2 and WT that shown in result chapter 2 that 56B2 more resistant to wide range of cytokinin concentrations than Col-0.

A

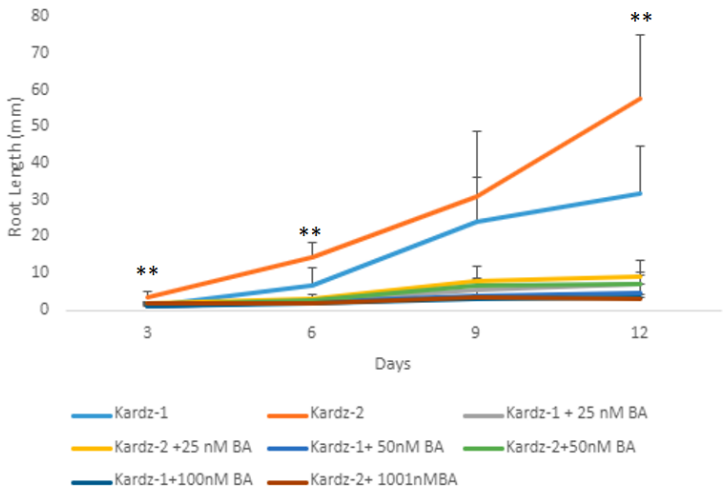

B

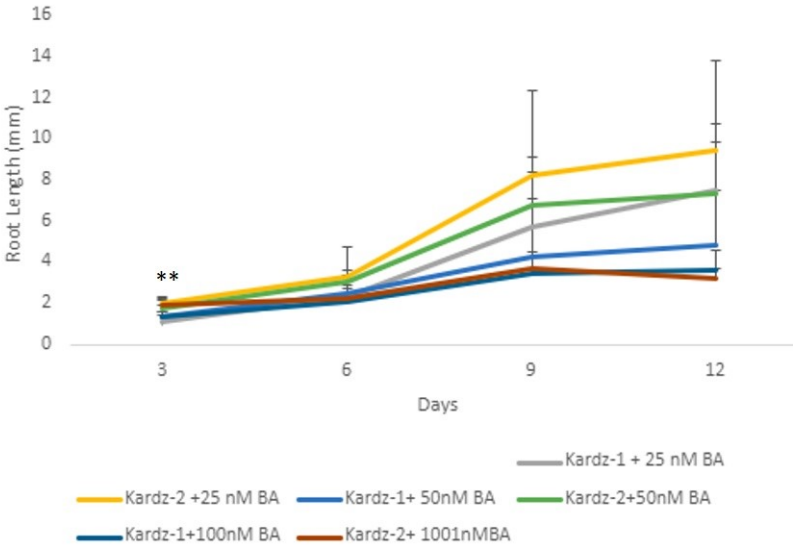

Figure 7.4: Kardz-2 is resistant to exogenous cytokinin at 3 days after germination with respect to root elongation. Kardz-2 and Kardz-1 seedlings were grown with different concentration of cytokinin (25 nM BA, 50 nM BA, and 100 nM BA) for 3, 6, 9 and 12 days. A students' T-test comparing growth in Kardz-1 versus Kardz-2 showed Kardz-2 root significantly longer than Kardz-1at 3,6 and 12 days without BA and only a statistically significant difference in growth at 3 days old in 25nM, 50nM and 100nM. B show only the cytokinin treatments. **=p≤0.01,*=p≤0.05. Error Bars=SD.n=8.

7.6 The expression of *CKX5* and *PIN7* is non-significant different in the Kardz lines.

To examine whether *CKX5* and *PIN7* mRNA was altered in the Kardz lines qRT-PCR was performed. RNA was extracted from the whole roots of 7 days old seedlings of Kardz-1 and Kardz-2, and 3 replicates were used for each and around 30 roots for each replicate. Then, cDNA was synthesised, and qRT-PCRs was run to measure levels of the *CKX5* and *PIN7* transcripts.

The level of *CKX5* mRNA is increased only slightly in Kardz-2 (Figure 7.5 A). Also, the mRNA levels of *PIN7* was tested. The level of *PIN7* in Kardz-2 was similar to that in Kardz-1 (figure 7.5 B). A student's T-test proved that there is not statistically significant different in either the level of *CKX5* and *PIN7* mRNA in Kardz-1 and Kardz-2. This is very different from the large differences observed in Col-0 and 56B2 in the first results chapter. Collectively, these qRT-PCR results do not support our hypothesis which state that the polymorphism within the poly (dA-dT) tract in the promoter of *CKX5* led to induce the expression of *CKX5* and therefore reduce the expression of *PIN7* by modulation the level of cytokinin and suggests a scenario in which the poly (dA-dT) does not bear a significant effect on the transcriptional level of CKX5 in the plant.

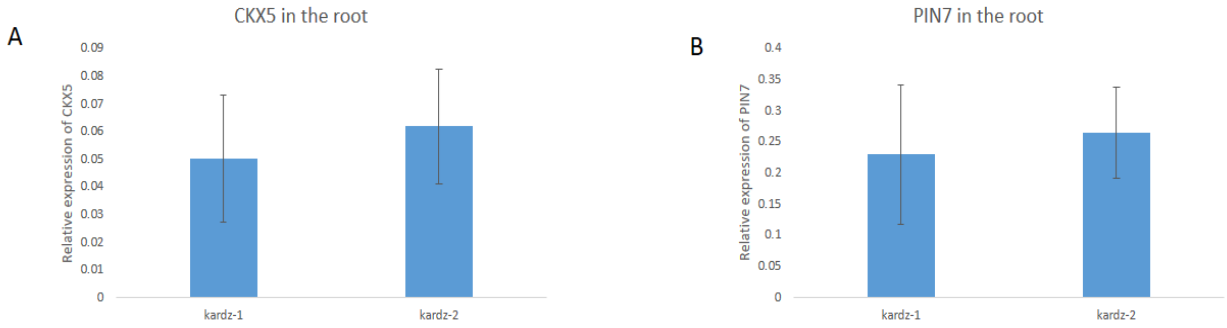

Figure 7.5: There is no significant difference in the mRNA levels of *CKX5* and *PIN7* in the Kardz-1 and Kardz-2 backgrounds.
The RNA from the whole roots of about 30 seedlings 7 days old was extracted for three replicates of each ecotype. qRT-PCR was run for *CKX5* (A) and *PIN7* (B). There is no significant difference between Kardz-1 and Kardz-2 in the level of the transcription of either *CKX5* or *PIN7* for whole roots. Error bars= SD.

7.7 Discussion

Several ecotypes were ordered from 1001 genome collection from different locations. At least 2 ecotypes as geographically close to each other as possible were ordered, with the aim of obtaining one that expected based on sequencing data would have an intact poly (dA-dT) tract and another without an intact poly (dA-dT) tract. The sequence provided in the 1001 genome was not high quality within this region as most of the genomes has at least one ambiguous nucleotide. Twelve ecotypes were selected and re-sequenced. After analysing sequences for each line, it was found that most of the ecotypes were unlike Col-0 in that they did not have an intact poly (dA-dT) tract. Kardz-1 was an exception to this as it has 17 consecutives As (an intact poly (dA-dT) tract). Based on this only two lines were pursued further; Kardz-1 that had a sequence similar to Col-0 and Kardz-2 that had a sequence similar to 56B2. This variation within natural populations provided an independent way to determine the role that the poly (dA-dT) tract in the promoter of *CKX5* plays on its expression.

The species *A. thaliana* contains individuals that can be classified as either summer or winter annual flowering (Lee et al., 1993). In the summer flowering lines, plants are annual and complete their lifecycle in one season (spring to summer) and the flowering does not commonly require vernalization. For winter annuals, plants germinate in the autumn and over winter in the rosette stage. In spring or early summer, they produce flower after exposure to vernalization. This biogeography is maintained in the laboratory, and winter annual plants require vernalization to accelerate early flowering. This variation in the flowering time caused problems when the natural populations were studied during my project. The flowering time for natural population (all lines that selected) was more than 60 days while the life cycle of Col-0 and 56B2 is about 8 weeks. Some lines that were analysed, such as *Bela-4 Hov1-7 Fja1-2* and *Fja1-5,* never flowered. It is recommended that vernalization (4ºC) at rosette stage for several weeks to promote early flowering for all lines except ecotypes from Spain (*IP-Lch-0* and *IP-Lam-0)* which are recommended to be vernalized for just one week (https://www.arabidopsis.org). Spraying plants with GA helped enhance flowering but may have been responsible for the germination problems that was faced later during germination. Also, other problems were faced where plants died before they were ready to be harvested or plants which give only few seed.

Comparing the phenotype of Col-0 versus 56B2 and Kardz-1 versus Kardz-2 was very revealing. Like 56B2 Kardz-2 did not have an intact poly (dA-dT) tract within the *CKX5* promoter. It also shared a number of phenotypic similarities with 56B2. Like 56B2, the number of leaves in Kardz-2 was found to be greater than the relevant control (Col-0 and Kardz-1 respectively). Like 56B2, Kardz-2 is also more cytokinin resistant than the relative control. Taken alone these phenotypic similarities in lines with and without the poly (dA-dT) tract suggest that these phenotypes could be tightly associated with

regulation of *CKX5*. There are also differences between the EMS and natural alleles. Kardz-2 has a root length phenotype in the absence of cytokinin, and this was not observed in other lines (Kardz-1, C0l-0 and 56B2).

To test if these phenotypes are associated with the poly (dA-dT) tract in the *CKX5* promoter it would be important to look for co-segregation of this polymorphism with the above phenotypes. Crossing Kardz-1 & Kardz-2 was performed but unfortunately plants died before harvesting. Had it managed to obtain F2 plants, it would determine whether plants homozygous for either the Kardz-1 or Kardz-2 polymorphisms within the *CKX5* promoter display the same phenotypes as their respective parents.

The hypothesis that the polymorphism within the poly (dA-dT) tract in the promoter of *CKX5* would result in the phenotypes seen due to over expression of CKX5 was not corroborated with qRT-PCR experiments. It was originally hypothesised that the phenotype of *PIN7::PIN7:GFP* observed in 56B2 state might be due to overexpression of *CKX5*. Based on this hypothesis it was expected that the expression of the level of *CKX5* mRNA would be greater in Kardz-2 compared to Kardz-1, and the level of *PIN7* mRNA would be reduced in Kardz-2. Therefore, the level of mRNA of *CKX5* and *PIN7* was measured via qRT-PCR. Whilst chapter 3 saw large changes in the level of *CKX5* expression between 56B2 and Col-0, only small non-significant differences between Kardz-1 and Kardz-2 was detected. The non-significant differences do not support our original hypothesis in which the polymorphism in the poly (dA-dT) tract in the *CKX5* promoter regulates expression levels for this gene. However, one important difference between these experiments was that in chapter 3 the level of *CKX5* was measured in the root tips, whereas in this chapter whole roots were used. It might be that local differences in levels of CKX5 expression in the root tip are masked by when looking at whole roots.

In order to examine the polymorphism in the *CKX5* across the natural accessions in context with changes in the mRNA sequence, an additional bioinformatic analysis was performed. This was performed by analysing SNPs within *CKX5* loci across the 12 natural accessions used in the previous experiment (alongside Col-0) based on sequence data from the 1001 genome project (Weigel and Mott, 2009). For every polymorphism the frequency of occurrence was counted (i.e., how many of the accessions contained this SNP). Additionally for SNPs in the exon, it was also noted if these resulted in synonymous or missense changes to the CKX5 protein. The analysis revealed several polymorphisms within *CKX5*. Six SNPs were found in the 3′ UTR, 1 SNP were found in 5′ UTR and 18 SNPs were found within the gene body (Figure 7.6 A&B). Of these 18, only five were found within the coding sequence, with the remaining 13 found within introns. Two out of the five SNPs resulted in only synonymous changes. SNP densities are 3.08 per kb within exons and 10.89 per kb within introns that means the density within introns higher than within exons. In most cases, SNPs were only identified in one or two accessions, that could represent recent variation. Collectively, these results show that there is a high degree of conservation within the *CKX5* gene, supporting the idea that this is an important and evolutionarily conserved locus.

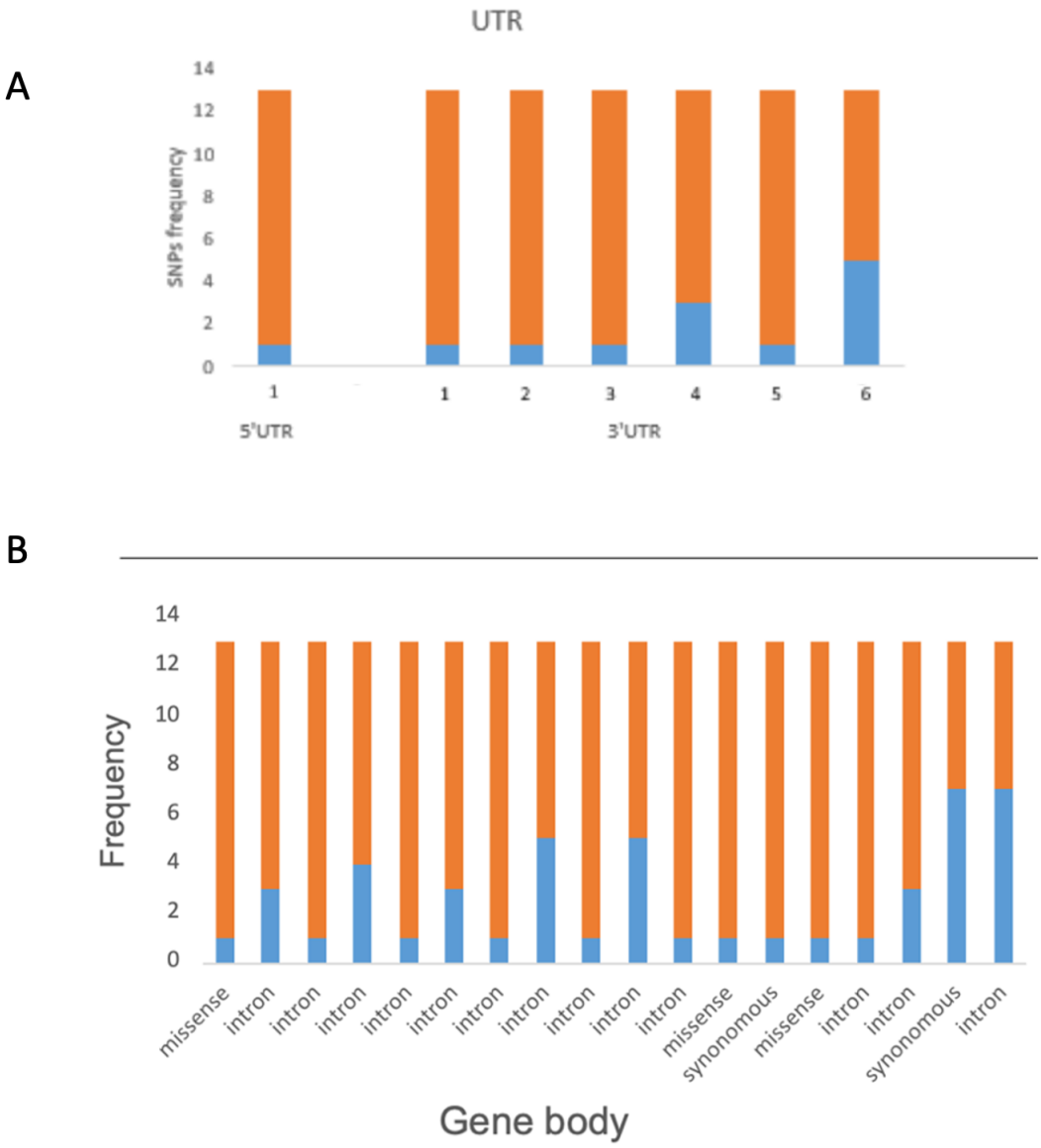

Figure 7.6: Polymorphisms frequency within *CKX5* amongst natural accessions.

A. The SNP frequency within the *CKX5* 5 and 3' UTR regions. This region is 1.08 kb and therefore has a density of 6.4 SNPs per kb. which is relatively few. The X axis indicate the position of polymorphisms within the UTR, with 1 occurring in the 5' UTR and 1-6 occurring in the 3' UTR. The two colours represent different alleles. B. SNP frequency within the gene body. The polymorphisms are arranged form 5-3' and SNPs within introns are marked. Additionally, for exons, synonymous versus missense mutations are marked. SNP densities are 10.89 SNPs per kb within introns and 3.08 SNPs per kb within exons.

Chapter 8. General discussion and conclusion

A previous student performed an EMS forward genetic screen of *PIN7::PIN7:GFP* to detect novel lines mis-expressing PIN7 in the root tip. Although he identified twelve lines showing altered PIN7 expression, this project focused on just one of the mutations, namely 56B2. After re-sequencing of the 56B2 genome at 50x coverage, the student identified a number of polymorphisms that were enriched in bulk segregant pools selected based on reduced *PIN7*. One strong candidate for in line 56B2 that may be causal to altered *PIN7* expression was a mutation within the *CKX5* promoter. *CKX5* is a member of the CYTOKININ OXIDASE/DEHYDROGENASE family which degrades cytokinin (Mok and Mok, 2001b). This seemed like a strong candidate because, by searching bioinformatic expression databases, it was found that CKX5 is expressed in vascular cells within the primary root tip, and because it is well documented that cytokinin response promotes the expression of PIN7 (Bishopp et al., 2011a).

Previously, there was incomplete temporal resolution about how “directly” cytokinin modulated the expression of PIN7. To address this knowledge gap, an experiment with a time series in which *PIN7::PIN7:GFP* was treated with cytokinin was set up. Plants at 3h, 6h, 9h and 12h timepoints were imaged. Changes in PIN7:GFP only after 12h cytokinin treatment was seen. Normally, PIN7 expression matches the domain of high cytokinin response and is located in the phloem and procambial cells flanking the xylem axis (Bishopp et al., 2011a). However, after 12h cytokinin treatment, it could be clearly seen that the domain of PIN7 expression had expanded into the xylem axis. These results were similar to those seen previously (Bishopp et al., 2011), however it was extended our knowledge of this interaction by showing that there was PIN7 expression was not responsive to treatments of cytokinin of nine hours or less.

After confirming the link between cytokinin response and PIN7 expression, this project was focused to the 56B2 mutant. This contains a mutation within a poly(dA-dT) tract upstream of the transcriptional start of *CKX5*. Presence of poly(dA-dT) tracts in the promotive elements of genes have previously been shown to have a role in modulating transcription of associate genes (Struhl, 1985). Although there is scant research in the role of poly(dA-dT) tracts in *Arabidopsis*, it was hypothesised that, like in other eukaryote systems, a polymorphism within such an element in the *CKX5* promoter could alter its expression. To this end, the level of *CKX5* mRNA in wild-type versus 56B2 was tested and saw higher levels of *CKX5* in root tips of 56B2 than it was observed in wild-type. This led to propose a hypothesis in which increased *CKX5* levels would occur in the root tips of 56B2. This would in turn reduce the pool of active cytokinin in these tissues, and therefore *PIN7* would be expressed at a lower level. In this project, it was set out to investigate the role of 56B2 closely. In particular, it was focused on the question of whether the alteration in the *CKX5* promoter was causal for the altered expression of PIN7.

If altered *CKX5* expression was behind the changes in PIN7 expression seen in 56B2, then it was reasoned that this effect may manifest itself in several ways. Firstly, as cytokinin affects many aspects of plant development, the 56B2 mutant may show a more pleotropic range of phenotypes associated with cytokinin responsiveness than purely the modulation of PIN7 expression. To this end, in chapter 4, a range of cytokinin-related developmental processes were examined in both the shoot and the root. Secondly, it was reasoned that if the mutation of 56B2 would affect *CKX5* levels, then it may do so in more tissues than just the root apical meristem. To investigate this further required an understanding of when and where CKX5 is expressed during development. To address this, in chapter 5, the expression of transcriptional *CKX5*

reporters were developed and analysed. This analysis prompted to then ask whether a mutation in the poly(dA-dT) tract upstream of *CKX5* would be sufficient to alter the levels of *CKX5* mRNA in the root. Here, three approaches were designed which were discussed in chapters six and seven. Although the research is presented as separate chapters, the work was done simultaneously. The first approach was based on transgenics. In these two versions of the *CKX5* promoter were created, one with and one without an intact poly(dA-dT) tract. It was hypothesised that like 56B2, the version of the promoter without an intact poly(dA-dT) tract would have higher levels of *CKX5* expression. The second approach was CRISPR based. Here, it was hypothesised that if the reduction of *PIN7* in 56B2 was based on elevated *CKX5* expression, then *PIN7* expression should return to a near normal level if over-expressing a non-functional version of the protein. Finally, it had been thought that as well as generating novel material to dissect the role of the poly(dA-dT) tract within the promoter, I may be able to exploit the variation that occurs within natural populations of *Arabidopsis*. this was done by exploring variability within the 56B2 promoter of germplasm sequenced as part of the 1001 genome sequencing project. Due to time restrictions, it was unable to complete all of this work, but it did provide key data that allowed to probe the question of whether the mutation reducing PIN7 expression in 56B2 was due to a polymorphism within the *CKX5* promoter.

8.1 Characterising the phenotype

Firstly, phenotypes that differed between 56B2 and wild-type (Col-0) were observed in both the shoot and the root. A range of phenotypes were studied relating to leaf number, lateral root density and sensitivity to cytokinin in a root elongation assay. Briefly, 56B2 developed more leaves than Col-0, showed increased lateral root density compared to Col-0, and roots were less sensitive to intermediate levels of cytokinin

(25-50 nM benzyl adenine). Given that all three of these phenotypes are in processes in which cytokinin is known to have an effect, this is supportive of a situation in which cytokinin levels may be affected more broadly in 56B2.

In many cases the phenotypic differences between the two lines were quite subtle. The project was started by only using twelve replicates for some of the root assays. During the course of this work, it has been learnt that increasing the number of replicates (in some cases to 27) was important to tease out the more subtle phenotypes. In the case of the leaf number, only five plants were examined. Although the difference between 56B2 and Col-0 was not statistically significant, it was close to being so. I think that, had I been able to look at a greater number of plants, then it is feasible that this difference would have been significant. The aim of this chapter was to survey whether the 56B2 line showed a broad range of phenotypes, rather than phenotypes that only related to the primary root apical meristem. Towards that aim, this chapter was successful in showing a broad range of phenotypes. It was not focus more on the phenotypes present but there is much more that could be done to explore these further. For example, it had only looked at emerged lateral roots in the lateral root density analysis. If looked at initiation too, it would be able to determine whether the defects observed in 56B2 were due to initiation or emergence.

Just as noteworthy as the phenotypes that were observed, were the ones that where did not presented a change. Given that the 56B2 mutant was identified as having reduced PIN7 in the root vascular cylinder, it would be expected to see phenotypes in the root apical meristem. Vascular patterning was investigated by comparing xylem differentiation in 56B2 and Col-0 but could not determine a difference between the two. This may not be surprising since a reduction (but not a complete loss) in PIN7 expression alone would be unlikely to produce a vascular phenotype, as single loss-

of-function *pin* mutants (except *pin1*) do not show root vascular phenotypes. Often multiple mutation in combination (e.g., *pin3 pin7*) are required to result in defects in protoxylem development (Bishopp et al., 2011). However, cytokinin is known to have a strong effect on xylem patterning. If *CKX5* was over-expressed, it may have expected to see vascular phenotypes. In this case too, the xylem axis is quite robust to changes in cytokinin levels. Even if the two of the three most root abundant cytokinin receptors are knocked out there are only weak and not penetrant phenotypes. For example, in the *cre1ahk3* double cytokinin receptor mutant, many individuals look like wild-type and only occasionally do plants produce ectopic xylem (Mähönen et al., 2006). Surprising too was that there was no phenotype relating to root meristem size, as it was known that PIN7 is mis-expressed in the root meristem of 56B2. However, this could be in part explained for a very tight spatial requirement for cytokinin in the transition zone of roots in order to determine root meristem size (Dello Ioio et al., 2008).

8.2 Studying the expression pattern by using reporter lines

Based on the wide range of phenotypes present in 56B2, it was reasoned that if changes in the levels of *CKX5* was responsible for these phenotypes, then it should be expressed in these tissues. This was based on the assumption that changes in a poly(dA-dT) tract may increase levels of expression, but would not necessarily drive expression in tissues which CKX5 is not normally expressed. To this end, the expression of two reporters were studied; a GUS line and a GFP line. These reporters were elected to use as they both offered different benefits: the GUS line would be useful to report the expression pattern of *CKX5* in a broad range of tissue types, including those that were awkward to visualise with our confocal microscope set up. The GFP reporter would allow more detailed cell level analysis of expression within

the root tip. To be carried out using the GUS reporter, it showed that CKX5 is expressed in the shoot apical meristem, the primary root tip and lateral root primordia. These findings are consistent with the broad range of phenotypes that were observed for 56B2 in the shoot and in the root. The analysis of expression in both lateral root primordia and in the shoot apical meristem was somewhat crude. With more time this could be extended to determine exactly when (i.e. in what stage) CKX5 is expressed in lateral root primordia. This could be more tightly coupled with phenotyping of lateral root initiation and emergence. In doing so, it could be explored at a temporal resolution whether the expression of CKX5 coincided with the lateral root phenotype in 56B2. Likewise, the observation of CKX5 in the shoot apical meristem, only looked at young seedlings about the time that the first two true leaves formed. If *CKX5* had a role in regulating the development of subsequent leaves, then it would be predicted that it would also be expressed in the SAM of older plants. This is a question that could be addressed using the material that was generated.

Additionally, the expression of CKX5 was examined in the root tip using a transcriptional GFP reporter. Here it showed that CKX5 is expressed in the procambium cells flanking xylem axis in the root tip, mirroring domains previously been shown to have high expression of PIN7 and a high cytokinin response (Bishopp et al., 2011). By using bioinformatic tools that provide spatiotemporal expression of genes such as eFP browser (Brady et al., 2007a) and scRNA-seq (Wendrich et al., 2020), it was confirmed that the data on CKX5 expression in the procambium cells matched data from these resources. Another advantage of GFP, is that it allows non-invasive imaging of gene expression in plants. This was exploited to look at the effect that cytokinin treatment would have in modulating *CKX5* expression. Although it was not a primary aim of this work, it was showed that *CKX5* likely plays a role in a mechanism

by which cytokinin feeds back on its own levels, as *CKX5* is induced by cytokinin. Collectively, these data were consistent with the idea that the mutation in the phenotypes in 56B2 could be caused by elevated *CKX5* expression. This encouraged development a series of experiments that would test this putative mechanism.

8.3 Transgenic lines and CRISPR/Cas9 explore whether the polymorphism in the promoter of *CKX5* cause the alteration in the level of *CKX5* and *PIN7*

A pair of transgenic lines were developed to test whether the polymorphism in the poly(dA-dT) in the *CKX5* promoter caused elevated *CKX5* expression in 56B2. The first line had the same mutation in the promoter of *CKX5* that is present in 56B2 (pro*CKX5mut::GFP*) and second had the wild-type promoter (pro*CKX5::GFP*). Both promoters were fused to GFP and confocal microscopy and qRT-PCR were used to compare their expression. Although the hypothesis was that changes in the poly(dA-dT) tract directly resulted in the increased levels of *CKX5*, an alternative hypothesis that could not be ruled out would be that in 56B2 there may be a mutation in a second site gene regulating *CKX5* transcription. By comparing both forms of the *CKX5* promoter, it could dissect the role that the poly(dA-dT) tract played. It has been known that transgenics have a wide range of line-to-line variation, therefore it was set out to obtain five independent lines for pro*CKX5::GFP* and pro*CKX5mut::GFP*. It was managed to obtain four for pro*CKX5mut::GFP* line and two for pro*CKX5::GFP*. Using both confocal to quantify GFP fluorescence, and qRT-PCR to quantify *GFP* mRNA, it was found that the expression and transcription of *GFP* in the lines with a wild-type promoter was greater than that in mutation promoter lines. It is hard to conclude with so few transgenics lines, but this preliminary finding was opposite the hypothesis. Taken alone, this data suggests that the polymorphism in the poly(dA-dT) tract is not

sufficient to make meaningful changes in the gene expression of *CKX5*. However, there are a few factors that need to be considered. Firstly, the total fluorescence and *GFP* mRNA do not correlate well. Only one of the two pro*CKX5::GFP* had higher levels of *GFP* mRNA than the two with the polymorphism, whereas both lines had higher fluorescence. This may be due differences in mRNA stability between the lines, but it may also be due to tissue specific differences. The qRT-PCR experiments were based on whole roots, whereas the confocal microscopy considered only the root meristems. With more time, the differences in the expression of *GFP* in the tissues in which it has been showing a phenotype in 56B2 could be explored, namely lateral roots and in the shoot apical meristem. In conclusion, even though this experiment would be better done with a greater number of transgenic lines, it suggests that alterations in the poly(dA-dT) tract do not significantly affect the levels of *CKX5* transcription in the root meristem. As this was the tissue in which *PIN7* was observed to be mis-expressed in the 56B2 mutant was identified, this is a strong case against my original hypothesis.

Whilst the previous result was not encouraging, it was not conclusive; it could be that the packaging around the nucleosomes was not the same in my transgenic lines as it is in the native context. In this case, the poly(dA-dT) tract may not have the same effect in the transgenics as in Col-0. In tandem, a CRISPR/Cas9 approach was pursued to produce intragenic knockouts in *CKX5*. Here, it was reasoned that if the polymorphism in the *CKX5* promoter caused changes in *PIN7* via modulation of *CKX5* levels, knocking out *CKX5* in 56B2 and Col-0 should equalize *PIN7* expression between the two lines. To develop CRISPR lines, the pKIR1.1 plasmid was used which has previously been shown to be a powerful tool for genomic editing in *Arabidopsis* (Tsutsui and Higashiyama, 2016). However, using a variety of guide RNA, it was failed

to obtain any plants with edited sequences. This was surprising as this plasmid had previously worked reliably when used in the lab.

Based on the fact that the results of the transgenics and of the natural variation (discussed next) both suggested that the polymorphism in the poly(dA-dT) tract was not associated with altered *CKX5* expression, this work does not pursue this further. Later it was found out that exposing *Arabidopsis* plants to short periods of heat stress at 37°C increases the number of mutations produced by Cas9 (LeBlanc et al., 2018). This is because the Cas9 enzyme is more active at higher temperatures. If CRISPR/Cas9 experiment were to redo, the same heat shock strategy would be incorporate into the design of experiments.

8.4 Studying the natural accessions with polymorphism similar to 56B2

Whilst it was working on the CRISPR/Cas9 lines, it also reasoned that if the poly(dA-dT) tract was important for determining levels of *CKX5* expression, then it would be expected to see it relatively well conserved across the wealth of *Arabidopsis* germplasm. Furthermore, if natural accessions with polymorphisms within the poly(dA-dT) track could be identified, then it could be tested whether these behaved the same way as 56B2. Not only the expression of *CKX5* could be examined, but it could be also tested whether these lines showed similar phenotypes to those that were observed in results chapter 4. Looking for variation in the poly(dA-dT) tract within the natural population in the 1001 genome project was complex ast the sequencing quality was quite poor in this region. Despite this, it was managed to identify a number of populations, some of which was predicted would have an intact poly(dA-dT) tract and some of which would not. Many of these lines had ambiguous bases within the poly(dA-dT) tract and by re-sequencing this region, it was discovered that many of the

accessions that had identified as potentially having an intact poly(dA-dT) tract, in fact had a polymorphism within this region.

It is intriguing to note that in context of the poly(dA-dT) tract within the *CKX5* promoter, the commonly used wild-type, Col-0, is somewhat of an outlier. Whilst Col-0 contains an intact poly(dA-dT), the analyses suggest this is something of a rarity. This was based on the following: only 1/36 of the genomes in the collection without an ambiguous base had an intact poly(dA-dT) tract, and only 1/6 lines that were identified as potentially having a poly(dA-dT) tract was able to be confirmed by re-sequencing. The seed batch of *Col-0* (carrying the *PIN7::PIN7:GFP*) certainly had the intact poly(dA-dT) tract as the 56B2 polymorphism was not present in any of the other 11 original EMS lines that were re-sequenced. Therefore, this is a real difference between Col-0 and most other accessions, and not due to an error in the Col-0 annotation. As my re-sequencing analysis involved European accessions, it is also possible that in other geographical locations, an intact poly(dA-dT) tract might be more common. This would be interesting to consider in the context of the original Col-0 lines, however the origin of these lines is not entirely clear. Although the Columbia lines were first described at the University of Missouri in Columbia by György Rédei (Rédei et al., 1992), they were originally taken from Friedrich Laibach's collection in the early twentieth century and have a Central European origin (Laibach, 1907).

Nevertheless, by re-sequencing this region, a line (Kardz-1) was discovered that had an intact poly(dA-dT) tract and a closely related line (Kardz-2) that had exactly the same polymorphism within this region as 56B2. It was amazing to find that a mutation produced randomly in the laboratory exists within natural populations, and even more surprising that this polymorphism would make Col-0 more similar to the majority of natural accessions. Based on the similarity of Kardz-1 to the Col-0 promoter (with an

intact poly(dA-dT) tract) and the similarity of Kardz-2 to the 56B2 promoter, it was set about examining whether the phenotypic differences between Col-0 and 56B2 were mirrored between Kardz-1 and Kardz-2.

It was found that like 56B2, Kardz-2 produced more leaves than Kardz-1. It also observed that like 56B2, Kardz-2 was resistant to cytokinin in a root elongation assay. These experiments would have benefitted from more technical replicates, but this was not trivial as there was difficulties with both seed propagation and germination. Given more time, these would have investigated more thoroughly and could have also looked at lateral root density. Next, the level of *CKX5* and *PIN7* expression in the Kardz lines was compared using qRT-PCR. It had predicted that the level of *CKX5* mRNA would be higher in Kardz-2. However, it was observed that the level of *CKX5* mRNA and *PIN7* mRNA in Kardz-1 and Kardz-2 was very similar.

When all the lines of evidence across the results chapters were considered, some of the results seem contradictory, suggesting that we do not yet fully understand the mutation. There are certainly similarities between 56B2 mutants and plants with altered cytokinin response; this is particularly evident in the experiment in which showed that 56B2 lines are resistant to cytokinin. With more time, it would be valuable to explore how attributable these phenotypes are due to alterations in cytokinin levels/response. This could be done simply by quantifying cytokinin levels in different tissues (e.g., root tips, lateral roots, shoot apical meristems) by mass-spectrometry. This can even be done for very small tissue samples (Antoniadi et al., 2015). Likewise, cytokinin response can be determined using qRT-PCR of known cytokinin primary response genes. However, whilst the 56B2 phenotypes are consistent with altered cytokinin response, the evidence that the polymorphism in the poly(dA-dT) tract causes alterations in *CKX5* is not present. Two experiments were finished to check

this. In both cases (transgenics in which GFP is driven by CKX5 and $CKX5_{mut}$ & comparisons between two related natural accessions with and without an intact poly(dA-dT) tract) the results from these experiments did not find any association between the poly(dA-dT) tract and *CKX5* mRNA levels. This was forced to challenge the initial findings in which *CKX5* showed increased expression in 56B2. To this end a new qRT-PCR was performed to measure the level of *CKX5* in 56B2. RNA was extracted from the root tips of 30 seedlings for each replicate. This new analysis yielded results quite different to the first experiment at the start of the project, and it was showed no significant difference in *CKX5* mRNA level in the WT and 56B2 (Figure 8.1). It is important to note that the environmental condition such as the light and temperature when the experiment was done could be affecting the expression of *CKX5*. It has been reported that light change chromatin organization and nuclear architecture which can modulate gene expression which effect plant adaptation (Bourbousse et al., 2015). Exposing *Arabidopsis* to temperature above 36°C induces alterations in nuclear architecture as reducing heterochromatin compaction (Pecinka et al., 2010). Furthermore, temperature regulates transcriptional responses, for example it was found that in *Arabidopsis* when plants are exposed to low temperature over long periods flowering is induced by repressing the expression of floral transcriptional repressor *FLC* (Sheldon et al., 2002). Moreover, the different in the time of day in the growth chamber and seed background as seeds used in the experiments from different bags could impact on the result. Consequently, the result of experiment might be affected by any changes or different in experiments condition between these two experiments. Taken together this new result, the fact that neither the poly(dA-dT) tract within the promoter of transcriptional reporters driving GFP nor the fact that two closely related natural accessions with differing sequences in their poly(dA-dT) tract

show altered levels of *CKX5*, supports a scenario in which mutation in the poly(dA-dT) tract does not affect expression of CKX5 at the root tip. It is worth noting that here the level of *CKX5* was measured in the root tip only. There is possibility that the level of *CKX5* is increased in other tissues. With more time, it could be valuable to measure the level of *CKX5* in different tissues, such as lateral roots, leaves and the shoot apical meristem. It is also worth noting that it is known that cytokinin is transported long distances from shoot to root (Matsumoto-Kitano et al., 2008) and that cytokinin transported by the phloem is required for correct vascular patterning and expression of *PIN7* in the root tip (Bishopp et al., 2011b). Therefore, it is still a possibility that depletion of cytokinin levels in other tissues, results in less phloem transported cytokinin and therefore causes non-autonomous effects at the root tip.

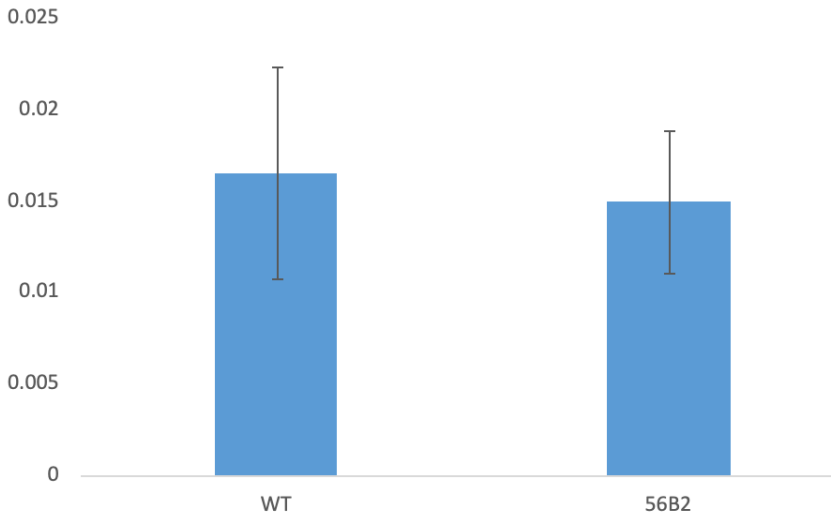

Figure 8.1: There is no significant different in the mRNA level of *CKX5* in Col-0 and 56B2 background.

The RNA from the root tips of 30 seedlings were harvest when they were 7 days old. Three biological replicates were performed for each sample. Student T-test showed that there is no significant difference between Col-0 and 56B2 in the level of transcription of *CKX5*. Error bars=SD, n=30.

Collectively, these findings leave two outstanding questions. Firstly, is there any basis for the phenotypic similarities between 56B2 and Kardz-2? Secondly, is *CKX5* involved in regulating PIN7 and vascular patterning in the root apical meristem?

With the data produced in this project, it is not possible to determine whether the mutation in the *CKX5* promoter is causal for the phenotype in the shoot. Indeed, it would seem surprising that both 56B2 and Kardz-2 share this polymorphism, and both have an almost identical effect on leaf number relative to their respective wild-types. This may be coincidence, or it may be related to the mutation within the poly(dA-dT) tract. One important way to test this, would be to cross Kardz-1 and Kardz-2 to test whether the mutation and the phenotype related to leaf number co-segregate. Here, the F1 generation will consist of plants heterozygous for both polymorphisms. In the F2 generation, 1/4 of the plants would be homozygous for the Kardz-1 allele, and 1/4 of the plants would be homozygous for the Kardz-2 allele. If the polymorphism in the poly(dA-dT) tract in the promoter of *CKX5* is linked to the shoot phenotype, then the plants homozygous for Kardz-2 would have more leaves than those containing a Kardz-1 allele. This cross was attempted to make, but unfortunately, this was not successful due to the challenging requirements to grow these lines. The same is true for Col-0 and 56B2. Although the 56B2 mutant was backcrossed three times, co-segregation of leaf number was never followed. If these experiments showed that the leaf number phenotype was linked to the *CKX5* promoter, then it would make sense to consider the level of both *CKX5* expression and to measure cytokinin levels in the shoot. To examine whether there was a possibility that this mutation in the poly(dA-dT) tract could behind the leaf phenotype independently of *CKX5*, other transcripts near this motif were looked. Interestingly, there is an antisense long non-coding RNA transcript nearby recorded in the *Arabidopsis* information portal (Araport) 11

annotation. There is no information about the expression pattern of this non-coding RNA in any of the commonly used bioinformatics resources. If the data above provided a link between the *CKX5* promoter and the shoot phenotype, this could be further explored by knocking out *CKX5* and potentially the non-coding RNA via CRISPR as originally planned in 56B2 and Col-0, but also in Kardz-1 and Kardz-2. Given the different lifecycles of Kardz and Col-0, it would not seem appropriate to cross these backgrounds and look at the trans-heterozygotes.

Does *CKX5* have a role in root vascular patterning? the results suggest that if this was the case, then *CKX5* would have to have a non-autonomous role, as my current interpretation of the data is that levels of *CKX5* mRNA are not altered in root tips of 56B2. New research published towards the end of my PhD demonstrates a role for *CKX3* (in which CKX5 acts redundantly) in regulating cytokinin levels in the procambium to regulate cell division and identity (Yang et al., 2021a). As described in the introduction, the interaction between cytokinin and auxin is required to maintain both cell division and cell specification within the stele. TMO5 is a direct auxin target, and forms a heterodimer with LHW to promote periclinal cell division (De Rybel et al., 2013). This complex stimulates the synthesis of active cytokinin by driving the expression of *LOG4* in the xylem axis (De Rybel et al., 2014a) . Cytokinin then diffuses into neighbouring cells (procambium and phloem) and promotes cell division and determines cell identity (De Rybel et al., 2014b). In this new research, Yang and colleagues (2021), show that in addition to *LOG4*, the TMO5/LHW heterodimer also promotes the expression of additional genes related to cytokinin homeostasis. The central one is a member of the glycoside hydrolase family 1 called BGLU44, which the authors showed acted cooperatively with LOG4 to convert inactive cytokinin conjugates into active cytokinin. They also demonstrated that the TMO5/LHW

heterodimer directly binds the promoter of the GRAS transcription factor *SHORT ROOT* (*SHR*) (Helariutta et al., 2000) and that SHR directly bound the *CKX3* promoter (Cui et al., 2011). This led the authors to propose a model in which via TMO5/LHW auxin regulates cytokinin homeostasis tightly by directly promoting cytokinin synthesis and indirectly regulation cytokinin catabolism. The single *ckx3* mutant did not show any alterations in vascular pattern, but when combined with CKX5 (its closest homologue) they observed a striking effect. The *ckx3 ckx5* double mutant showed an increase in the number of vascular cell files produced, and in most of the lines analysed they observed additional metaxylem cell files (Yang et al., 2021a). These clearly results demonstrate a requirement for *CKX5* as part of a module controlling root vascular patterning. Results in this project are consistent with this study on number of points. Firstly, the authors generated a new transcriptional reporter line for *CKX5*. This contained a 3.5 kb promoter, whilst construct in this project contained a 1.2 kb promoter. However, both constructs reported similar expression patterns and were expressed in cells flanking the xylem axis within the primary root tip. The authors did not investigate whether, like *CKX3*, *CKX5* is also induced by cytokinin. Chapter 5 was looked at this, and revealed that CKX5 was strongly increased in expression by cytokinin (BA) after six hours treatment. Although our experiments were not done the same way (benzyl adenine was applied exogenously, whereas Yang et al., used an inducible approach to drive the TMO5/LHW heterodimer), this is consistent with *CKX3* and *CKX5* being induced at a similar timepoint. It is therefore intriguing to speculate whether *CKX5* may also be a target of *SHR*. In order to finding SHR binding motif , 2 kb regions upstream of both *CKX5* and *CKX3* were imported into the binding site prediction tool on the PlantRegMap database (Tian et al., 2019) to search for GRAS binding sites. The *CKX3* promoter contained 3 potential GRAS binding sites, and the

CKX5 promoter contained 10. It is important to note the GRAS transcription factor family is large with more than 30 members in *Arabidopsis* (Pysh et al., 1999) and so the presence of these sites do not necessarily mean that SHR binds. Moreover, according to list that created to identify SHR direct target by combining a ChIP-chip method and microarray analysis (Cui et al., 2011). By combining the two datasets, the genome-wide location of SHR targets is determined. This list contains 200 genes, among these genes *CKX3* was found but not *CKX5*.

8.5 Conclusion

In conclusion, this thesis was aimed to characterise novel mutants that affected PIN7 expression in the root meristem. The involvement of *CKX5* in regulating the defects in PIN7 in a mutant called 56B2 was explored. Originally it had been planned for this to be a platform from which to study other mutants, but due to time restrictions and the complexity of this mutant it was exclusively focused on 56B2. The results are somewhat contradictory, and it will take further research to completely understand the role that this protein plays in vascular patterning. Based on results published late during my thesis (Yang et al., 2021a)., it is clear that CKX5 has an important role in vascular patterning. The results are consistent with these, and this project was provided novel data showing both the tissue specific expression of *CKX5* and showing that its expression is regulated as part of a feedback loop with cytokinin. 56B2 had a range of phenotypes which were broadly consistent with a plant showing changes in cytokinin homeostasis. However, experiments in this project looking at *CKX5* levels in the root tip could not support a mechanism which could link the mutation in the *CKX5* promoter to changes in *CKX5* levels in the root tip. However, whilst it was started out focused on root vascular pattern, this research showed a wider range of phenotypes

including lateral root and shoot development. Also, a natural accession with exactly the same polymorphism in the *CKX5* promoter phenocopied the 56B2 mutant was observed with respect to alterations in leaf number. This leaves a tantalising question whether this is a coincidence or if the 56B2 mutant affects cytokinin levels in other parts of the plant. Exploring this would be beyond the timescale of my PhD, but I have made suggestions about how this could be pursued.

References

ABAS, L., BENJAMINS, R., MALENICA, N., PACIOREK, T., WIŠNIEWSKA, J., MOULINIER–ANZOLA, J. C., SIEBERER, T., FRIML, J. & LUSCHNIG, C. 2006. Intracellular trafficking and proteolysis of the Arabidopsis auxin-efflux facilitator PIN2 are involved in root gravitropism. *Nature cell biology,* 8**,** 249-256.

AL-SHEHBAZ, I. A. & O'KANE, S. L., JR. 2002. Taxonomy and phylogeny of Arabidopsis (brassicaceae). *Arabidopsis Book,* 1**,** e0001.

ALONSO-BLANCO, C., ANDRADE, J., BECKER, C., BEMM, F., BERGELSON, J., BORGWARDT, K. M., CAO, J., CHAE, E., DEZWAAN, T. M., DING, W., ECKER, J. R., EXPOSITO-ALONSO, M., FARLOW, A., FITZ, J., GAN, X., GRIMM, D. G., HANCOCK, A. M., HENZ, S. R., HOLM, S., HORTON, M., JARSULIC, M., KERSTETTER, R. A., KORTE, A., KORTE, P., LANZ, C., LEE, C.-R., MENG, D., MICHAEL, T. P., MOTT, R., MULIYATI, N. W., NÄGELE, T., NAGLER, M., NIZHYNSKA, V., NORDBORG, M., NOVIKOVA, P. Y., PICÓ, F. X., PLATZER, A., RABANAL, F. A., RODRIGUEZ, A., ROWAN, B. A., SALOMÉ, P. A., SCHMID, K. J., SCHMITZ, R. J., SEREN, Ü., SPERONE, F. G., SUDKAMP, M., SVARDAL, H., TANZER, M. M., TODD, D., VOLCHENBOUM, S. L., WANG, C., WANG, G., WANG, X., WECKWERTH, W., WEIGEL, D. & ZHOU, X. 2016. 1,135 Genomes Reveal the Global Pattern of Polymorphism in Arabidopsis thaliana. *Cell,* 166**,** 481-491.

ANTONIADI, I., PLAČKOVÁ, L., SIMONOVIK, B., DOLEŽAL, K., TURNBULL, C., LJUNG, K. & NOVÁK, O. 2015. Cell-type-specific cytokinin distribution within the Arabidopsis primary root apex. *The Plant Cell,* 27**,** 1955-1967.

ASHIKARI, M., SAKAKIBARA, H., LIN, S., YAMAMOTO, T., TAKASHI, T., NISHIMURA, A., ANGELES, E. R., QIAN, Q., KITANO, H. & MATSUOKA, M. 2005. Cytokinin Oxidase Regulates Rice Grain Production. *Science,* 309**,** 741-745.

BARNES, T. & KORBER, P. 2021. The Active Mechanism of Nucleosome Depletion by Poly (dA: dT) Tracts In Vivo. *International Journal of Molecular Sciences,* 22**,** 8233.

BARTRINA, I., OTTO, E., STRNAD, M., WERNER, T. & SCHMÜLLING, T. 2011. Cytokinin regulates the activity of reproductive meristems, flower organ size, ovule formation, and thus seed yield in Arabidopsis thaliana. *Plant Cell,* 23**,** 69-80.

BENT, A. F. 2000. Arabidopsis in planta transformation. Uses, mechanisms, and prospects for transformation of other species. *Plant physiology,* 124**,** 1540-1547.

BERNARD, G., GAGNEUL, D., SANTOS, H. A. D., ETIENNE, A., HILBERT, J.-L. & RAMBAUD, C. 2019. Efficient genome editing using CRISPR/Cas9 technology in chicory. *International Journal of Molecular Sciences,* 20**,** 1155.

BHARGAVA, A., CLABAUGH, I., TO, J. P., MAXWELL, B. B., CHIANG, Y. H., SCHALLER, G. E., LORAINE, A. & KIEBER, J. J. 2013. Identification of cytokinin-responsive genes using microarray meta-analysis and RNA-Seq in Arabidopsis. *Plant Physiol,* 162**,** 272-94.

BISHOPP, A., HELP, H., EL-SHOWK, S., WEIJERS, D., SCHERES, B., FRIML, J., BENKOVÁ, E., MÄHÖNEN, A. P. & HELARIUTTA, Y. 2011a. A mutually inhibitory interaction between auxin and cytokinin specifies vascular pattern in roots. *Current Biology,* 21**,** 917-926.

BISHOPP, A., LEHESRANTA, S., VATÉN, A., HELP, H., EL-SHOWK, S., SCHERES, B., HELARIUTTA, K., MÄHÖNEN, ARI P., SAKAKIBARA, H. & HELARIUTTA, Y. 2011b. Phloem-Transported Cytokinin Regulates Polar Auxin Transport and Maintains Vascular Pattern in the Root Meristem. *Current Biology,* 21**,** 927-932.

BLILOU, I., XU, J., WILDWATER, M., WILLEMSEN, V., PAPONOV, I., FRIML, J., HEIDSTRA, R., AIDA, M., PALME, K. & SCHERES, B. 2005. The PIN auxin efflux facilitator network controls growth and patterning in Arabidopsis roots. *Nature,* 433**,** 39-44.

BOSCÁ, S., KNAUER, S. & LAUX, T. 2011. Embryonic development in Arabidopsis thaliana: from the zygote division to the shoot meristem. *Frontiers in Plant Science,* 2**,** 93.

BÖTTGER, M. 1974. Apical dominance in roots of Pisum sativum L. *Planta,* 121**,** 253-261.

BOURBOUSSE, C., MESTIRI, I., ZABULON, G., BOURGE, M., FORMIGGINI, F., KOINI, M. A., BROWN, S. C., FRANSZ, P., BOWLER, C. & BARNECHE, F. 2015. Light signaling controls nuclear architecture reorganization during seedling establishment. *Proceedings of the National Academy of Sciences,* 112**,** E2836-E2844.

BRADY, S. M., ORLANDO, D. A., LEE, J.-Y., WANG, J. Y., KOCH, J., DINNENY, J. R., MACE, D., OHLER, U. & BENFEY, P. N. 2007a. A high-resolution root spatiotemporal map reveals dominant expression patterns. *Science,* 318**,** 801-806.

BRADY, S. M., ORLANDO, D. A., LEE, J. Y., WANG, J. Y., KOCH, J., DINNENY, J. R., MACE, D., OHLER, U. & BENFEY, P. N. 2007b. A high-resolution root spatiotemporal map reveals dominant expression patterns. *Science,* 318**,** 801-6.

BRANDSTATTER, I. & KIEBER, J. J. 1998. Two genes with similarity to bacterial response regulators are rapidly and specifically induced by cytokinin in Arabidopsis. *The Plant Cell,* 10**,** 1009-1019.

BRENNER, W. G., RAMIREDDY, E., HEYL, A. & SCHMÜLLING, T. 2012. Gene regulation by cytokinin in Arabidopsis. *Frontiers in plant science,* 3**,** 8.

BRENNER, W. G., ROMANOV, G. A., KÖLLMER, I., BÜRKLE, L. & SCHMÜLLING, T. 2005. Immediate-early and delayed cytokinin response genes of Arabidopsis thaliana identified by genome-wide expression profiling reveal novel cytokinin-sensitive processes and suggest cytokinin action through transcriptional cascades. *The Plant Journal,* 44**,** 314-333.

CAESAR, K., THAMM, A. M., WITTHÖFT, J., ELGASS, K., HUPPENBERGER, P., GREFEN, C., HORAK, J. & HARTER, K. 2011. Evidence for the localization of the Arabidopsis cytokinin receptors AHK3 and AHK4 in the endoplasmic reticulum. *Journal of Experimental Botany,* 62**,** 5571-5580.

CALDERON-VILLALOBOS, L. I., TAN, X., ZHENG, N. & ESTELLE, M. 2010. Auxin perception—structural insights. *Cold Spring Harbor perspectives in biology,* 2**,** a005546.

CASIMIRO, I., MARCHANT, A., BHALERAO, R. P., BEECKMAN, T., DHOOGE, S., SWARUP, R., GRAHAM, N., INZÉ, D., SANDBERG, G. & CASERO, P. J. 2001. Auxin transport promotes Arabidopsis lateral root initiation. *The Plant Cell,* 13**,** 843-852.

CASSIDY, E. S., WEST, P. C., GERBER, J. S. & FOLEY, J. A. 2013. Redefining agricultural yields: from tonnes to people nourished per hectare. *Environmental Research Letters,* 8**,** 034015.

CHALFIE, M., TU, Y., EUSKIRCHEN, G., WARD, W. W. & PRASHER, D. C. 1994. Green fluorescent protein as a marker for gene expression. *Science,* 263**,** 802-805.

CHANG, L., RAMIREDDY, E. & SCHMÜLLING, T. 2013. Lateral root formation and growth of Arabidopsis is redundantly regulated by cytokinin metabolism and signalling genes. *Journal of experimental botany,* 64**,** 5021-5032.

CHEN, Q., LIU, Y., MAERE, S., LEE, E., VAN ISTERDAEL, G., XIE, Z., XUAN, W., LUCAS, J., VASSILEVA, V. & KITAKURA, S. 2015. A coherent transcriptional feed-forward motif model for mediating auxin-sensitive PIN3 expression during lateral root development. *Nature communications,* 6**,** 1-12.

CHEN, R., HILSON, P., SEDBROOK, J., ROSEN, E., CASPAR, T. & MASSON, P. H. 1998. The Arabidopsis thaliana AGRAVITROPIC 1 gene encodes a component of the polar-auxin-transport efflux carrier. *Proceedings of the National Academy of Sciences,* 95**,** 15112-15117.

COLE, M. B., AUGUSTIN, M. A., ROBERTSON, M. J. & MANNERS, J. M. 2018. The science of food security. *npj Science of Food,* 2**,** 14.

CUI, H., HAO, Y., KOVTUN, M., STOLC, V., DENG, X.-W., SAKAKIBARA, H. & KOJIMA, M. 2011. Genome-wide direct target analysis reveals a role for SHORT-ROOT in root vascular patterning through cytokinin homeostasis. *Plant Physiology,* 157**,** 1221-1231.

D'AGOSTINO, I. B., DERUERE, J. & KIEBER, J. J. 2000. Characterization of the response of the Arabidopsis response regulator gene family to cytokinin. *Plant physiology,* 124**,** 1706-1717.

DABRAVOLSKI, S. A. & ISAYENKOV, S. V. 2021. Evolution of the Cytokinin Dehydrogenase (CKX) Domain. *Journal of Molecular Evolution,* 89**,** 665-677.

DE RUIJTER, N., VERHEES, J., VAN LEEUWEN, W. & VAN DER KROL, A. 2003. Evaluation and comparison of the GUS, LUC and GFP reporter system for gene expression studies in plants. *Plant Biology,* 5**,** 103-115.

DE RYBEL, B., ADIBI, M., BREDA, A. S., WENDRICH, J. R., SMIT, M. E., NOVÁK, O., YAMAGUCHI, N., YOSHIDA, S., VAN ISTERDAEL, G. & PALOVAARA, J. 2014a. Integration of growth and patterning during vascular tissue formation in Arabidopsis. *Science,* 345**,** 1255215.

DE RYBEL, B., ADIBI, M., BREDA, A. S., WENDRICH, J. R., SMIT, M. E., NOVÁK, O., YAMAGUCHI, N., YOSHIDA, S., VAN ISTERDAEL, G., PALOVAARA, J., NIJSSE, B., BOEKSCHOTEN, M. V., HOOIVELD, G., BEECKMAN, T., WAGNER, D., LJUNG, K., FLECK, C. & WEIJERS, D. 2014b. Plant development. Integration of growth and patterning during vascular tissue formation in Arabidopsis. *Science,* 345**,** 1255215.

DE RYBEL, B., MÖLLER, B., YOSHIDA, S., GRABOWICZ, I., DE REUILLE, P. B., BOEREN, S., SMITH, R. S., BORST, J. W. & WEIJERS, D. 2013. A bHLH complex controls embryonic vascular tissue establishment and indeterminate growth in Arabidopsis. *Developmental cell,* 24**,** 426-437.

DE SMET, I. & BEECKMAN, T. 2011. Asymmetric cell division in land plants and algae: the driving force for differentiation. *Nature Reviews Molecular Cell Biology,* 12**,** 177-188.

DECHERING, K. J., KONINGS, R. N., CUELENAERE, K. & LEUNISSEN, J. A. 1998. Distinct frequency-distributions of homopolymeric DNA tracts in different genomes. *Nucleic acids research,* 26**,** 4056-4062.

DEDOW, L. K., OREN, E. & BRAYBROOK, S. A. 2022. Fake news blues: A GUS staining protocol to reduce false-negative data. *Plant direct,* 6**,** e367-e367.

DOLAN, L., JANMAAT, K., WILLEMSEN, V., LINSTEAD, P., POETHIG, S., ROBERTS, K. & SCHERES, B. 1993. Cellular organisation of the Arabidopsis thaliana root. *Development,* 119**,** 71-84.

DONNELLY, P. M., BONETTA, D., TSUKAYA, H., DENGLER, R. E. & DENGLER, N. G. 1999. Cell cycling and cell enlargement in developing leaves of Arabidopsis. *Developmental biology,* 215**,** 407-419.

DUBROVSKY, J. G., ROST, T. L., COLÓN-CARMONA, A. & DOERNER, P. 2001. Early primordium morphogenesis during lateral root initiation in Arabidopsis thaliana. *Planta,* 214**,** 30-36.

EFRONI, I., HAN, S.-K., KIM, H. J., WU, M.-F., STEINER, E., BIRNBAUM, K. D., HONG, J. C., ESHED, Y. & WAGNER, D. 2013. Regulation of leaf maturation by chromatin-mediated modulation of cytokinin responses. *Developmental cell,* 24**,** 438-445.

FAO, IFAD & WFP 2015. The State of Food Insecurity in the World 2015. Meeting the 2015 international hunger targets: taking stock of uneven progress. *FAO, Rome*.

FERREIRA, F. J. & KIEBER, J. J. 2005. Cytokinin signaling. *Current Opinion in Plant Biology,* 8**,** 518-525.

FERRERO-SERRANO, Á. & ASSMANN, S. M. 2019. Phenotypic and genome-wide association with the local environment of Arabidopsis. *Nature Ecology & Evolution,* 3**,** 274-285.

FIELD, Y., KAPLAN, N., FONDUFE-MITTENDORF, Y., MOORE, I. K., SHARON, E., LUBLING, Y., WIDOM, J. & SEGAL, E. 2008. Distinct modes of regulation by chromatin encoded through nucleosome positioning signals. *PLoS computational biology,* 4**,** e1000216.

FRIML, J., BENKOVÁ, E., BLILOU, I., WISNIEWSKA, J., HAMANN, T., LJUNG, K., WOODY, S., SANDBERG, G., SCHERES, B. & JÜRGENS, G. 2002a. AtPIN4 mediates sink-driven auxin gradients and root patterning in Arabidopsis. *Cell,* 108**,** 661-673.

FRIML, J., VIETEN, A., SAUER, M., WEIJERS, D., SCHWARZ, H., HAMANN, T., OFFRINGA, R. & JÜRGENS, G. 2003. Efflux-dependent auxin gradients establish the apical–basal axis of Arabidopsis. *Nature,* 426**,** 147-153.

FRIML, J., WIŚNIEWSKA, J., BENKOVÁ, E., MENDGEN, K. & PALME, K. 2002b. Lateral relocation of auxin efflux regulator PIN3 mediates tropism in Arabidopsis. *Nature,* 415**,** 806-809.

GALWEILER, L., GUAN, C., MULLER, A., WISMAN, E., MENDGEN, K., YEPHREMOV, A. & PALME, K. 1998. Regulation of polar auxin transport by AtPIN1 in Arabidopsis vascular tissue. *Science,* 282**,** 2226-2230.

GELVIN, S. B. 2003. Agrobacterium-mediated plant transformation: the biology behind the "gene-jockeying" tool. *Microbiology and molecular biology reviews,* 67**,** 16-37.

GELVIN, S. B. 2017. Integration of Agrobacterium T-DNA into the plant genome. *Annual review of genetics,* 51**,** 195-217.

GONZALEZ, N., VANHAEREN, H. & INZÉ, D. 2012. Leaf size control: complex coordination of cell division and expansion. *Trends in Plant Science,* 17**,** 332-340.

GREENE, E. A., CODOMO, C. A., TAYLOR, N. E., HENIKOFF, J. G., TILL, B. J., REYNOLDS, S. H., ENNS, L. C., BURTNER, C., JOHNSON, J. E. & ODDEN, A. R. 2003. Spectrum of chemically induced mutations from a large-scale reverse-genetic screen in Arabidopsis. *Genetics,* 164**,** 731-740.

HAAGEN-SMIT, A., DANDLIKER, W., WITTWER, S. & MURNEEK, A. 1946. Isolation of 3-indoleacetic acid from immature corn kernels. *American Journal of Botany***,** 118-120.

HELARIUTTA, Y., FUKAKI, H., WYSOCKA-DILLER, J., NAKAJIMA, K., JUNG, J., SENA, G., HAUSER, M.-T. & BENFEY, P. N. 2000. The SHORT-ROOT gene controls radial patterning of the Arabidopsis root through radial signaling. *Cell,* 101**,** 555-567.

HENDERSON, I. R. & DEAN, C. 2004. Control of Arabidopsis flowering: the chill before the bloom. *Development,* 131**,** 3829-3838.

HOUBA-HÉRIN, N., PETHE, C., D'ALAYER, J. & LALOUE, M. 1999. Cytokinin oxidase from Zea mays: purification, cDNA cloning and expression in moss protoplasts. *The Plant Journal,* 17**,** 615-626.

HWANG, I. & SHEEN, J. 2001. Two-component circuitry in Arabidopsis cytokinin signal transduction. *nature,* 413**,** 383-389.

HWANG, I., SHEEN, J. & MÜLLER, B. 2012. Cytokinin signaling networks. *Annual review of plant biology,* 63**,** 353-380.

INOUE, T., HIGUCHI, M., HASHIMOTO, Y., SEKI, M., KOBAYASHI, M., KATO, T., TABATA, S., SHINOZAKI, K. & KAKIMOTO, T. 2001. Identification of CRE1 as a cytokinin receptor from Arabidopsis. *Nature,* 409**,** 1060-1063.

IOIO, R. D., LINHARES, F. S. & SABATINI, S. 2008a. Emerging role of cytokinin as a regulator of cellular differentiation. *Current opinion in plant biology,* 11**,** 23-27.

IOIO, R. D., LINHARES, F. S., SCACCHI, E., CASAMITJANA-MARTINEZ, E., HEIDSTRA, R., COSTANTINO, P. & SABATINI, S. 2007. Cytokinins determine Arabidopsis root-meristem size by controlling cell differentiation. *Current biology,* 17**,** 678-682.

IOIO, R. D., NAKAMURA, K., MOUBAYIDIN, L., PERILLI, S., TANIGUCHI, M., MORITA, M. T., AOYAMA, T., COSTANTINO, P. & SABATINI, S. 2008b. A genetic framework for the control of cell division and differentiation in the root meristem. *Science,* 322**,** 1380-1384.

IYER, V. & STRUHL, K. 1995. Poly (dA: dT), a ubiquitous promoter element that stimulates transcription via its intrinsic DNA structure. *The EMBO journal,* 14**,** 2570-2579.

JEFFERSON, R. A., KAVANAGH, T. A. & BEVAN, M. W. 1987. GUS fusions: beta-glucuronidase as a sensitive and versatile gene fusion marker in higher plants. *The EMBO Journal,* 6**,** 3901-3907.

JIANG, J. & GILL, B. S. 2006. Current status and the future of fluorescence in situ hybridization (FISH) in plant genome research. *Genome,* 49**,** 1057-68.

JINEK, M., CHYLINSKI, K., FONFARA, I., HAUER, M., DOUDNA, J. A. & CHARPENTIER, E. 2012. A programmable dual-RNA–guided DNA endonuclease in adaptive bacterial immunity. *science,* 337**,** 816-821.

KAUFMANN, K., PAJORO, A. & ANGENENT, G. C. 2010. Regulation of transcription in plants: mechanisms controlling developmental switches. *Nature Reviews Genetics,* 11**,** 830-842.

KIEBER, J. J. & SCHALLER, G. E. 2018. Cytokinin signaling in plant development. *Development,* 145.

KLEINE-VEHN, J. & FRIML, J. 2008. Polar Targeting and Endocytic Recycling in Auxin-Dependent Plant Development. *Annual Review of Cell and Developmental Biology,* 24**,** 447-473.

KÖLLMER, I., NOVÁK, O., STRNAD, M., SCHMÜLLING, T. & WERNER, T. 2014. Overexpression of the cytosolic cytokinin oxidase/dehydrogenase (CKX 7) from A rabidopsis causes specific changes in root growth and xylem differentiation. *The Plant Journal,* 78**,** 359-371.

KOMAKI, M., OKADA, K., NISHINO, E. & SHIMURA, Y. 1988. Isolation and characterization of novel mutants of Arabidopsis thaliana defective in flower development. *Development,* 104**,** 195-203.

KRÄMER, U. 2015. Planting molecular functions in an ecological context with Arabidopsis thaliana. *eLife,* 4**,** e06100.

KÜMPERS, B. M., HAN, J., VAUGHAN-HIRSCH, J., REDMAN, N., WARE, A., ATKINSON, J. A., LEFTLEY, N., JANES, G., CASTIGLIONE, G. & TARR, P. T. 2022. Dual expression and anatomy lines allow simultaneous visualization of gene expression and anatomy. *Plant physiology,* 188**,** 56-69.

LAIBACH, F. 1907. *Zur Frage nach der Individualität der Chromosomen im Pflanzenreich.*

LAMPROPOULOS, A., SUTIKOVIC, Z., WENZL, C., MAEGELE, I., LOHMANN, J. U. & FORNER, J. 2013. GreenGate---a novel, versatile, and efficient cloning system for plant transgenesis. *PLoS One,* 8**,** e83043.

LAUX, T., WÜRSCHUM, T. & BREUNINGER, H. 2004. Genetic regulation of embryonic pattern formation. *The Plant Cell,* 16**,** S190-S202.

LEBLANC, C., ZHANG, F., MENDEZ, J., LOZANO, Y., CHATPAR, K., IRISH, V. F. & JACOB, Y. 2018. Increased efficiency of targeted mutagenesis by CRISPR/Cas9 in plants using heat stress. *The Plant Journal,* 93**,** 377-386.

LEE, D. J., PARK, J.-Y., KU, S.-J., HA, Y.-M., KIM, S., KIM, M. D., OH, M.-H. & KIM, J. 2007. Genome-wide expression profiling of ARABIDOPSIS RESPONSE REGULATOR 7 (ARR7) overexpression in cytokinin response. *Molecular Genetics and Genomics,* 277**,** 115-137.

LEE, I., BLEECKER, A. & AMASINO, R. 1993. Analysis of naturally occurring late flowering in Arabidopsis thaliana. *Molecular and General Genetics MGG,* 237**,** 171-176.

LOMIN, S., KRIVOSHEEV, D., STEKLOV, M. Y., OSOLODKIN, D. & ROMANOV, G. 2012. Receptor properties and features of cytokinin signaling. *Acta Naturae (англоязычная версия),* 4**,** 31-45.

LOMIN, S. N., KRIVOSHEEV, D. M., STEKLOV, M. Y., ARKHIPOV, D. V., OSOLODKIN, D. I., SCHMÜLLING, T. & ROMANOV, G. A. 2015. Plant membrane assays with cytokinin receptors underpin the unique role of free cytokinin bases as biologically active ligands. *Journal of Experimental Botany,* 66**,** 1851-1863.

MÄHÖNEN, A. P., BISHOPP, A., HIGUCHI, M., NIEMINEN, K. M., KINOSHITA, K., TÖRMÄKANGAS, K., IKEDA, Y., OKA, A., KAKIMOTO, T. & HELARIUTTA, Y. 2006. Cytokinin Signaling and Its Inhibitor AHP6 Regulate Cell Fate During Vascular Development. *Science,* 311**,** 94-98.

MALAMY, J. E. & BENFEY, P. N. 1997. Organization and cell differentiation in lateral roots of Arabidopsis thaliana. *Development,* 124**,** 33-44.

MARHAVÝ, P., BIELACH, A., ABAS, L., ABUZEINEH, A., DUCLERCQ, J., TANAKA, H., PAŘEZOVÁ, M., PETRÁŠEK, J., FRIML, J. & KLEINE-VEHN, J. 2011. Cytokinin modulates endocytic trafficking of PIN1 auxin efflux carrier to control plant organogenesis. *Developmental cell,* 21**,** 796-804.

MARHAVÝ, P., DUCLERCQ, J., WELLER, B., FERARU, E., BIELACH, A., OFFRINGA, R., FRIML, J., SCHWECHHEIMER, C., MURPHY, A. & BENKOVÁ, E. 2014. Cytokinin controls polarity of PIN1-dependent auxin transport during lateral root organogenesis. *Current Biology,* 24**,** 1031-1037.

MARTÍN, B., RAMIRO, M., MARTÍNEZ-ZAPATER, J. M. & ALONSO-BLANCO, C. 2009. A high-density collection of EMS-induced mutations for TILLING in Landsberg erecta genetic background of Arabidopsis. *BMC Plant Biology,* 9**,** 147.

MARTINDALE, W. 2017. The potential of food preservation to reduce food waste. *Proceedings of the Nutrition Society,* 76**,** 28-33.

MASON, M. G., LI, J., MATHEWS, D. E., KIEBER, J. J. & SCHALLER, G. E. 2004. Type-B response regulators display overlapping expression patterns in Arabidopsis. *Plant physiology,* 135**,** 927-937.

MATSUMOTO-KITANO, M., KUSUMOTO, T., TARKOWSKI, P., KINOSHITA-TSUJIMURA, K., VÁCLAVÍKOVÁ, K., MIYAWAKI, K. & KAKIMOTO, T. 2008. Cytokinins are central regulators of cambial activity. *Proceedings of the National Academy of Sciences,* 105**,** 20027-20031.

MATTE RISOPATRON, J. P., SUN, Y. & JONES, B. J. 2010. The vascular cambium: molecular control of cellular structure. *Protoplasma,* 247**,** 145-161.

MEINKE, D. W., CHERRY, J. M., DEAN, C., ROUNSLEY, S. D. & KOORNNEEF, M. 1998. Arabidopsis thaliana: a model plant for genome analysis. *Science,* 282**,** 662-682.

MELLOR, N. L., VOS, U., JANES, G., BENNETT, M. J., WELLS, D. M. & BAND, L. R. 2020. Auxin fluxes through plasmodesmata modify root-tip auxin distribution. *Development,* 147.

MILLER, C. O., SKOOG, F., VON SALTZA, M. H. & STRONG, F. 1955. Kinetin, a cell division factor from deoxyribonucleic acid1. *Journal of the American Chemical Society,* 77**,** 1392-1392.

MIRONOVA, V. V., OMELYANCHUK, N. A., NOVOSELOVA, E. S., DOROSHKOV, A. V., KAZANTSEV, F. V., KOCHETOV, A. V., KOLCHANOV, N. A., MJOLSNESS, E. & LIKHOSHVAI, V. A. 2012. Combined in silico/in vivo analysis of mechanisms providing for root apical meristem self-organization and maintenance. *Annals of Botany,* 110**,** 349-360.

MIYATA, S.-I., URAO, T., YAMAGUCHI-SHINOZAKI, K. & SHINOZAKI, K. 1998. Characterization of genes for two-component phosphorelay mediators with a single HPt domain in Arabidopsis thaliana. *FEBS letters,* 437**,** 11-14.

MOK, D. W. & MOK, M. C. 1994. *Cytokininschemistry, activity, and function*, CRC press.

MOK, D. W. & MOK, M. C. 2001a. CYTOKININ METABOLISM AND ACTION. *Annu Rev Plant Physiol Plant Mol Biol,* 52**,** 89-118.

MOK, D. W. & MOK, M. C. 2001b. Cytokinin metabolism and action. *Annual review of plant biology,* 52**,** 89.

MORRIS, R. O., BILYEU, K. D., LASKEY, J. G. & CHEIKH, N. N. 1999. Isolation of a gene encoding a glycosylated cytokinin oxidase from maize. *Biochemical and biophysical research communications,* 255**,** 328-333.

MOUBAYIDIN, L., PERILLI, S., IOIO, R. D., DI MAMBRO, R., COSTANTINO, P. & SABATINI, S. 2010. The rate of cell differentiation controls the Arabidopsis root meristem growth phase. *Current Biology,* 20**,** 1138-1143.

MÜLLER, A., GUAN, C., GÄLWEILER, L., TÄNZLER, P., HUIJSER, P., MARCHANT, A., PARRY, G., BENNETT, M., WISMAN, E. & PALME, K. 1998. AtPIN2 defines a locus of Arabidopsis for root gravitropism control. *The EMBO journal,* 17**,** 6903-6911.

MÜLLER, B. & SHEEN, J. 2008. Cytokinin and auxin interaction in root stem-cell specification during early embryogenesis. *Nature,* 453**,** 1094-1097.

NAPP-ZINN, K. 1987. Vernalization-environmental and genetic regulation. *Manipulation of flowering***,** 123-132.

NELSON, H., FINCH, J. T., LUISI, B. F. & KLUG, A. 1987. The structure of an oligo (dA)· oligo (dT) tract and its biological implications. *Nature,* 330**,** 221-226.

NIEMANN, M. C., WEBER, H., HLUSKA, T., LEONTE, G., ANDERSON, S. M., NOVÁK, O., SENES, A. & WERNER, T. 2018. The cytokinin oxidase/dehydrogenase CKX1 is a membrane-bound protein requiring homooligomerization in the endoplasmic reticulum for its cellular activity. *Plant Physiology,* 176**,** 2024-2039.

OKADA, K., UEDA, J., KOMAKI, M. K., BELL, C. J. & SHIMURA, Y. 1991. Requirement of the auxin polar transport system in early stages of Arabidopsis floral bud formation. *The plant cell,* 3**,** 677-684.

OSAKABE, Y., WATANABE, T., SUGANO, S. S., UETA, R., ISHIHARA, R., SHINOZAKI, K. & OSAKABE, K. 2016. Optimization of CRISPR/Cas9 genome editing to modify abiotic stress responses in plants. *Scientific reports,* 6**,** 1-10.

PECINKA, A., DINH, H. Q., BAUBEC, T., ROSA, M., LETTNER, N. & SCHEID, O. M. 2010. Epigenetic regulation of repetitive elements is attenuated by prolonged heat stress in Arabidopsis. *The Plant Cell,* 22**,** 3118-3129.

PEER, W. A. 2013. From perception to attenuation: auxin signalling and responses. *Current opinion in plant biology,* 16**,** 561-568.

PÉRET, B., DE RYBEL, B., CASIMIRO, I., BENKOVÁ, E., SWARUP, R., LAPLAZE, L., BEECKMAN, T. & BENNETT, M. J. 2009. Arabidopsis lateral root development: an emerging story. *Trends in plant science,* 14**,** 399-408.

PERNISOVÁ, M., KLÍMA, P., HORÁK, J., VÁLKOVÁ, M., MALBECK, J., SOUČEK, P., REICHMAN, P., HOYEROVÁ, K., DUBOVÁ, J. & FRIML, J. 2009. Cytokinins modulate auxin-induced organogenesis in plants via regulation of the auxin efflux. *Proceedings of the National Academy of Sciences,* 106**,** 3609-3614.

PIGLIUCCI, M. 2002. Ecology and evolutionary biology of Arabidopsis. *The arabidopsis book,* 1**,** e0003-e0003.

PIMENTEL, D. & PIMENTEL, M. 2003. Sustainability of meat-based and plant-based diets and the environment. *The American journal of clinical nutrition,* 78**,** 660S-663S.

PUNWANI, J. A., HUTCHISON, C. E., SCHALLER, G. E. & KIEBER, J. J. 2010. The subcellular distribution of the Arabidopsis histidine phosphotransfer proteins is independent of cytokinin signaling. *The Plant Journal,* 62**,** 473-482.

PYSH, L. D., WYSOCKA-DILLER, J. W., CAMILLERI, C., BOUCHEZ, D. & BENFEY, P. N. 1999. The GRAS gene family in Arabidopsis: sequence characterization and basic expression analysis of the SCARECROW-LIKE genes. *Plant J,* 18**,** 111-9.

RASHOTTE, A. M., CARSON, S. D., TO, J. P. & KIEBER, J. J. 2003. Expression profiling of cytokinin action in Arabidopsis. *Plant Physiology,* 132**,** 1998-2011.

RÉDEI, G., KONCZ, C., CHUA, N. & SCHELL, J. 1992. Methods in Arabidopsis research. *Vol World Scientific***,** 16-21.

RIEFLER, M., NOVAK, O., STRNAD, M. & SCHMÜLLING, T. 2006. Arabidopsis cytokinin receptor mutants reveal functions in shoot growth, leaf senescence, seed size, germination, root development, and cytokinin metabolism. *The Plant Cell,* 18**,** 40-54.

ROMANOV, G. A., LOMIN, S. N. & SCHMÜLLING, T. 2018. Cytokinin signaling: from the ER or from the PM? That is the question! *New Phytologist,* 218**,** 41-53.

ROY, A., EXINGER, F. & LOSSON, R. 1990. cis-and trans-acting regulatory elements of the yeast URA3 promoter. *Molecular and Cellular Biology,* 10**,** 5257-5270.

RUIZ ROSQUETE, M., WAIDMANN, S. & KLEINE-VEHN, J. 2018. PIN7 auxin carrier has a preferential role in terminating radial root expansion in Arabidopsis thaliana. *International Journal of Molecular Sciences,* 19**,** 1238.

RŮŽIČKA, K., ŠIMÁŠKOVÁ, M., DUCLERCQ, J., PETRÁŠEK, J., ZAŽÍMALOVÁ, E., SIMON, S., FRIML, J., VAN MONTAGU, M. C. & BENKOVÁ, E. 2009. Cytokinin regulates root meristem activity via modulation of the polar auxin transport. *Proceedings of the National Academy of Sciences,* 106**,** 4284-4289.

SADIK, N. 1997. State of world population.

SAKAI, H., AOYAMA, T. & OKA, A. 2000. Arabidopsis ARR1 and ARR2 response regulators operate as transcriptional activators. *The Plant Journal,* 24**,** 703-711.

SAKAKIBARA, H. 2006. Cytokinins: activity, biosynthesis, and translocation. *Annual review of plant biology,* 57**,** 431-449.

SALEHIN, M., BAGCHI, R. & ESTELLE, M. 2015. SCFTIR1/AFB-based auxin perception: mechanism and role in plant growth and development. *The Plant Cell,* 27**,** 9-19.

SCHALLER, G. E., BISHOPP, A. & KIEBER, J. J. 2015. The Yin-Yang of Hormones: Cytokinin and Auxin Interactions in Plant Development. *The Plant Cell,* 27**,** 44-63.

SCHERES, B., WOLKENFELT, H., WILLEMSEN, V., TERLOUW, M., LAWSON, E., DEAN, C. & WEISBEEK, P. 1994. Embryonic origin of the Arabidopsis primary root and root meristem initials. *Development,* 120**,** 2475-2487.

SCHMÜLLING, T., WERNER, T., RIEFLER, M., KRUPKOVÁ, E. & BARTRINA Y MANNS, I. 2003. Structure and function of cytokinin oxidase/dehydrogenase genes of maize, rice, Arabidopsis and other species. *Journal of plant research,* 116**,** 241-252.

SEGAL, E. & WIDOM, J. 2009. Poly (dA: dT) tracts: major determinants of nucleosome organization. *Current opinion in structural biology,* 19**,** 65-71.

SHELDON, C. C., CONN, A. B., DENNIS, E. S. & PEACOCK, W. J. 2002. Different regulatory regions are required for the vernalization-induced repression of FLOWERING LOCUS C and for the epigenetic maintenance of repression. *The Plant Cell,* 14**,** 2527-2537.

SKALÁK, J., VERCRUYSSEN, L., CLAEYS, H., HRADILOVÁ, J., ČERNÝ, M., NOVÁK, O., PLAČKOVÁ, L., SAIZ-FERNÁNDEZ, I., SKALÁKOVÁ, P. & COPPENS, F. 2019. Multifaceted activity of cytokinin in leaf development shapes its size and structure in Arabidopsis. *The Plant Journal,* 97**,** 805-824.

SKOOG, F. & MILLER, C. O. 1957. Chemical regulation of growth and organ formation in plant tissues cultured in vitro. *Symp Soc Exp Biol,* 11**,** 118-30.

SMIT, M. E. & WEIJERS, D. 2015. The role of auxin signaling in early embryo pattern formation. *Current opinion in plant biology,* 28**,** 99-105.

STEEVES, T. A. & SUSSEX, I. M. 1989. *Patterns in plant development*, Cambridge University Press.

STRNAD, M. 1997. The aromatic cytokinins. *Physiologia plantarum,* 101**,** 674-688.

STRUHL, K. 1985. Naturally occurring poly (dA-dT) sequences are upstream promoter elements for constitutive transcription in yeast. *Proceedings of the National Academy of Sciences,* 82**,** 8419-8423.

SUGIMOTO, K., JIAO, Y. & MEYEROWITZ, E. M. 2010. Arabidopsis regeneration from multiple tissues occurs via a root development pathway. *Developmental cell,* 18**,** 463-471.

SUTER, B., SCHNAPPAUF, G. & THOMA, F. 2000. Poly (dA· dT) sequences exist as rigid DNA structures in nucleosome-free yeast promoters in vivo. *Nucleic acids research,* 28**,** 4083-4089.

SUZUKI, T., IMAMURA, A., UEGUCHI, C. & MIZUNO, T. 1998. Histidine-containing phosphotransfer (HPt) signal transducers implicated in His-to-Asp phosphorelay in Arabidopsis. *Plant and cell physiology,* 39**,** 1258-1268.

SUZUKI, T., MIWA, K., ISHIKAWA, K., YAMADA, H., AIBA, H. & MIZUNO, T. 2001. The Arabidopsis Sensor His-kinase, AHK4, Can Respond to Cytokinins. *Plant and Cell Physiology,* 42**,** 107-113.

SWARBRECK, D., WILKS, C., LAMESCH, P., BERARDINI, T. Z., GARCIA-HERNANDEZ, M., FOERSTER, H., LI, D., MEYER, T., MULLER, R., PLOETZ, L., RADENBAUGH, A., SINGH, S., SWING, V., TISSIER, C., ZHANG, P. & HUALA, E. 2007. The Arabidopsis Information Resource (TAIR): gene structure and function annotation. *Nucleic Acids Research,* 36**,** D1009-D1014.

SZEMENYEI, H., HANNON, M. & LONG, J. A. 2008. TOPLESS mediates auxin-dependent transcriptional repression during Arabidopsis embryogenesis. *Science,* 319**,** 1384-1386.

TAKATSUKA, H. & UMEDA, M. 2014. Hormonal control of cell division and elongation along differentiation trajectories in roots. *Journal of experimental botany,* 65**,** 2633-2643.

TEN HOVE, C. A., LU, K.-J. & WEIJERS, D. 2015. Building a plant: cell fate specification in the early Arabidopsis embryo. *Development,* 142**,** 420-430.

TEOTIA, P. S., MUKHERJEE, S. K. & MISHRA, N. S. 2008. Fine tuning of auxin signaling by miRNAs. *Physiology and Molecular Biology of Plants,* 14**,** 81-90.

THE ARABIDOPSIS GENOME, I. 2000. Analysis of the genome sequence of the flowering plant Arabidopsis thaliana. *Nature,* 408**,** 796-815.

TIAN, F., YANG, D.-C., MENG, Y.-Q., JIN, J. & GAO, G. 2019. PlantRegMap: charting functional regulatory maps in plants. *Nucleic Acids Research,* 48**,** D1104-D1113.

TIAN, H., DE SMET, I. & DING, Z. 2014. Shaping a root system: regulating lateral versus primary root growth. *Trends in Plant Science,* 19**,** 426-431.

TO, J. P., HABERER, G., FERREIRA, F. J., DERUÈRE, J., MASON, M. G., SCHALLER, G. E., ALONSO, J. M., ECKER, J. R. & KIEBER, J. J. 2004. Type-A Arabidopsis response regulators are partially redundant negative regulators of cytokinin signaling. *Plant Cell,* 16**,** 658-71.

TSUTSUI, H. & HIGASHIYAMA, T. 2016. pKAMA-ITACHI Vectors for Highly Efficient CRISPR/Cas9-Mediated Gene Knockout in Arabidopsis thaliana. *Plant and Cell Physiology,* 58**,** 46-56.

UBEDA-TOMÁS, S., BEEMSTER, G. T. S. & BENNETT, M. J. 2012. Hormonal regulation of root growth: integrating local activities into global behaviour. *Trends in Plant Science,* 17**,** 326-331.

UEGUCHI, C., KOIZUMI, H., SUZUKI, T. & MIZUNO, T. 2001. Novel family of sensor histidine kinase genes in Arabidopsis thaliana. *Plant and Cell Physiology,* 42**,** 231-235.

ULMASOV, T., HAGEN, G. & GUILFOYLE, T. J. 1999. Activation and repression of transcription by auxin-response factors. *Proceedings of the National Academy of Sciences,* 96**,** 5844-5849.

VAUGHAN-HIRSCH, J., GOODALL, B. & BISHOPP, A. 2018. North, East, South, West: mapping vascular tissues onto the Arabidopsis root. *Current Opinion in Plant Biology,* 41**,** 16-22.

VERBELEN, J.-P., CNODDER, T. D., LE, J., VISSENBERG, K. & BALUŠKA, F. 2006. The Root Apex of Arabidopsis thaliana Consists of Four Distinct Zones of Growth Activities. *Plant Signaling & Behavior,* 1**,** 296-304.

WEIGEL, D. & MOTT, R. 2009. The 1001 Genomes Project for Arabidopsis thaliana. *Genome Biology,* 10**,** 107.

WENDRICH, J. R., YANG, B., VANDAMME, N., VERSTAEN, K., SMET, W., VAN DE VELDE, C., MINNE, M., WYBOUW, B., MOR, E. & ARENTS, H. E. 2020. Vascular transcription factors guide plant epidermal responses to limiting phosphate conditions. *Science,* 370**,** eaay4970.

WERNER, T., MOTYKA, V., STRNAD, M. & SCHMÜLLING, T. 2001a. Regulation of plant growth by cytokinin. *Proc Natl Acad Sci U S A,* 98**,** 10487-92.

WERNER, T., MOTYKA, V., STRNAD, M. & SCHMÜLLING, T. 2001b. Regulation of plant growth by cytokinin. *Proceedings of the National Academy of Sciences,* 98**,** 10487-10492.

WERNER, T. & SCHMÜLLING, T. 2009. Cytokinin action in plant development. *Current opinion in plant biology,* 12**,** 527-538.

WERNER, T. S., MOTYKA, V., LAUCOU, V., SMETS, R., VAN ONCKELEN, H. & SCHMÜLLING, T. 2003. Cytokinin-deficient transgenic Arabidopsis plants show multiple developmental alterations indicating opposite functions of cytokinins in the regulation of shoot and root meristem activity. *The Plant Cell,* 15**,** 2532-2550.

WULFETANGE, K., LOMIN, S. N., ROMANOV, G. A., STOLZ, A., HEYL, A. & SCHMÜLLING, T. 2011. The cytokinin receptors of Arabidopsis are located mainly to the endoplasmic reticulum. *Plant physiology,* 156**,** 1808-1818.

XUE, Z., LIU, L. & ZHANG, C. 2020. Regulation of Shoot Apical Meristem and Axillary Meristem Development in Plants. *International Journal of Molecular Sciences,* 21**,** 2917.

YANG, B., MINNE, M., BRUNONI, F., PLAČKOVÁ, L., PETŘÍK, I., SUN, Y., NOLF, J., SMET, W., VERSTAEN, K. & WENDRICH, J. R. 2021a. Non-cell autonomous and spatiotemporal signalling from a tissue organizer orchestrates root vascular development. *Nature plants,* 7**,** 1485-1494.

YANG, B., MINNE, M., BRUNONI, F., PLAČKOVÁ, L., PETŘÍK, I., SUN, Y., NOLF, J., SMET, W., VERSTAEN, K., WENDRICH, J. R., EEKHOUT, T., HOYEROVÁ, K., VAN ISTERDAEL, G., HAUSTRAETE, J., BISHOPP, A., FARCOT, E., NOVÁK, O., SAEYS, Y. & DE RYBEL, B. 2021b. Non-cell autonomous and spatiotemporal signalling from a tissue organizer orchestrates root vascular development. *Nature Plants,* 7**,** 1485-1494.

YANG, S. H., YU, H. & GOH, C. J. 2003. Functional characterisation of a cytokinin oxidase gene DSCKX1 in Dendrobium orchid. *Plant Molecular Biology,* 51**,** 237-248.

YOKOYAMA, A., YAMASHINO, T., AMANO, Y.-I., TAJIMA, Y., IMAMURA, A., SAKAKIBARA, H. & MIZUNO, T. 2007. Type-B ARR Transcription Factors, ARR10 and ARR12, are Implicated in Cytokinin-Mediated Regulation of Protoxylem Differentiation in Roots of Arabidopsis thaliana. *Plant and Cell Physiology,* 48**,** 84-96.

YOSHIDA, S., DE REUILLE, P. B., LANE, B., BASSEL, G. W., PRUSINKIEWICZ, P., SMITH, R. S. & WEIJERS, D. 2014. Genetic control of plant development by overriding a geometric division rule. *Developmental cell,* 29**,** 75-87.

YUAN, G.-C., LIU, Y.-J., DION, M. F., SLACK, M. D., WU, L. F., ALTSCHULER, S. J. & RANDO, O. J. 2005. Genome-scale identification of nucleosome positions in S. cerevisiae. *Science,* 309**,** 626-630.

Appendix:

Methods Supp 1. Working Concentrations of Antibiotics Utilised

Antibiotic	Concentration (µg/ml)
Kanamycin	50
Spectinomycin	100
Ampicillin	100
Gentamicin	50
Tetracycline	5
Rifampicin	25
Basta (PTT)	10

Methods Supp 2. CRISPR Related Primers

F Primer Name	F Primer Sequence	R Primer Name	R Primer Sequence
CKX5.1-3 Poly Seq F	CCTCAGACTTCGGTATGCTG	CKX5.1-3 Poly Seq R	TAACTCTCCACCCCATACATC
CAS9-F	CGCTAATCTTGCAGGTAGCC	CAS9-R	CCGTTGTGTGATCAGTTTGG
CRISPRpKIRg3-F-	ATCTCTCTCGAACCAGCTCC	CRISPRpKIRg3-R	cCTCTGGCTTCTTCTTCATGTCC

CKX-CRISPR-guideF	GTTTTCCCAGTCACGAC	CKX-CRISPR-gudeR	CAGACAAACCGGCCAGGATTTC
CKX5-Genotyping-F	GCAGGAATCAGTGGTCAAGC	CKX5-Genotyping-R	GAGGAGATCTTGACGGGGTT

Methods Supp 3. Primers for sequence natural accession:

F Primer Name	F Primer Sequence	R Primer Name	R Primer Sequence
ckx5ttrackF	TGTCGATGAAGCCAAAGAGAG	ckx5ttrackR	TGAAAGAGCAGGGTCCACAT
Seq56B2F	TGGTACCATATCGACCCACCA	Seq56B2R	GGATGAGGTCACACGTGTGT